



Hochschule für Angewandte Wissenschaften Hamburg
Hamburg University of Applied Sciences

Master Thesis

Conceptual Design Optimization of a Strut Braced Wing Aircraft

Author: Víctor Julián Sánchez Barreda

Examiner: Prof. Dr.-Ing. Dieter Scholz, MSME

Delivery date: 12.07.2013



Hochschule für Angewandte Wissenschaften Hamburg
Fakultät Technik und Informatik
Department Fahrzeugtechnik und Flugzeugbau
Berliner Tor 9
20099 Hamburg

Author: Víctor Julián Sánchez Barreda

Examiner: Prof. Dr.-Ing. Dieter Scholz, MSME

Abstract

Aircraft design has changed a lot during years. In the beginning everything was done by hand and following a *test and error* philosophy. With time, scientific methods and empirical results allowed a great improvement on the field. With the arrival of computers, more complicated calculations were possible, as well as an increase in the accuracy of the existing methods. All these improvements made possible the evaluation and optimization of new configurations for the future. These configurations are expected to show an improvement in aircraft cost, as well as in fuel consumption and respect for the environment, which is what currently our World needs. Some of the new configurations rise as the best potential candidates to achieve this goal. Configurations like the Blended Wing Body and the Box Wing are clear examples of what the future aircraft may look like. The goal of this Thesis is the evaluation of the potential benefit of the Strut Braced Wing configuration for a passenger aircraft comparable in size and range to the Airbus A320. This aircraft is designed following the requirements given by the German Aerospace Center (DLR) in the frame of their *Design Challenge*, aiming to find the future aircraft. With that purpose, an optimization tool based on Microsoft Office Excel is used (OPerA). Such tool was created at AERO Group, at Hamburg University of Applied Sciences, with the aim of applying formal optimization to aircraft preliminary design. One of the objectives is to test the tool itself and the VBA optimization code implemented in it. Therefore, OPerA is modified in the present Thesis in order to add some features not available in the original code and to improve the calculation. This modified version of OPerA is then used to evaluate different configurations and to choose the most attractive in terms of fuel consumption or cash operating cost (COC). Once the program was ready, a series of calculations are performed, first to evaluate the potential of all possible configurations, and then to observe how far they can go with their improvements. Finally, a new aircraft is proposed. Configuration of this aircraft includes folding high wing (48.57 m span) with engines installed on it, conventional (low) tail and a supporting strut mounted under the wing. Thus, potential savings in fuel consumption of 33.64 % with respect to an optimized airbus A320, and 12.71 % in cash operation cost were obtained. The takeoff mass was reduced as well by 12.65 %, which has a positive effect on the COC and DOC. In addition, an alternative configuration is presented, limited to 36 m span. This alternative airplane has no folding wings, and reaches savings of 5.57 % in COC and 16.19 % in fuel mass. This proves the great benefit of using struts to achieve greater wingspans, and thus SBW becomes an attractive alternative to the classic cantilever wing aircraft.



DEPARTMENT OF AUTOMOTIVE AND AERONAUTICAL ENGINEERING

Conceptual Design Optimization of a Strut Braced Wing Aircraft

Background

The first step in aircraft design consists of finding consistent aircraft parameters that ensure the aircraft meets given requirements. Subsequently, this first set of aircraft parameters is varied such that an objective function is optimized. The objective function most often applied in civil aviation are Direct Operating Costs (DOC) which are to be minimized. The optimization involves – even in conceptual design – so many parameters that an aircraft specific optimization algorithm has to be used. The program Optimization in Preliminary Aircraft Design (OPerA) is available for this purpose at Hamburg University of Applied Sciences. A Strut Braced Wing (SBW) Aircraft is seen to have a potential replacing today's short-medium range aircraft. The strut relieves bending moments at the wing root. This advantage can be used to reduce wing mass maintaining span or to increase span at constant wing mass. Both approaches will reduce induced drag. Alternatively, relative wing thickness may be reduced at constant wing mass offering the chance to reduce wing sweep and supporting natural laminar flow, hence reducing zero lift drag. Snowball effects will reduce aircraft mass even more, reducing fuel consumption and emissions.

Task

Task of this Master Thesis is to investigate possible configurations and to optimize aircraft parameters (with and without wing span limitation) for a jet propelled Strut Braced Wing Aircraft (SBWA). The optimization shall consider various typical objective functions and should finally also include questioning and optimizing requirements like cruise Mach number, take-off and landing distance. Subtasks are listed below.

- Brief review of the SBWA concept including a brief discussion of wing span limitations at airports.
- Brief introduction to OPerA and description of modification in OPerA to allow also for optimization of other configurations than the standard tail aft, low wing passenger aircraft. Inclusion of the new DLR/HAW proposed Unified Cost Method (UCM) in OPerA.

- Investigation and preliminary optimization of SBWA configurations including high versus low wing, standard tail versus T-Tail, engines on wing versus engines on aft fuselage, wing mounted landing gear versus fuselage mounted landing gear – all based on “DLR Design Challenge 2012” requirements for a short-medium range passenger aircraft.
- Selection of a SBWA configuration and further optimization with respect to various cost functions: Primarily working with the UCM (COC and DOC) investigating also other basic and more sophisticated methods like Added Values.
- Final proposal of a SBWA and presentation as an electronic 3-D model either for X-Plane with the Plane Maker or with OpenVSP.

The report will be written in English based on German or international standards on report writing.

Declaration

Herewith I affirm that this master thesis is entirely my own work. Where use has been made of the work of others, it has been fully acknowledged and referenced.

Date

Signature

Contents

	Page
Abstract	3
Task	5
Declaration	6
List of Figures	9
List of Tables	11
Nomenclature	12
List of Abbreviations	14
1 Introduction	15
1.1 Motivation.....	15
1.2 Objectives.....	15
1.3 Review of Literature.....	16
1.4 Structure of this Thesis.....	16
2 Overview of the Strut Braced Wing Aircraft Concept	17
2.1 Introduction to SBW	17
2.2 Strut Braced Wing Aircraft Geometry	18
2.3 Advantages and Disadvantages of a SBW against Cantilever Wing.....	21
2.4 Bigger Span Considerations	22
3 Overview of OPerA	26
3.1 OPerA Concept.....	26
3.2 Methodology in OPerA	28
3.2.1 Requisites in OPerA	28
3.2.1.1 Airport Runway Lengths	29
3.2.1.2 Second Segment and Missed Approach	30
3.2.1.3 Cruise Mach Number	31
3.2.2 Design Parameters in OPerA.....	32
3.2.3 Matching Chart.....	33
3.3 Overview of the Tool	34
3.3.1 Modules Description.....	36
3.3.2 VBA Optimization in OPerA	39
3.3.2.1 Single Parameter Optimization.....	39
3.3.2.2 Multiple Parameter Optimization.....	40
3.4 Changes Done in OPerA.....	42
3.4.1 Changes in Tail Sizing.....	43
3.4.2 Centre of Gravity	46
3.4.3 Folding Wing Technology.....	51

3.4.4	New COC Method	58
3.4.4.1	TUB Cost Method	59
4	SBW Design Optimization	62
4.1	Mission Objectives	62
4.2	Single Parameter Study	67
4.2.1	m_{ML}/m_{MTO}	68
4.2.2	Aspect Ratio	70
4.2.3	Sweep Angle (φ_{25})	71
4.2.4	Taper Ratio	74
4.2.5	By-Pass Ratio	75
4.2.6	Relative Distance between Engine and Wing	77
4.2.7	Horizontal Tail Position	79
4.2.8	Engine Position	81
4.2.9	Main Landing Gear Position	81
4.2.10	$C_{L,max,TO}$ and $C_{L,max,L}$	82
4.3	A320 Optimization	83
4.3.1	First A320 Optimization	85
4.3.2	Second A320 Optimization	86
4.4	Preliminary Evaluation of Possible Configurations	87
4.4.1	Folding Wing Technology	88
4.4.2	New COC Method	90
4.5	Further Optimization of Chosen Configurations	93
4.6	Final Design Optimization Results	98
4.7	Visual Representation of the HCW52 SBW + FWS + NLF	102
5	Conclusions and Future Work	105
	References	106
	Acknowledgements	109
	Appendix A Results of first iteration round	110
	Appendix B CD-Rom contents	113

List of Figures

Figure 2.1	1919 British Sopwith Tabloid with strut connectors	17
Figure 2.2	Strut view of a Cessna Skyhawk	18
Figure 2.3	Typical strut configuration	19
Figure 2.4	Modified Fly Baby with top struts	20
Figure 2.5	Wing-strut connection with offset.....	21
Figure 3.1	Example of a Matching Chart delivered by OPerA	34
Figure 3.2	OPerA Layout.....	35
Figure 3.3	Scheme of the structure of OPerA.....	36
Figure 3.4	Example of DOE result obtained with OPerA	40
Figure 3.5	Scheme of a standard DE algorithm.....	41
Figure 3.6	Tail aft positioning	46
Figure 3.7	Position of the fuselage mass centre depending on engine position.....	48
Figure 3.8	Tail surfaces' centre of mass	48
Figure 3.9	Wing centre of mass position	50
Figure 3.10	Engine and nacelle mass centre position.....	50
Figure 3.11	Wing mass increase separated in its different parts	53
Figure 3.12	Plot of the three equations for the reinforcing system mass	54
Figure 3.13	Interpolated line for the mass reinforcing system	54
Figure 3.14	Plot of the equations for the folding mechanism and join mechanism masses	55
Figure 3.15	Folding system and joining system masses corrected.....	56
Figure 3.16	Relative mass of the three systems involved in folding wing technology.....	56
Figure 3.17	Mass increase of the wing with folding wing technology	57
Figure 3.18	Comparison of the wing weight when using one or two folding actuators	57
Figure 3.19	Folding system installed on a wing	58
Figure 3.20	Airbus fuel price tendency prediction	61
Figure 4.1	Blended wing body concept	63
Figure 4.2	Box wing aircraft concept	64
Figure 4.3	Cargo less aircraft concept cabin.....	65
Figure 4.4	COC variations with m_{ML}/m_{MTO}	69
Figure 4.5	Evolution of fuel mass and takeoff mass with m_{ML}/m_{MTO}	69
Figure 4.6	Results of experiment varying the wing aspect ratio	70
Figure 4.7	Flow over a swept wing.....	71
Figure 4.8	Results of varying the sweep angle for different cruise Mach numbers.....	72
Figure 4.9	Wing mass variation with the sweep angle for various speeds.....	73
Figure 4.10	Thickness ratio variation versus sweep angle	73
Figure 4.11	Wing mass variation with the taper ratio ($M = 0.76$)	74
Figure 4.12	COC variations with taper ratio ($M = 0.76$).....	75
Figure 4.13	Engine with high by-pass ratio	76
Figure 4.14	BPR variations versus COC	76

Figure 4.15	By-pass ratio versus altitude.....	77
Figure 4.16	h_P/D_N versus main landing gear length for various BPR.....	78
Figure 4.17	Different tail configurations	79
Figure 4.18	Comparison of the effect of centre of gravity calculation in tail position	80
Figure 4.19	Effect of tail position in tail mass	80
Figure 4.20	Variation of engine position over the fuselage.....	81
Figure 4.21	Influence of the main landing gear position over the COC	82
Figure 4.22	Influence of the maximum lift coefficients on the COC.....	83
Figure 4.23	DOC pie chart for A320 (CFM) 2009.....	84
Figure 4.24	COC pie chart for A320 (CFM) 2009	84
Figure 4.25	Design point of braced HXW52 in Raymer suggestion plot	93
Figure 4.26	COC chart comparison of the optimized aircraft.....	101
Figure 4.27	COC distribution of the designed airplane.....	102
Figure 4.28	3D representation of the final design	103
Figure 4.29	4 view representation of the final design.....	103
Figure 4.30	Final design with folded wings	104
Figure 4.31	Artistic representation of the final design	104

List of Tables

	Page
Table 2.1	ICAO recommendations for aircraft classification 23
Table 2.2	FAA Aircraft Design Group classification used in airport geometric design 24
Table 4.1	DLR Design Challenge requirements 64
Table 4.2	List of requirements, fixed parameters and design parameters for the design 66
Table 4.3	Cabin parameters 67
Table 4.4	OPerA results for reference standard A320 (CFM) 2009 67
Table 4.5	Variation of A320 cost through years (€/ton/mile) 83
Table 4.6	Requirements of standard A320 85
Table 4.7	Optimization results with original A320 requirements 85
Table 4.8	Requirements for Design Challenge 86
Table 4.9	A320 optimized for Design Challenge requirements 87
Table 4.10	Summary of all tested configurations 89
Table 4.11	Preliminary test round best results (separated on groups) 90
Table 4.12	COC results of preliminary test round compared with optimized A320 91
Table 4.13	Preliminary optimization round best results separated in groups 92
Table 4.14	Second round optimizations requirements and limits 94
Table 4.15	Best results obtained for HCW36 SBW with free parameters 95
Table 4.16	Best results obtained for HCW52 SBW with free parameters 95
Table 4.17	Best results obtained for HCW52 SBW + Folding with free parameters 96
Table 4.18	Best results obtained for HCW52 SBW+FWS+NLF with free parameters 97
Table 4.19	Main results of the final configurations 98
Table 4.20	Optimization results for HCW52 SBW+FWS+NLF 100

Nomenclature

a	annuity factor, component of parent vector
\bar{A}	parent vector
AR	aspect ratio
b	wing span, component of parent vector
\bar{B}	parent vector
c	chord length
C	cost
\bar{C}	parent vector
C_D	drag coefficient
C_H	horizontal tail volume coefficient
C_L	lift coefficient
C_M	moment coefficient
C_V	vertical tail coefficient
d	distance
E	lift-to-drag ratio
g	gravity acceleration
h	height, altitude
k_{APP}	statistical factor for approach
k_L	statistical factor for landing
k_{TO}	statistical factor for take off
l	length, lever arm
m	mass
M	Mach number
n_E	number of engines
n_{PAX}	number of passengers
n_{SA}	number of seat abreast
p	price, pressure
P	range
S_{LFL}	landing field length
S_{TOFL}	take off field length
S	surface
T	thrust power
V	speed
W	weight
x	position along x axis, distance
y	position along y axis, distance
z	position along z axis, distance

Greek Symbols

γ	climb angle
λ	taper ratio
π	pressure ratio
ρ	density
σ	density ratio
φ	sweep angle

Indices

$()_0$	zero lift, initial, 0 % of chord length
$()_{25}$	25 % of the chord length
$()_{100}$	100 % of the chord length
$()_{CAP}$	capital
$()_{CG}$	centre of gravity
$()_{ENG,E}$	engine
$()_F$	fuselage
$()_{H,T}$	horizontal tail
$()_{INS}$	insurance
$()_L$	landing
$()_{LEMAC}$	referred to the leading edge mean aerodynamic chord
$()_M$	maintenance
$()_{MAC}$	mean aerodynamic chord
$()_R$	root
$()_{RV}$	revenue
$()_T$	tip
$()_{TO}$	takeoff
$()_V$	vertical tail
$()_W$	wing

List of Abbreviations

AC	aerodynamic center
AEA	Association of European Airlines
AERO	Aircraft Design and Systems Group
AR	Aspect ratio
BPR	By-pass ratio
BWB	Blended Wing Body
CD-Rom	Compact Disc – Read Only Memory
CG	Centre of Gravity
COC	Cash Operating Cost
CFD	Computational Fluid Dynamics
DE	Differential Evolution
DOC	Direct Operating Cost
DOE	Design of Experiments
EASA	European Aviation Safety Agency
FAA	Federal Aviation Administration
FEM	Finite Element Method
FWS	Folding Wing System
FWT	Folding Wing Technology
HAW	Hochschule für Angewandte Wissenschaften Hamburg
ICAO	International Civil Aviation Organization
ISA	International Standard Atmosphere
JAA	Joint Aviation Authorities
MAC	Mean Aerodynamic Chord
MAI	Moscow Aviation Institute
MF	Maximum Fuel mass
ML	Maximum Landing mass
MLG	Main Landing Gear
MTO	Maximum Take Off mass
MZFW	Maximum Zero Fuel Weight
NASA	National Aeronautics and Space Administration
NOSA	NASA Open Source Agreement
NLG	Nose Landing Gear
NLF	Natural Laminar Flow
OEW	Operating Empty Weight
OPerA	Optimization in Preliminary Aircraft Design
PreSTo	Preliminary Sizing Tool
SAS	Simple Aircraft Sizing
SBW	Strut Braced Wing
TBW	Truss Braced Wing
SFC	Specific Fuel Consumption

TUB	Technische Universität Berlin
UCM	Unified Cost Method
VBA	Visual Basic for Applications
VSP	Vehicle Sketch Pad

1 Introduction

1.1 Motivation

Airplane trips are a very important part in many people's life. From business trips to holiday travels, the world is every day smaller and smaller thanks to airplanes. With time, more people uses more regularly this way of transport, and the business of air transport is grows increasingly more. However, this way of transport is not free of disadvantages. Air pollution produced by the airplane engines is one of them. In addition, air transport is an expensive business: each aircraft costs many dozen million of euro, and the operation costs are very high, which directly affects on the final ticket price, making it sometimes hard to afford by everybody.

For that reasons many development groups exist. Groups that are researching different projects with the aim of design the future aircraft. Aircraft with innovative looking that are cheaper and respectful with the environment. One on these groups is the AERO research group, from the Hamburg University of Applied Sciences (HAW); AERO collaborates with the project *Airport2030*, a joint project in which many universities in Germany and many different aeronautical companies collaborate. *Airport2030* aims to research new aircraft configurations that have great potential to be very beneficial for the future. This Thesis presents and analyzes one of these configurations: the Strut Braced Wing Aircraft, whose potential for increasing efficiency and therefore reduce fuel consumption makes of it a very attractive option from the economic point of view, as well as for the environment.

1.2 Objectives

This Thesis has the objective of performing an optimized preliminary design of a Strut Braced Wing Aircraft (SBW). The design will be created following the proposed requirements by the German Aerospace Center (DLR) for their *Design Challenge*. The final goal is to achieve a total 35 % of savings in cash operation cost (COC), as well as 25 % less fuel burn, compared to the Airbus A320 (CFM) 2009. The new aircraft must be designed to start service in 2025.

In order to do that, the tool called OPerA will be used. OPerA is a tool developed at the AERO research group. The tool is based in *Microsoft Excel*, and allows the user to perform preliminary aircraft design in an automatic way. It also has the ability to optimize the design under certain conditions defined by the user before starting the optimization process, such as using different objective functions or multiple parameter optimizations. The tool will be updated as part of this project in order to improve its functionality. In addition, using the tool for this project serves as well as test to check how OPerA works with non conventional configurations like the SBW.

1.3 Review of Literature

Despite the concept of the strut braced wing aircraft is not new, it has not been conveniently researched in the past, because the cantilever wing aircraft became more popular in the early years of aeronautical history than the SBW, and thus this last one was abandoned.

The first idea of using a truss braced wing structure came from Werner Pfenninger (**Pfenninger 1958**) who investigated the best way to reduce drag in an aircraft, and with that purpose he came to the idea of a TBW aircraft with laminar boundary layer. On other side, Maurice Hurel used the concept of a SBW to create great span wings, whose advantage is a great lift-to-drag ratio (**Hurel 1952**).

NASA conducted some researches as well investigating the advantages and viability of the strut braced wing aircraft (**NASA 1980** and **NASA 1981**), where it was shown that strut braced wing could save 20 % of fuel compared to the cantilever wing and increase the range by 5 %.

In the last years, due to the increasing interest in creating new aircraft configurations that are more efficient and respectful with the environment, the SBW concept has returned to the point of view of many researchers that see in it enough potential to become one of the aircraft of the future. Many of these researches were conducted at the Virginia Polytechnic Institute and State University, Blacksburg, VA, USA. Studies such as **Gundlach 1999**, **Gern 2000**, **Grasmeyer 1998** or **Ko 2002** agree on the potential advantages of the strut braced wing aircraft.

Ko 2002 includes a complete CFD focused on the strut-wing joint, proposing different solutions to reduce the shock wave produced there, with interesting results. On other side, **Gundlach 2000** and **Gern 2000** introduce the idea of using a telescopic sleeve on the union between the wing and the strut, so the strut never suffers compression, and thus buckling is avoided, apart that this way the strut mass can be optimized. However, other research studies like **Carrier 2012** suggest another different solution for this: the use of an arch shaped strut that is structurally simpler as the telescopic sleeve, and can act as a spring in negative g maneuvers, releasing bending moment in the wing root for these cases. This research performs a CFD and FEM study of the strut, in order to find the optimum configuration and shape.

1.4 Structure of this Thesis

This work has been structured as follows:

- Chapter 2** Gives an overview of the concept of the Strut Braced wing aircraft, its advantages and disadvantages.
- Chapter 3** Introduces OPerA to the reader, gives a summarized vision of its theoretical background, and describes the changes done within this project.
- Chapter 4** Explains the design process followed to create the SBW aircraft. Gives an overview of the mission, and comments the results. It also includes a computer model of the aircraft created with OpenVSP.

2 Overview of the Strut Braced Wing Aircraft Concept

2.1 Introduction to SBW

The strut braced wing concept (SBW), basically consist on the idea of adding a pair of supporting struts to the wing. This design will bring a series of different effects to the aerodynamics and performance of the aircraft, which will be further detailed.

This kind of design is not new, it is possible to find aircraft provided with supporting struts since the very beginning of the Aviation History. Early plane designers considered both monoplane and biplane designs. However, due to the materials available at the first decades of the 20th century, and the belief that thinner profiles were the most convenient for aircraft, the biplane design became very popular. A biplane aircraft allowed the designer to sketch lighter aircraft with very thin profiles, and the supporting structure keeping things together were the struts.



Figure 2.1 1919's British Sopwith Tabloid with strut connectors (**Agentsmart 2013**)

As years were passing, further investigations showed that it was possible to use cantilever wings with thicker profiles and low drag, keeping a good lift-to-drag ratio. They were also easier to manufacture, and did not have the drag penalty associated with the struts. As a result, biplane designs were being abandoned as the monoplane cantilever wing design was becoming the most used one.

In the early 50s, the supporting struts were rescued by Werner Pfenninger. His investigations were directed to reduce the induced drag of a transonic airplane, and that led him of higher aspect ratio wings which were not possible without the use of struts. Nowadays, SWB concept is commonly used in small aircraft, like the widely spread Cessna 172.



Figure 2.2 Strut view of a Cessna Skyhawk (Cessna 2013)

2.2 Strut Braced Wing Aircraft Geometry

The configuration of a strut braced wing aircraft on its most common form is very similar to a standard cantilever wing aircraft. Normally a SBW aircraft shows a high wing configuration, with standard or T-Tail. The strut then connects the lower surface of the wing with the lower part of the fuselage.

Figure 2.3 shows a wing with the typical strut configuration. As it can be seen, it is not much different to the standard cantilever wing. The strut is located in the lower part of the wing, and connects it with the fuselage, at an angle that may vary depending on the design. Later this point will be discussed. On a different perspective, the cross section of the strut has a profile-like shape. This is done to minimize its drag impact as much as possible, and in some designs even to contribute to the lifting force or the controllability of the plane. This section design is limited by the compromise of having a strut strong enough to support the different loads during flight and the already mentioned drag efficient shape.

In addition, a great variety of configurations can be considered in the design of a SBW. Apart from the already mentioned biplane configuration, other designs such as struts over the wing instead of under it, or double strut among others can be seen nowadays in the airplanes that use this configuration.

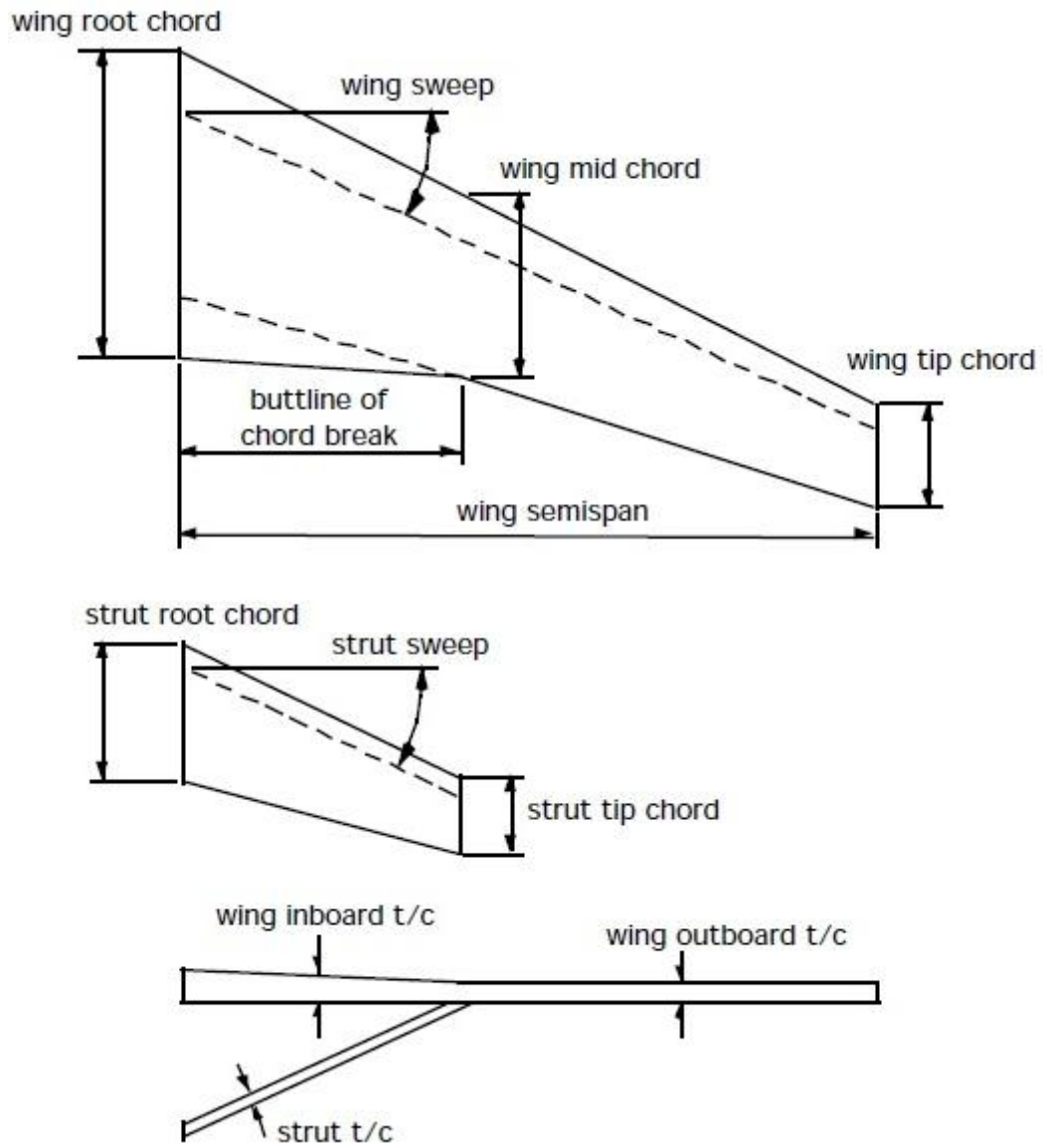


Figure 2.3 Typical strut configuration (Grasmeyer 1998)



Figure 2.4 Modified Fly Baby with top struts (FlyBaby 2013)

When it comes to the conceptual design of strut braced wing airplanes, many different configurations based on very different considerations come across. Two important factors are of vital importance when choosing a suitable strut for the aircraft: the interaction between the fuselage, the wing and the strut, and the capability of this last one to support the required loads. For the first one several aerodynamic studies have been conducted, such as **Ko 2002**, or **Grasmeyer 1998**.

About the capability of the strut to support loads, the most important consideration is to create a design that avoids buckling on the strut. The strut, when placed under the wing, usually supports traction loads, but there are few cases to consider in which the strut will be under compression loads. These are the $-1g$ case considered for certification purposes, and the taxi bump. Many solutions have been proposed, but the most common are hinged joints between the strut and body/fuselage, and telescopic sleeve. The hinged joints bring along an extra complication: by using them, the aerodynamic interactions become more complicated, and the additional drag due to the installation of the strut increases, so a detailed design is required. On the other hand, the telescopic sleeve is a promising device that “activates” the strut only when it has to support traction loads, so the buckling is not anymore a problem. The weight of such device and the parasite drag increase are its disadvantages. In addition, another proposed design to avoid the strut buckling is the arch shaped strut. This design makes the strut bend in a controlled way under compression loads, but stretches under traction loads, hence supporting them. This way, is it possible to say that the arch shaped strut “activates” the strut the same way the telescopic sleeve does. However, this design increases slightly the weight of the strut, so a further analysis is required. More designs combine the three possibilities mentioned above, like partially arched

struts in combination with hinges, or offsets in the wing-strut joint plus telescopic sleeve or, again, joints. Further information on this topic can be found on various studies conducted on the SBW, like **Carrier 2012**, **Gundlach 2000** and **Gern 2000**.

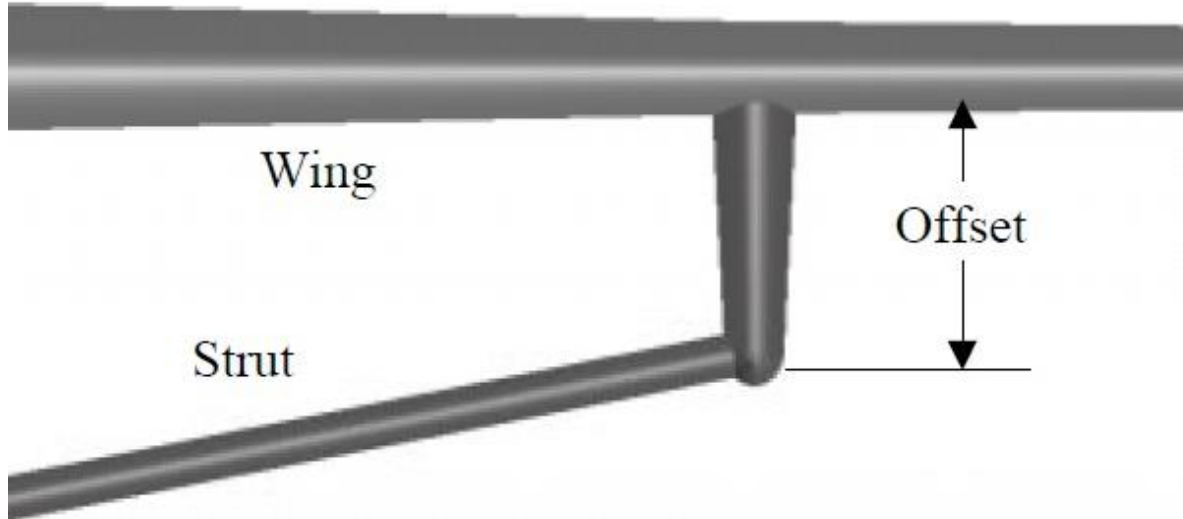


Figure 2.5 Wing-strut connection with offset (**Gundlach 1999**)

2.3 Advantages and Disadvantages of a SBW against Cantilever Wing

The use of a strut in order to design a SBW aircraft has several effects on the aircraft performance, with some positive outcomes, and some negative that have to be evaluated and optimized for the design.

The first effect when a strut is added to the wing is that it relieves some bending moment from the wing by carrying part of its load. This way the structure of the wing can reduce weight, since the structural complexity is smaller and lighter reinforcements in the wing box are required. Having a lighter wing means having a lighter aircraft, and the final result of it is lower fuel consumption, hence reducing the cash operating cost (COC) for the companies.

Using a lighter wing structure means that it is possible to build a bigger wing and keep the same weight. In this case, it is of interest to build higher aspect ratio wings. Having a higher aspect ratio wing has a positive impact in the lift to drag ratio (L/D), known also as *aerodynamic efficiency*. This ratio is very positively affected by the higher span, achieving increases up to 30 % in certain configurations compared to the current cantilever wing designs (**Grasmeyer 1998**). A higher lift to drag ratio reduces the induced drag produced by the wing, making the aircraft more fuel efficient.

In addition, adding struts makes possible to build wings with thinner profiles. Thinner profiles reduce significantly the wave drag that the wing produces, making it easier to fly at transonic

speeds, and thus again improving the fuel efficiency of the airplane. Moreover, thinner profiles combined with a reduction of the wing sweep allow natural laminar flow to be applied, which reduces also the zero-lift drag of the aircraft.

All the effects mentioned before have an important consequence: drag is significantly reduced, increasing the fuel efficiency of the aircraft. As mentioned before, this improve in fuel efficiency means that the aircraft requires less fuel for the same mission, having this a very positive impact in the cost of aircraft operation, which makes this configuration quite interesting for the airlines.

In fact, this improvement in fuel efficiency turns into the use of less fuel, which reduces the take off mass of the plane, amplifying the effect of the strut advantages. This is called *snowball effect*, for the resemblance with a snowball rolling down a hill. The snowball effect keeps increasing the advantages of the fuel efficiency increase to a certain point, and does not keep improving to the infinite.

However, adding a strut has also some disadvantages that must be taken into account when it comes to decide whether to use it or not. For instance, although the use of the strut significantly reduces the wing weight, it comes also with a weight penalty, for the strut has its own mass. Anyway, this penalty is not so big, but must be taken into account when designing a new wing. Furthermore, the strut addition comes along with a drag penalty mainly caused by the strut itself and the design of the joint between strut and fuselage/wing. This turn the design of this mentioned joint critical in further stages of the design process, and is convenient to adopt some of the configurations mentioned in the previous chapter.

Finally, it is important to say that the addition of a strut or a truss to support the wing may imply an increase in the aircraft price, as the manufactured parts are different than the standard cantilever wing ones. This can mean that the technology used to create them, especially when telescopic sleeves, hinges or any sort of arch shaped strut is used, can be different or new, so further consideration in this topic is needed, but the lack of real data on transonic strut braced aircraft makes it complicated to asses.

2.4 Bigger Span Considerations

It has been introduced in the previous chapter that the addition of struts to a standard cantilever wing allows it to increase to bigger span, and doing so increasing the lift-to-drag ratio (L/D), which comes with an important reduction of the induced drag produced by the wing, and hence increasing the fuel efficiency of the aircraft.

However, it is important to consider if a span increase is desirable or not. It seems clear that increasing the span will come eventually in a reduction of the cash operation cost of the aircraft, so, from a technical point of view, it is recommended to increase the span as much as possible,

or at least as much as the fuel efficiency increases with it. Still, there is another factor which has not been yet considered: the airport.

This Thesis is part of the *Airport2030* project, whose objective is the conceptual design of future aircraft that are more efficient from the airport point of view. That includes ground handling, noise, fuel consumption, etc.

In this section the focus will be set on the fact that adding a strut to the wing allows increasing the wing span, and thus increasing the aircraft efficiency. However, this has also an impact from the airport point of view. ICAO recommends a category system based on the landing field length, the wing span and the outer main gear wheel span.

Table 2.1 ICAO recommendations for aircraft classification (**COSCAP 1999**)

Code element 1		Code element 2		
Code number (1)	Aeroplane reference field length (2)	Code letter (3)	Wing span (4)	Outer main gear wheel span ^a (5)
1	Less than 800 m	A	Up to but not including 15 m	Up to but not including 4.5 m
2	800 m up to but not including 1 200 m	B	15 m up to but not including 24 m	4.5 m up to but not including 6 m
3	1 200 m up to but not including 1 800 m	C	24 m up to but not including 36 m	6 m up to but not including 9 m
4	1 800 m and over	D	36 m up to but not including 52 m	9 m up to but not including 14 m
		E	52 m up to but not including 65 m	9 m up to but not including 14 m
		F	65m up to but not including 80m	14m up to but not including 16m

a. Distance between the outside edges of the main gear wheels.

Nowadays, the Aviation Authorities like the American Federal Aviation Administration (FAA), or the European Aviation Safety Agency (EASA) as well as the Joint Aviation Authority (JAA) have adopted ICAO's recommendations for aircraft classification. For example, on Table 2.2 is it shown the system by FAA, which is similar to ICAO's:

Table 2.2 FAA Aircraft Design Group classification used in airport geometric design

Design Group	Wingspan (ft)	Example Aircraft
I	< 49	Cessna 152-210, Beechcraft A36
II	49 - 78	Saab 2000, EMB-120, Saab 340, Canadair RJ-100
III	79 - 117	Boeing 737, MD-80, Airbus A-320
IV	118 - 170	Boeing 757, Boeing 767, Airbus A-300
V	171 - 213	Boeing 747, Boeing 777, MD-11, Airbus A-340
VI	214 - 262	A3XX-200 or VLCA (planned)

As it can be seen, Boeing 737 and Airbus A320 belong to Category III, which is equivalent to ICAO Category C. This is a very important fact, for those mentioned aircraft are the most common in the current times. This is not a coincidence: most airports are designed with this category in mind, and thus they have most of their parking positions designed for this category. Airport limitations must be considered when designing a SBW Aircraft. The span increase can be very beneficial for the efficiency of the aircraft and, indeed, many aircraft designers tend to increase it as much as possible. The problem appears when the airport category comes into consideration. As mentioned before, most of the airports are intended mostly for Category C, and this way the airlines are interested on buying aircraft that fit into that category. If the airplane fits in a bigger category, less space for it is available in the airport. This can increase the airport time (which could reduce its utilization), or force the plane to park in a remote position, which delays ground handling and it is uncomfortable for the passenger, since they have to take a shuttle bus to reach the vessel.

This way, despite increasing the aircraft span can be useful; the desired category must be taken into account. It must be considered whether is worth to fit into the desired category with the penalty of being less efficient, or it is better to choose aircraft efficiency over all and sacrifice the number of airports on which is possible to land, and the space in those.

Another solution would be the research of different means that allow increasing the aspect ratio without incrementing the category. On one hand, for example, companies try to get permission from the airport authorities to slightly increase the span, i.e. to reduce the minimum distance between adjacent aircraft. Other possible solution would be the redesign of the parking places at the airport to a new shape on which is easier to park bigger span aircraft. This redesign would not need building works on the airport, just repainting the parking place lines for the new and more efficient shape.

On the other hand, alternative means to achieve the span increase while sticking to the same category are technical means. Here the creativity of the engineers plays an important role, as well as the technology available at the moment of the design. Nowadays, a much extended solution is the use of winglets. Winglets are, in a rough description, an “extension” of the wings, which is folded normally upwards, and by means of the *end plate effect* lets the effective span grow higher.

Finally, the use of a folding wing system is considered in this Thesis. This system will allow the pilot to fold the wing, once the plane is on the ground, reducing the aircraft span to an extent that fits in the desired category. It has been included in the OPerA tool the possibility of adding this system to the aircraft optimizations, evaluating its impact on the vehicle mass and efficiency.

These systems have been designed taking into account that most of the world airports are built with category C in mind, so designing a bigger category airplane is pointless if this aircraft is intended to be an alternative to the Boeing B737 and the Airbus A320. Both A320 and B737 are category C aircraft, so, in order to compete with them and not with bigger planes in both the Boeing and Airbus families, a category C airplane must be designed. Besides, to accommodate the new airplane in all the future airports, if having a bigger category, it would force them to build new infrastructures to hold these planes in bigger numbers.

3 Overview of OPerA

3.1 OPerA Concept

The preliminary design of an aircraft requires the union of several areas of the aeronautic knowledge, as well as the use of many equations deeply interacting one with each other. The designers that approach design process in a manual way must have deep and clear knowledge of all those branches, and an exceptional calculus and understanding ability for the implied expressions and its interactions. This, in practice, is impossible or requires an exaggerated amount of work. For that reason many different methods are created, with the objective of simplifying the task or even bringing the possibility to solve problems that cannot be solved in a different way. Thus many authors developed their own methods for preliminary aircraft design, such as **Torenbeek 1992** or **Roskam 1989**, allowing the systematic calculation of all necessary parameters to achieve proper designs. These methods have been widely used for long time, and they are still valid. However, nowadays exists an increasing concern for obtaining planes that are as cheap as possible, which the smallest fuel consumption or with very specific features. Is in this purpose where optimization takes its place. Optimization not only aims to obtain a valid parameter combination that matches the design requirement, but it aims to obtain the best parameter combination under certain conditions, such as lowest cost or highest range.

Optimize consists on indentify a series of variable parameters, namely *design parameters*, and look for a certain combination of them in order to maximize o minimize a specific function, called the *target function*. A typical example of this is the problem of achieving the maximum area with a fixed perimeter. This problem would be solved by considering the many different shapes that the perimeter can take, and for each one of them identify the parameters from which the area depends (like the length of the sides in a rectangle), and find the combination that brings the biggest area. Then, the best results for each considered shape must be compared, and thus choose the largest one. As soon as this is done, optimization has been completed.

This example was a very simple optimization, and this one can be easily made in a manual way. However, not all the optimizations can be performed so easily, or even manually. Some of them require the use of many simplifications that make them affordable for manual calculation, with the penalty of losing accuracy, or missing possible solutions. That is the reason why computer assisted optimization started. In order to solve complicated problems, or solve the simple one in a faster and even more accurate way, a computer program or algorithm can be used. Computer programs calculate and evaluate the possible solutions, taking the best and presenting it to the user. This way, different programs that allow to not only design but also to optimize results and solutions are created. Of course, many programs exist for this task in aircraft design, and in this group is where OPerA is found.

OPerA (Optimization in Preliminary Aircraft Design) is tool that joins the possibility of preliminary design aircraft with the optimization of these designs, in an automated way that is

also simple for the user (especially after the interface improvements added during this Master Thesis). It was designed by Michaela Nita (**Nita 2012**) in the framework her PhD Thesis. OPerA is a Microsoft Excel based tool because it is used worldwide, it is easy to control equations and edit them, and because the program is transparent and all the processes taking part into it can be easily followed, like parameter interaction. Another reason for choosing MS Excel is because this program integrates VBA (Visual Basic for Applications) programming and can interact with external programs that are able to execute many specific optimization tasks, such as *Optimus*®, created by **Noesis Solutions**, which has already fully support in OPerA.

OPerA is part of a tool suite created in the Aircraft Design and Systems Group (AERO) from the Hamburg University of Applied Sciences (HAW Hamburg), in the frame of *Airport2030* project. The tool consists of three different levels of design, from the simplest to the most complex, and each level has its own program.

The first level corresponds to SAS (Simple Aircraft Sizing). This is the most basic level, based on the method that can be found in the lecture notes of Professor Dieter Scholz (**Scholz 1999**). The program allows the user to find a suitable design point in a matching chart that is obtained after fixing five different requirements (see section 3.2.1). It is possible to use it for simple aircraft optimization, though this must be done manually, and this task requires deep knowledge of the subject and understanding of the whole process. This tool has been used by students for 10 years, and it has proved its educational value. Currently, many changes are being prepared for the tool, such as a version that is suitable for designing prop fan aircraft, or an optimization algorithm that is being implemented in the tool.

However, SAS just makes a very simple and rough design, and it only has to be taken as the beginning of a new design. For further design, a different program must be used. This program is OPerA, which is found in the second level of the tool suite. OPerA follows the philosophy of SAS and it is as well based in the method found in **Scholz 1999**, but it takes a step beyond. OPerA is able to obtain complete preliminary aircraft designs, equally from the same 5 requisites as SAS, and, in addition, it can optimize the design parameters in order to maximize or minimize any of the target functions included within the program. In order to do so, OPerA can use an external program, such as *Optimus*, or can use its own integrated algorithm, which is based in a technique named *Differential Evolution* to achieve the optimum.

Finally, in the last level of the tool suite PreSTo is found. PreSTo stands for Preliminary Sizing Tool, and allows the user to not only perform preliminary design, but also to dive in conceptual design. The tool, still in development in the AERO group, is modular-based. This means that the tool features many modules, each one of them taking care of a different step in the aircraft design process. PreSTo allows only manual optimization if the different configurations, but it can be connected to diverse external tools for aircraft design, so it can take advantage of their features, like FEM analysis or CFD simulations, as well as many different optimizers. This characteristic makes OPerA a perfect starting point for PreSTo, since the design data coming from OPerA is already optimized, and thus they can be used to perform a complete conceptual design in PreSTo in an easier way that requires less iteration, or even just one.

3.2 Methodology in OPerA

OPerA uses a method based on the lecture notes of Professor Dieter Scholz, supervisor of this Master Thesis (**Scholz 1999**). This method will be here briefly reviewed, and can be fully consulted in the mentioned lecture notes, as well as in **Nita 2012**.

As previously said, the method used in OPerA has a series of requisites as starting point, just like any other method. These requisites are combined with the chosen design parameters in order to perform the preliminary design of a complete airplane. The parameter combination can be varied in order to optimize the results, searching objectives such as minimum cost expenses, minimum take-off mass or minimum fuel consumption. Some of the requisites can be varied as well, for the sake of the optimization, and when there is a good reason to do it (for example, flying slower to spend less fuel).

The parameters and requisites used in OPerA will be summarized in the following section.

3.2.1 Requisites in OPerA

Every design starts from a set of requisites. Requisites are basically the reason to perform a new design. Every time that a new mission needs to be accomplished, a new design must be used, or an adaptation of a previous design, which is, in essence, a new design process. Requisites are the parameters that define this mission. When the design is able to meet those goals, then it is said that the design is finished and operational. Every mission has numerous design possibilities that can fit in the requirements. However, some of them can be better in some areas in which others are not, and vice versa. For that reason, is it possible also to set new additional evaluation systems that classify the different designs into better designs and worse designs. This is the mission of optimization.

In the field of aircraft design, the main goal requirements are the payload (m_{PL}) and the range (R), i.e. the amount of passengers or cargo that must be transported and the distance to which the payload is transported.

These requirements are fixed and known, for they define the designed airplane. However there are additional requirements and these can be subject to optimization. For example: the cruise Mach number (M_C) or the take-off and landing field lengths (S_{TOFL} and S_{LFL} , respectively). These two lengths are requisites imposed by the airport, and they are not fixed, but limited. Those requisites are used in OPerA to generate a Matching Chart, along with the climb gradients for the Second Segment Climb maneuver and Missed Approach maneuver. This Matching Chart plots all the requirements together and allows an easy visualization of the design space and the design window.

In the next section the way in which OPerA works with these requirements will be explained.

3.2.1.1 Airport Runway Lengths

The first requirement used in the OPerA Matching Chart comes from the airports. Airport field lengths are limited, and an airplane must be able to take off and land in as many as possible. The ICAO classification system (Table 2.1) defines certain runway lengths to separate the different categories. This way, all airplanes in a certain category must be able to take off and land within a certain runway length. Conversely, when designing runways for an airport, this category system tells the designer how long must the runway be in order to be able to operate with the selected category. For example, an airport intended to operate with Class D aircraft must have at least one runway 1800m long. Nowadays airports have longer runways than those, for they are intended to hold the biggest categories as well as the small ones. In order to use this requisite, both the take off field length and landing field length must be introduced as an input in OPerA.

On one hand, the landing requirement can be expressed in terms of the landing field distance (S_{LFL}) or the landing approach speed (V_{APP}). The expression that relates both is:

$$V_{APP} = k_{APP} \cdot \sqrt{S_{LFL}} \quad (3.1)$$

Where the factor that relates both terms, k_{APP} , is obtained from statistical data and is influenced by the braking capacity of the aircraft. Currently OPerA uses the value $k_{APP} = 1.86 [(m/s^2)^{0.5}]$. In addition, from the Flight Mechanics for landing the following expression is obtained:

$$m_{ML} \cdot g = \frac{1}{2} \cdot \rho \cdot V_{APP}^2 \cdot S_W \cdot C_{L,max,L} \quad (3.2)$$

And, reordering the terms and adding expression (3.1), it is:

$$\frac{m_{ML}}{S_W} = \frac{1}{2g} \cdot \rho_0 \cdot k_{APP}^2 \cdot \sigma \cdot C_{L,max,L} \cdot S_{LFL} \quad (3.3)$$

Finally, combining all the constants together into a new one called k_T , it yields:

$$\begin{aligned} \frac{m_{ML}}{S_W} &= k_L \cdot \sigma \cdot C_{L,max,L} \cdot S_{LFL} \\ k_L &= 0.036957 \cdot k_{APP}^2 \end{aligned} \quad (3.4)$$

To meet the requirement, wing loading must not be exceeded. Introducing m_{MTO} in (3.4) and reorganizing terms:

$$\frac{m_{MTO}}{S_W} \leq \frac{k_L \cdot \sigma \cdot C_{L,max,L} \cdot S_{LFL}}{m_{ML}/m_{MTO}} \quad (3.5)$$

Equation (3.5) represents the first limit line that OPerA will plot in the Matching Chart, and introduces m_{ML}/m_{MTO} , and $C_{L,max,L}$, which are design parameters.

On the other hand, take off distance is the other requirement imposed by the airport characteristics. Following a similar process to obtain the landing field length limit equation (3.5), the following question for takeoff is derived:

$$\frac{T_{TO}/(m_{MTO} \cdot g)}{m_{MTO}/S_W} \geq \frac{k_{TO}}{s_{TOFL} \cdot \sigma \cdot C_{L,max,TO}} \quad (3.6)$$

In this equation (3.6) another statistical factor is included: k_{TO} . This factor has currently a value in OPerA of $k_{TO} = 2.3216 \text{ m}^3/\text{kg}$. $C_{L,max,TO}$ is another design parameter, and it is related with $C_{L,max,L}$. Normally, $C_{L,max,TO} \cong 0.8C_{L,max,L}$. This equation represents the second line plotted in the Matching Chart.

3.2.1.2 Second Segment and Missed Approach Climb Gradients

According to certification rules FAR25 and CS25, an airplane must be able to achieve a certain climb angle when performing the second segment climb and the missed approach maneuver.

For the second segment climb maneuver, the Flight Mechanics equations for climb are taken:

$$\begin{aligned} T &= D + m \cdot g \cdot \sin\gamma \\ L &= m \cdot g \cdot \cos\gamma \cong m \cdot g \end{aligned} \quad (3.7)$$

Combining both we get to:

$$\frac{T}{m \cdot g} = \frac{1}{L/D} + \sin\gamma \quad (3.8)$$

And adapting the equation to one engine failure, it gets to:

$$\frac{T_{TO}}{m_{MTO} \cdot g} \geq \left(\frac{n_E}{n_E - 1} \right) \cdot \left(\frac{1}{E_{TO}} + \sin\gamma \right) \quad (3.9)$$

Where E_{TO} is the lift-to-drag ratio for takeoff and n_E the number of engines. This last number is as well a design parameter.

Operations are done in the same way to get the equation for the missed approach:

$$\frac{T_{TO}}{m_{MTO} \cdot g} \geq \left(\frac{n_E}{n_E - 1} \right) \cdot \left(\frac{1}{E_{TL}} + \sin\gamma \right) \cdot \frac{m_{ML}}{m_{MTO}} \quad (3.10)$$

In which E_L is the lift-to-drag ratio for landing.

Both E_{TO} and E_L are estimated through many other parameters, being aspect ratio AR, the parasite drag $C_{D,0}$ and the Oswald factor e the most important of them. The simple preliminary

design uses statistical values of the Oswald factor in this part of the process, normally $e = 0.7$. However, given the iterative structure of the tool, OPerA allows the user to choose between different ways to estimate it, from simple statistical values, to more accurate methods that estimate E in a more exact way.

Equations (3.9) and (3.10) represent two more curves in the Matching Chart, and thus opera plots them in the appropriate module.

3.2.1.3 Cruise Mach Number

The last requisite for the Matching Chart is the intended cruise Mach number. This parameter represents the speed at which the airplane is designed to fly in the cruise phase, and it is not the maximum speed that the vessel can achieve. To express it in the same terms as the other requirements, i.e. in terms of wing loading to the takeoff mass and thrust to weight ratio, the equations for cruise flight are used. These are:

$$T_{CR} = D_{CR} \quad (3.11a)$$

$$L = W \quad (3.11b)$$

Dividing the second equation in (3.11) by D it comes to:

$$D = \frac{W}{L/D} \cong \frac{m_{MTO} \cdot g}{L/D} \quad (3.12)$$

Taking (3.12) into the first equation of (3.11) and dividing by T_{TO} :

$$\frac{T_{TO}}{m_{MTO} \cdot g} = \frac{1}{(T_{CR}/T_{TO}) \cdot E} \quad (3.13)$$

T_{CR}/T_{TO} is obtained from Scholz approximation (**Scholz 1999**):

$$\frac{T_{CR}}{T_{TO}} = (0.0013BPR - 0.0397) \cdot \frac{1}{km} \cdot h_{CR} - 0.0248BCR + 0.7125 \quad (3.14)$$

Equation (3.14) is a function of the cruise altitude h_{CR} , so (3.13) is then function of E and h_{CR} . In addition, taking the second member from (3.11) the wing loading m_{MTO}/S_W , and setting it as a function of the altitude:

$$\frac{m_{MTO}}{S_W} = \frac{C_L \cdot M_{CR}^2}{g} \cdot \frac{\gamma}{2} \cdot p(h) \quad (3.15)$$

Where M_{CR} is the cruise Mach number, γ is the ratio of specific heats and $p(h)$ is the air pressure as a function of the altitude.

With equations (3.13) and (3.15) OPerA calculates the thrust to weight ratio and the wing loading for a certain number of altitudes, obtaining thus the curve plotted in the Matching Chart.

3.2.2 Design Parameters in OPerA

In the previous section was explained which are the main requisites in OPerA, and how the tool plots the Matching Chart to represent them and select the design point. The design requirements are, as already mentioned, the parameters that define the design and set the goal to achieve for the design. However, the requirements are not the only input in the tool. The requirements themselves define only the design window, but they do not define all the characteristics of the airplane. The parameters that fully define the aircraft and make a difference between designs for the same requirements are the design parameters.

The design parameters are introduced in the tool at the same time as the requirements, and thus OPerA does all the calculations automatically. Varying parameters is the way the explore the design space in order to find the design that delivers the best results such as low cost or low fuel consumption. These parameters are divided in OPerA in two groups: airframe parameters and cabin parameters.

Airframe parameters are:

- Maximum lift coefficients for takeoff and landing: $C_{L,max,TO}$ and $C_{L,max,L}$
- Aspect ratio: AR
- Maximum landing mass to maximum takeoff mass ratio: $\frac{m_{ML}}{m_{MTO}}$
- Number of engines: n_E
- Sweep angle of the 25 % chord line: φ_{25}
- Taper ratio: λ
- Relative distance between engine and wing: $\frac{h_P}{D_N}$
- By-pass ratio: BPR
- Relative height of the horizontal tail surface (if cruciform configuration is selected): $\frac{z_h}{b_v}$
- Relative distance on engines to fuselage end (for fuselage mounted engines): $d_{ENG,F}$
- Relative position of the main landing gear along the fuselage (when the MLG is chosen to be mounted in the fuselage): d_{MLG}

Cabin parameters are:

- Seat abreast: n_{SA}
- Seat pitch: SP

- Aisle width: w_{AISLE}
- Seat width: w_{SEAT}
- Armrest width: $w_{ARMREST}$
- Side clearance: $s_{CLEARANCE}$

3.2.3 Matching Chart

Once all the requisites are already analyzed, OPerA represents them on a Matching Chart. This Matching Chart is very useful because it lets the user to check in a visual way the design space and appreciate the design window where the design point can be located. In a manual design process, the design point is selected by the user after plotting all the requisites, such that meets the preferences of the designer. An optimum design will have the lowest thrust to weight ratio possible and the highest wing loading, in that order. OPerA does this in a totally automatic way, offering always the best design point for each parameter and requisite combination. An example of Matching Chart is shown in Figure 3.1. It is possible to appreciate the different lines corresponding to the different requirements, the design window and the optimal design point.

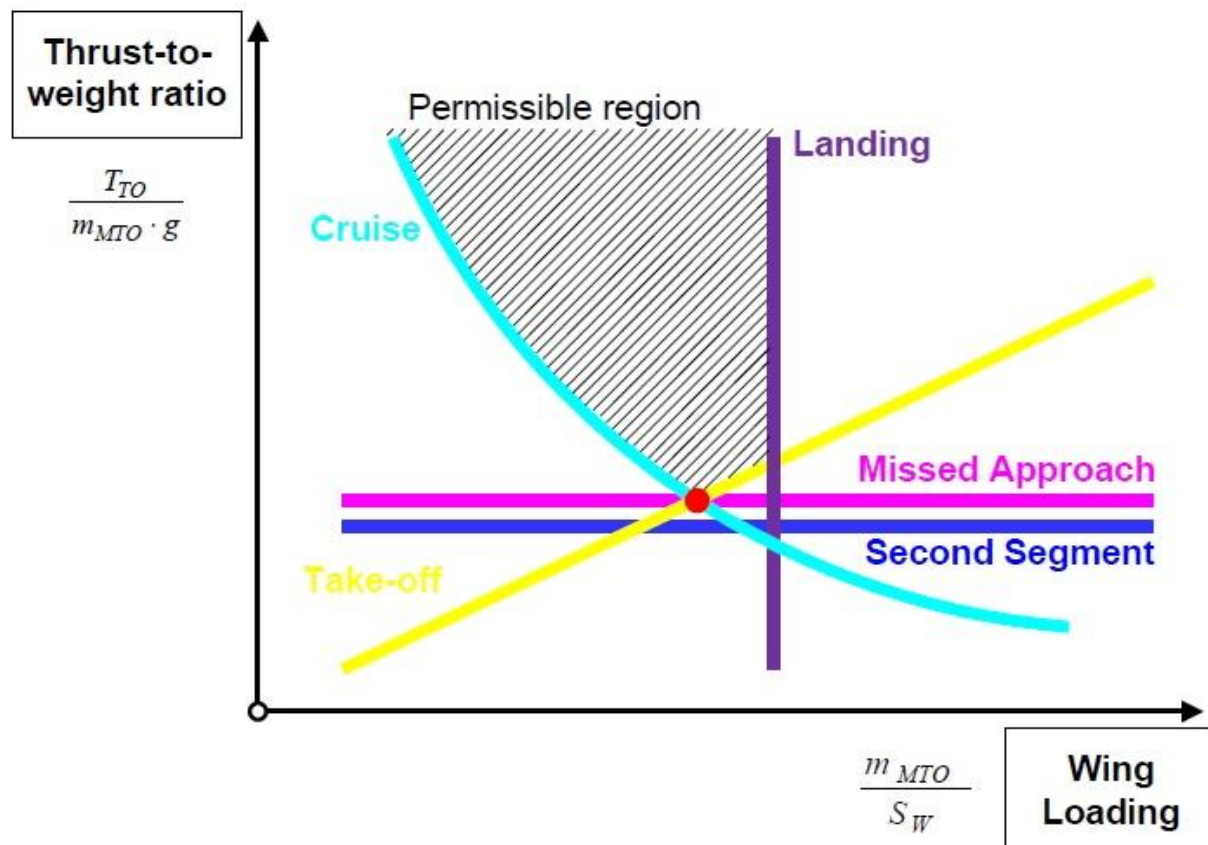


Figure 3.1 Example of a Matching Chart delivered by OPerA (Nita 2012)

Once this step is completed, what the user sees on the screen is a full preliminary design already optimized for the combination of requirements and parameters that were input in the program. This design can be further complete into concept design phase, with tools such as PreSTo.

3.3 Overview of the Tool

OPerA is a tool developed in Excel. Its goal is to support designers in the task of performing preliminary aircraft design. The program automates this task, making the use of the tool and thus the preliminary design process easier. Apart from this *inner optimization*, OPerA also optimizes the design parameters input and even the requirements. This process is called *formal optimization*. All this process is performed in a totally traceable design environment, which has the advantage for the user that all the steps of the process can be easily followed and understood, as well as editing the different equations and design factors.

OPerA looks like any other Excel sheet, as it is possible to see in Figure 3.2. This figure shows the Optimization Set up module, where the user configures the aircraft and inputs the parameters and requirements.

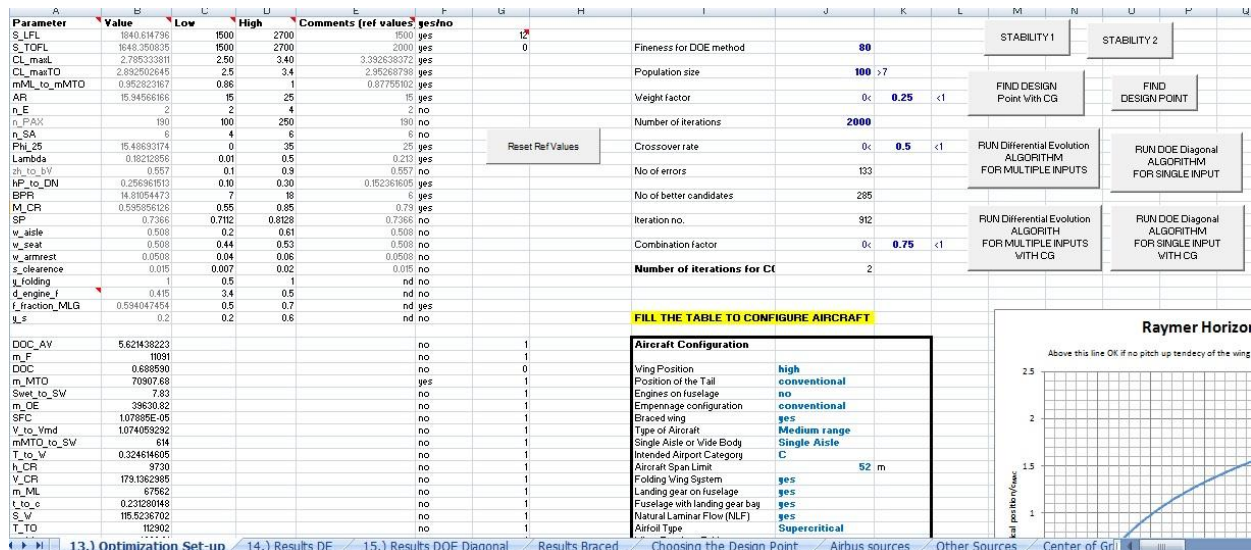


Figure 3.2 OPerA Layout (screenshot)

A description of the tool and its use will be presented in this section. A more detailed description is available in (Nita 2012).

A scheme of the tool organization is shown in Figure 3.3. Two different areas can be appreciated: On one hand, the *inner optimization* area. This area includes all the modules (or tabs in Excel) that take part in the design point determination. On the other hand, the *formal optimization* area includes the first area and includes also the requisites and the module that estimates the aircraft cost and the added values. The optimization of the different designs is performed through the variation of the parameters that come from the input in this area, and the requirements when needed. Finally, acting as input and output respectively, the design parameter box (List of Input Parameters) and the different result sheets, either for single parameter optimization and multiple parameter optimization.

The List of Input Parameters brings two different kinds of parameters into the *formal optimization* area: the *input parameters* and the *experience based parameters*. The first are marked in bold blue within the different modules of the tool, and are the parameters subject to variations during the optimization process. The second group are the values marked with like blue, and are, as their name suggests, factors obtained from experience or statistics, such like the approach and landing factors mentioned in section 3.2.1.1.

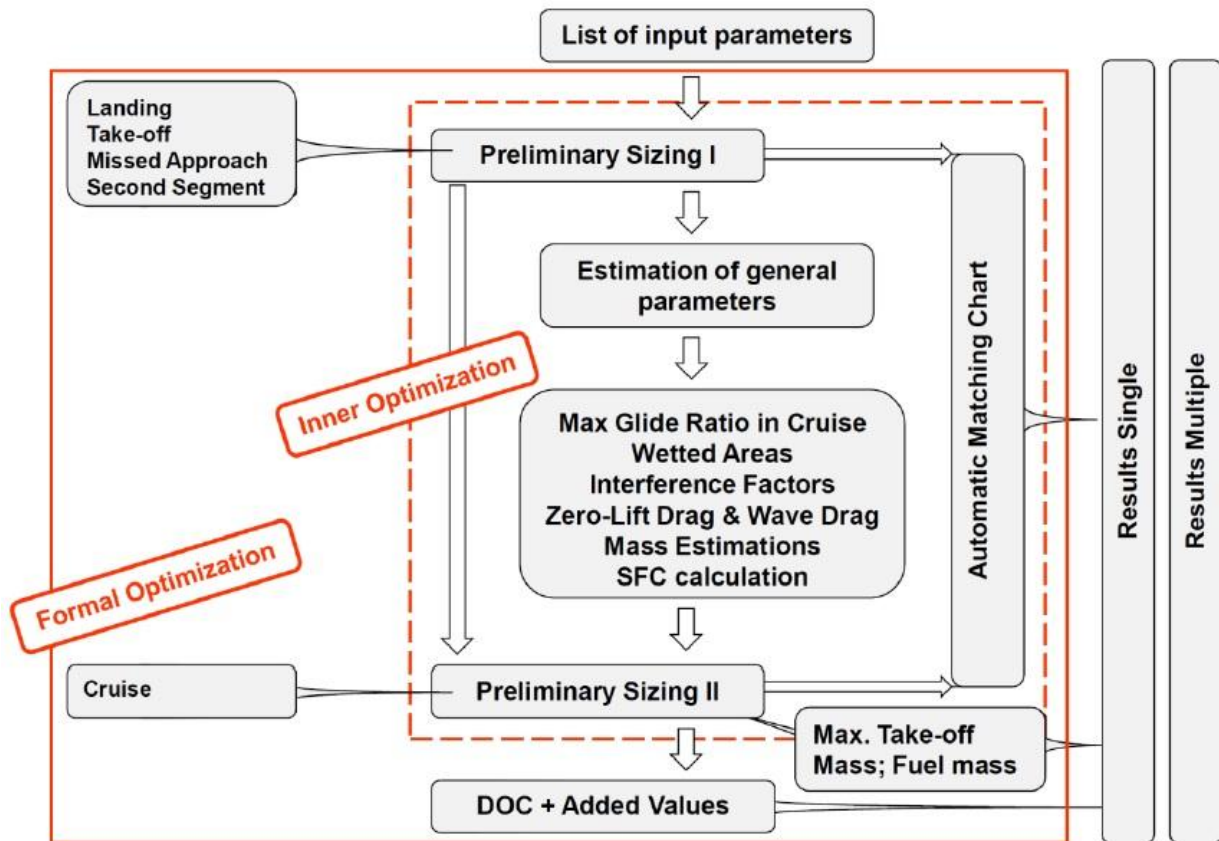


Figure 3.3 Scheme of the structure of OPerA (Nita 2012)

In order to facilitate the identification of the different parameters and factors, a tab in OPerA exists that summarizes the List of Input Parameters.

3.3.1 Modules Description

This section will shortly describe the different modules included in the tool, briefly detailing their mission and possibilities. The names referred here will be the same included in the program tabs.

- *Input parameters* is, as already said, a tab that summarizes all the parameters used by the tool, both the input variables and the experience based factors.

- *Estimation of General Parameters*: In this module every basic parameter is calculated so they can be used by the other modules. Here are performed the calculations that define the geometry of the wing, tail, fuselage, etc, as well as many cabin parameters.
- *Preliminary Sizing I*: In this module the first four lines for the Matching Chart are calculated, namely *Landing*, *Takeoff*, *Second Segment* and *Missed Approach*.
- *Max Glide Ratio in Cruise*: This module is responsible of calculating the Oswald factor of the wing and the maximum cruise lift-to-drag ratio. To obtain this last one, many methods are available for user choice. The methods vary from complexity: the simplest ones use only statistical values, and the most complex ones calculate each parameter involved in E_{MAX} calculation. Logically, the most complex methods deliver better results, but they require more time to perform calculations.
- *Wetted Areas Estimation*: Here the geometrical parameters obtained in *Estimation of General Parameters* are used to estimate the size of the wetted areas of all the components of the aircraft. These results will be later used for the calculation of the zero lift drag.
- *Interference factors* calculates the remain parameters needed to calculate the drag of every component of the aircraft.
- *Complete Drag Estimation*: Here the results from *Estimation of General Parameters*, *Wetted Areas Estimation* and *Interference factors* are used to calculate the zero lift drag $C_{D,0}$, which is necessary to estimate the maximum lift-to-drag ratio in some of the methods in the corresponding module.
- *Mass estimations*: This module computes the mass of the different components of the aircraft that, once added together, form the Operating Empty Weight (OEW) of the airplane. These estimations are performed following the method written by Torenbeek (**Torenbeek 2006**, **Scholz 1999**, **Nita 2012**). For the landing gear mass, the method from the German *Luftfahrttechnisches Handbuch* (**LTH 2008**, **Nita 2012**), and the engine mass from Hermann (**Herrmann 2010**, **Nita 2012**). For the wing mass increase due to the use of a folding wing system –a feature added within this Project-, the method produced by Yarygina (**Yarygina 2012**), with some own modifications is used.
- *SFC Calculation* uses the equations from Hermann to obtain the specific fuel consumption and some other engine parameters. This particular method was used due to the importance given to the engine by-pass-ratio, one of the design parameters in OPerA.
- *Preliminary Sizing II* calculates the last requirement curve for the Matching Chart. It also gathers together all the data from the other curves and checks if some of the results are out of the implemented constraints.

- *Matching Chart*: This module takes the results produced by *Preliminary Sizing I&II*, and plots them in the already mentioned Matching Chart.
- *DOC*: This is the module where every calculation regarding of the aircraft cost is performed. Initially this operations were done using the method from Scholz (**Scholz 1999**), but as part of this project, a new cost method has been added. This method is the method developed in the Technical University of Berlin (**TUB 2013**) and is available as a user option. In addition, both methods are adapted so they can derive both Direct Operating Cost (DOC) and Cash Operating Cost (COC) being once more a user option. This module also performs the fuel price estimation necessary for the cost calculation when designing future aircraft, another feature added for this Thesis.
- *Added Values* calculates every parameter that means added value for the aircraft. The method used here is fully described in **Nita 2012**, and consist on a value assignation to every airplane feature based on a statistic study of the value that different professionals of the aeronautical industry, pilots and customers give to them. Aspects like seat commodity or aircraft control are here taken into account. The aircraft obtains a score from zero to ten as an indication of the attractiveness of the design for the potential customers.
- *Optimization Set up*: This module is where the user will spend most of his OPerA time. This module is basically the control console of OPerA. Here the design parameters can be set, as well as the requirements and the boundaries for their variation. Every optimization can be started from this module, both mono parameter and multi parameter. The last version also permits the user to fully configure the aircraft from here, in an attempt of making OPerA much more user friendly and easy to use. Finally, this module is also the gate that the tool uses to communicate with external programs such as *Optimus*®.
- *Results DE and Results DOE* gather the results obtained from the DE and DOE optimizations, respectively. In these modules all the steps of the optimizations can be consulted and use for the design process. There is an extra sheet, called *Results braced*, that contains the results obtained by the creator of the tool on the strut braced wing aircraft. However, those results cannot be compared anymore with new results, due to the many changes done to the tool.
- *Choosing the Design Point* is a module that OPerA uses when calculating the design point using the SOLVER Add-In of Excel. The user will normally not need to be here.
- *Airbus Sources and Other Sources* is a complete collection of every statistical and experimental data used in OPerA, with their sources properly indicated.
- *Center of Gravity* is a new module added for this Thesis. This module expands the OPerA designing capacity by letting the tool estimate the position of the mass center of the plane. This module has proved to have a significant impact in the calculation results, and thus the

optimization results obtained with the new version of the tool cannot be compared with previous results (like the ones included in the module *Results Braced*).

3.3.2 VBA Optimization in OPerA

The most interesting feature in OPerA is its capacity to perform a complete optimization of the design parameter. This way is it possible to optimize the aircraft for a certain objective function, such as COC or DOC to obtain the minimum cost, or the fuel mass to achieve an aircraft with very low fuel consumption. In order to do so, OPerA offers the user two different alternatives.

On one hand, OPerA lets the user to connect it with an external optimization software, such as *Optimus*®, from **Noesis Solutions**, which is already fully supported by OPerA. This program offers multiple algorithms to calculate optimum solutions, such as *gradient based algorithms* or *evolutionary algorithms*. The advantage that this alternative offers is that using a program specific for optimizing offers more choices for the user, and is more configurable. Besides, optimizer software can obtain optimum results faster than the built-in code of OPerA. However, using an external optimizer needs the user to learn how to work with another software, which takes learning time, as well as obtaining a license for it. These advantages and disadvantages must be taken into account when choosing the use of an external optimizer. In the case of choosing *Optimus*®, **Nita 2012** includes complete instructions to connect it with OPerA.

On the other hand, the user has the option to use the optimization algorithm included with OPerA. This way, the tool itself becomes a completely independent optimizer. OPerA offer two different kinds of optimization: *single parameter optimization* and *multiple parameter optimizations*.

3.3.2.1 Single Parameter Optimization

Single parameter optimization in OPerA is quite simple. OPerA uses an algorithm called *DOE Diagonal*. DOE stands for “Design of Experiments”, a mathematical methodology that aims to get maximum possible information of the behaviour of the variables within the design space. The algorithm implemented in OPerA works only for single parameter optimizations: the code travels through the chosen boundaries of the selected variable, obtaining results for each experiment, and plotting them together so they can be easily read and interpreted. The user can choose the variable to optimize, as well as its boundaries and the fineness ratio. The fineness ratio is the number of experiments that will take place within the boundaries of the varied design parameter.

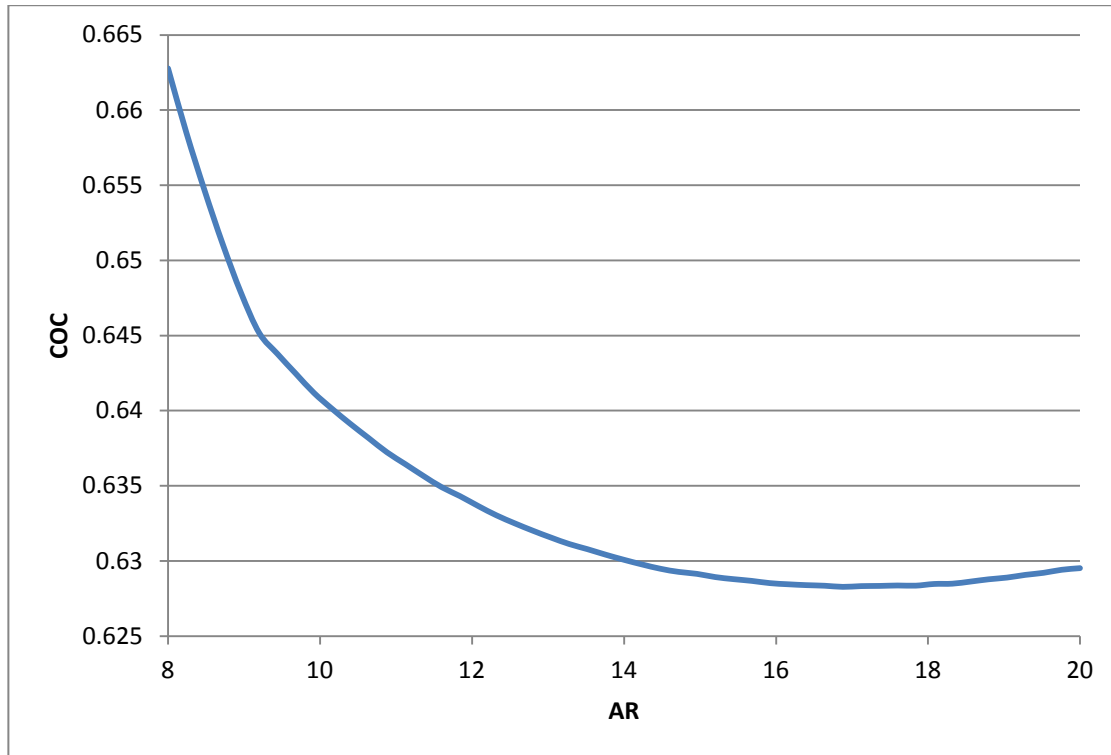


Figure 3.4 Example of DOE result obtained with OPerA

3.3.2.2 Multiple Parameter Optimization

The other optimization alternative included in OPerA is the multiple parameter optimization. In OPerA, this is done by means of an algorithm called *Differential Evolution*. This algorithm belongs to a group of optimization methods called *Evolutionary Algorithms*. The idea under the method of these algorithms is simple: When the optimization process starts, a population of different parameters is created. These population members are called parents, and during the process they change “evolving” towards the optimum. The OPerA algorithm, *Differential Evolution* (DE), was developed first by Price and Storm (**Price 1997**) and afterwards improved to adapt it to multiple objective optimizations. The algorithm operation is based on an iterative process for searching candidates, similar the one pictured in Figure 3.5.

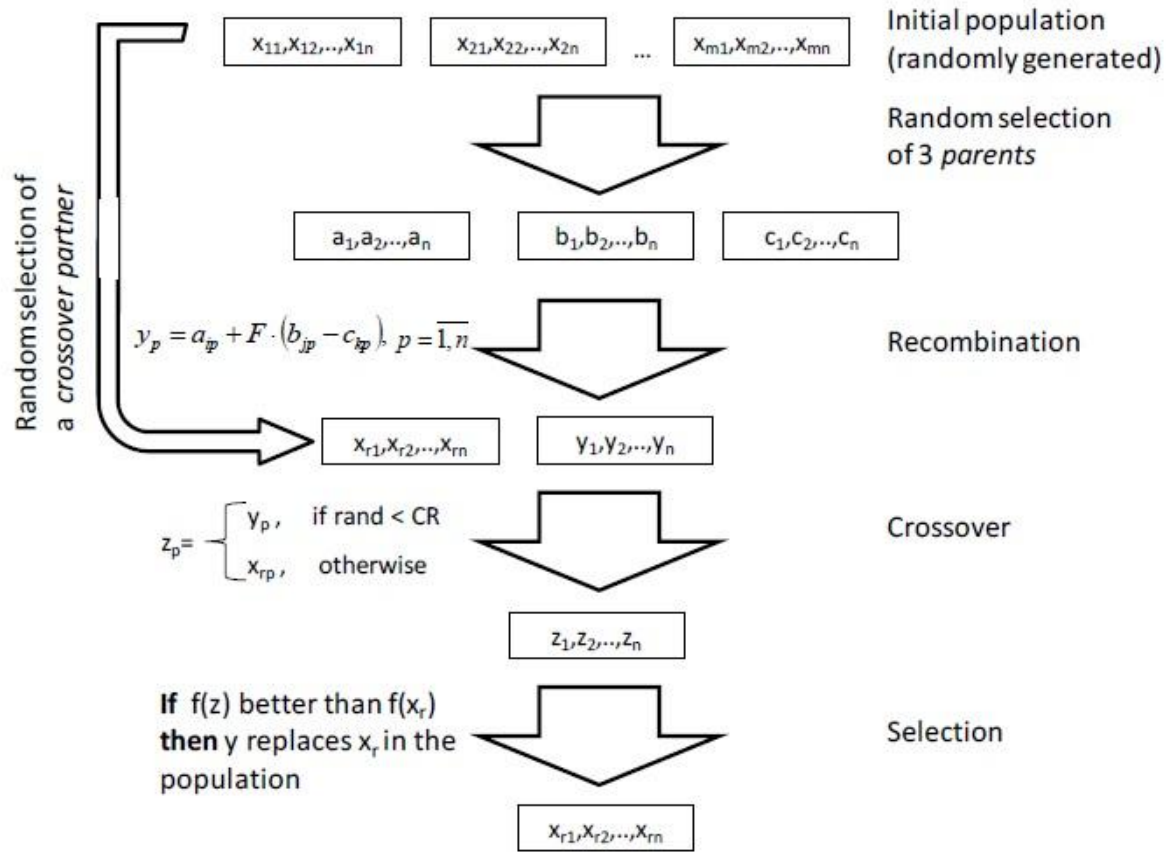


Figure 3.5 Scheme of a standard DE algorithm (Nita 2012)

The detailed process performed by the algorithm is the following:

- The first step consists of the identification of the design parameters that are going to be evaluated and their corresponding variation intervals, along with the objective function. With this data, the program generates a random population of parents. The population size is chosen by the user; although it should in any case be lower than 7. Recommended size is at least 5 times the number of free design parameters.
- Once the parent population is defined, the tool takes 4 random members of the population. One of them (\bar{X}_k , the crossover parent) will be subject of mutation, while the other three (\bar{A}_k , \bar{B}_k and \bar{C}_k) are used to create the trial vector \bar{Y}_k :

$$\bar{Y}_k = \bar{A}_k + F \cdot (\bar{B}_k - \bar{C}_k) + KF \cdot (\bar{M}_k + \bar{A}_k) \quad (3.16a)$$

$$y_i = a_i + F \cdot (b_i + c_i) + KF \cdot (m_i - a_i) \quad i = 1, \dots, n \quad (3.16b)$$

In equation (3.16) \bar{M}_k is the parent that offers the best result in the objective function (since the other four parents are randomly taken, it could happen that this last parent is equal to any of the other four). F is the *weighting factor* that determines which percentage of $(\bar{B}_k - \bar{C}_k)$ is added to \bar{A}_k . Recommended value is something between 0.5 and 1. Lower values make the

process become slower, but they also increase the possibilities of convergence. Finally, KF is the *combination factor*, a parameter that accounts how much will \bar{Y}_k move towards \bar{M}_k . This value must be between zero and 1, and the higher it is, the closer the trial vector gets to the best candidate, but a too high value increase the risk of finding a local optimum instead of a global optimum. Recommended is 0.75. After every iteration, OPerA performs a check to determine if the new candidate is better than the previous best. If this is so, the tool names this candidate the new best, and thus all the new iterations will move towards it until a better candidate is found.

- In the next step, once \bar{Y}_k is defined, the algorithm proceeds to mutate the crossover parent \bar{X}_k . In order to do that, the algorithm follows the following expression:

$$z_i = \begin{cases} y_i & \text{if } r_i \leq C \\ x_i & \text{if } r_i > C \end{cases} \quad (3.17)$$

Where $r_i \in [0,1]$ is a random value and C is the crossover factor. This factor indicates how many of the parents from previous steps are taken without changes. The recommended value is between 0.7 and 0.85.

- The \bar{Z}_k already created is compared by the tool with the original \bar{X}_k . The one that delivers the best result survives as \bar{X}_{k+1} .

This process is iteratively performed a number of times defined by the user. The minimum recommended is 10. However, a bigger number will increase the chances of finding the optimum.

3.4 Changes done in OPerA

The objective of the present Thesis is to analyze and optimize the preliminary design of a Strut Braced Wing Aircraft. In order to do so, the tool OPerA will be used, taking advantage of its optimization capabilities to obtain an optimum result that meets the requirements. However, despite OPerA is ready for SBW configurations, the program has been revised and modified in an attempt to improve this support, as well as to make it easier to use from the user point of view.

In addition, new functions have been added, so the tool now is able to calculate the gravity centre of the aircraft, derives different cost calculations with different methods and support for folding wing technology is now an option to configure the aircraft. This technology allows the airplane to grow in wingspan and fit in a desired ICAO category at the same time. The changes done in OPerA are the following.

3.4.1 Changes in Tail Sizing

OPerA incorporates a complete set of possibilities to configure the empennage of the aircraft, namely conventional tail, cruciform tail, and T-tail. In order to improve the equations already implemented in OPerA (Nita 2012), a few of changes have been made:

- When a T-tail is mounted on an empennage, is it possible to observe a certain endplate effect on the vertical surface. This is equivalent to say that the horizontal tail acts as a winglet for the vertical tail. This endplate effect affects the effective aspect ratio of the vertical tail, making it bigger than the geometrical aspect ratio. The consequence of this is that the vertical surface can be reduced, thus reducing slightly the empennage mass. Kundu (Kundu 2010) suggests that, in order to account for this effect, the vertical tail volume coefficient, which is used to calculate the vertical tail surface area, must be reduced by 6/7 when using a T-tail.
- The wing wake provokes that the dynamic pressure over the horizontal tail is lower than over the wing, making the empennage less efficient in producing lift. This effect is accounted in the equations with an efficiency factor η_H , that takes a value of 0.9 for conventional tail configuration, and getting bigger as the horizontal surfaces comes out of the wing wake, being 1 when T-tail is used. This effect is applied in the equation for the horizontal tail volume coefficient:

$$C_H = \frac{S_H \cdot l_H}{S_W \cdot c_{MAC}} \quad (3.18)$$

Where C_H is the tail volume coefficient, S_W and S_H are the wing and horizontal tail surfaces, l_H is the horizontal tail lever arm and c_{MAC} is the mean aerodynamic chord. OPerA calculates the horizontal tail surface by means of an statistical value for the tail volume coefficient: $C_H = 1.105$ that is taken for conventional tail. From Scholz (Scholz 1999), the following expression is obtained:

$$\frac{S_H}{S_W} = \frac{C_L}{C_{L,H} \cdot \eta_H \cdot \frac{l_H}{c_{MAC}}} \cdot \overline{x_{CG-AC}} + \frac{C_{M,W} + C_{M,E}}{C_{L,H} \cdot \eta_H \cdot \frac{l_H}{c_{MAC}}} \quad (3.19)$$

Where C_L and $C_{L,M}$ are the lift coefficients wing and horizontal tail, respectively, $C_{M,W}$ and $C_{M,E}$ are the moment coefficients of wing and engine, η_H is the horizontal tail efficiency and $\overline{x_{CG-AC}}$ is the dimensionless distance between the aircraft gravity centre and aerodynamic centre. Reorganising the terms of equation (3.18) and (3.19):

$$\frac{S_H}{S_W} = \frac{C_H \cdot c_{MAC}}{l_H} \quad (3.20)$$

$$\frac{S_H}{S_W} = \frac{c_{MAC}}{l_H} \cdot \left(\frac{C_L}{C_{L,H} \cdot \eta_H} \cdot \overline{x_{CG-AC}} + \frac{C_{M,W} + C_{M,E}}{C_{L,H} \cdot \eta_H} \right) \quad (3.21)$$

Combining both equations leads to:

$$C_H = \frac{A}{\eta_H} \quad (3.22)$$

$$A = \frac{C_L}{C_{L,H}} \cdot \overline{x_{CG-AC}} + \frac{C_{M,W} + C_{M,E}}{C_{L,H}} \quad (3.23)$$

Once in this point, knowing the value of the tail coefficient volume for conventional tail, and the efficiency of the tail surface for that configuration, it is possible to obtain the value of A:

$$A = C_H^* \cdot \eta_H = 1.105 \cdot 0.9 = 0.9945 \quad (3.24)$$

This way:

$$C_H = \frac{0.9945}{\eta_H} \quad (3.25)$$

And, introducing the horizontal tail position with respect to the vertical fin to calculate the tail efficiency, it comes to the final expression:

$$C_H = 1.105 - 0.1105 \cdot \frac{z_H}{b_V} \quad (3.26)$$

- Another consideration that has to be taken is the influence that the position of the wing has on the position of the tail. The optimizer sometimes delivers results that may look very promising, but some other checks must be made in order to achieve a good design. The influence of the position of the wing from the tail point of view is one of these cases. It must be noted that the wing wake always interacts with the horizontal tail surface, sometimes even make it more difficult to be controlled, or even impossible. When the angle of attack grows enough to make the wing stall, the horizontal tail is the responsible for taking the airplane out of the stall situation. However, if the horizontal tail is inside the wing wake when this happens, it will not be able to bring down the angle of attack again, and therefore the airplane will become unresponsive to control commands and eventually fall down. This is called *deep stall*. In order to take it into consideration, Raymer (**Raymer 2006**) produced a graphic to help the designer check if the tail will be inside the wing wake when the plane stalls. This graphic can be seen in Figure 3.6. On it, the lines that limit the allowable design can be appreciated. A good design would be when the design point lies over the upper boundary, or under the lowest one. If the designed airplane flies at sub sonic speeds, then it is enough if the design point lies within the two low lines. To determine the design point position, the x-axis shows the horizontal distance between the wing and the tail divided by the mean aerodynamic chord, and the vertical axis shows the vertical distance, divided as well by c_{MAC} . However, it is important to note that the results of the graphic are only a suggestion, as the author says. If the design point is inside the blanking area, it does not mean that the design is completely wrong, but that the designer should provide the airplane

with technical means or design solutions that avoid the deep stall. This graphic has been implemented in OPerA, so the user can check, after the design point is found or the optimization is over, if the design is in the blanketing area or not, and decide whether to continue with it, because some measures are going to be later applied. It is located in the module *Optimization Set up*, and the program shows automatically the location point when the design point Macro is used.

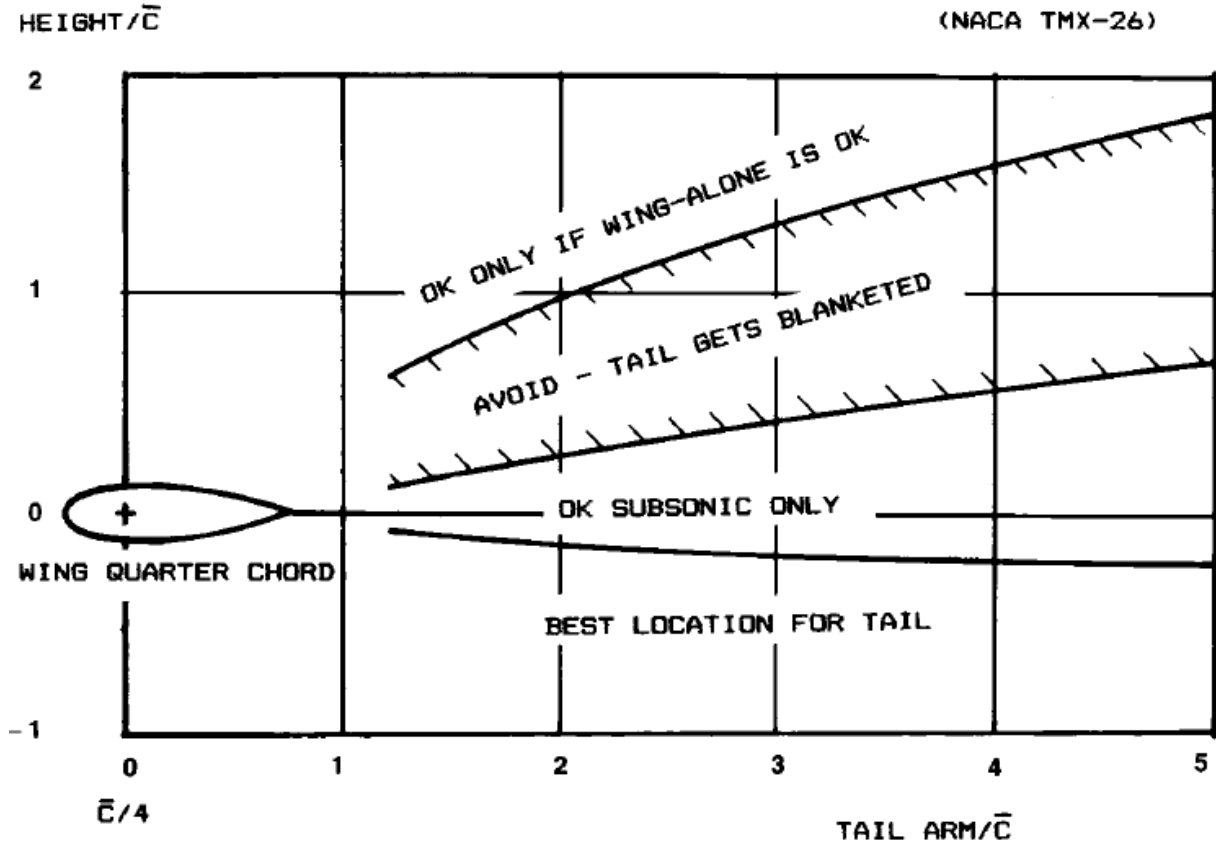


Figure 3.6 Tail aft positioning (Raymer 2006)

3.4.2 Centre of Gravity

The old version of OPerA was able to complete the preliminary design of an airplane, but it does not take into account the position of the gravity centre within the aircraft. This has specially a big impact in the sizing of the empennage, because the position of the CG determinates the position of the wing along the fuselage, varying the tail arm, and thus the needed tail surface. For this reason a new module was added to the tool that estimates the position of the CG and delivers it to others. This module works iteratively, so in order to make it work properly the own code of OPerA had to be changed. With this new feature the tool gains in accuracy and the effect of using different empennage configurations or aft mounted engines can be more realistically studied.

The method that the module uses to calculate the centre of gravity is taken from **Scholz 1999** and comes from the definition of CG:

$$\overline{x_{CG}} = \frac{\sum m_i \cdot \bar{x}_i}{\sum m_i} \quad (3.27)$$

The equation must be adapted to be used for an airplane. In order to do so, two mass groups are divided, the *wing group* and the *fuselage group*. Both groups have fixed elements, and elements that can belong to one or another group, depending on the configuration. Thus, the wing group is formed by the wing and the engines, when those are mounted on the wing; in the fuselage group are the fuselage, the nose landing gear, the tail and the engines, when they are mounted on the fuselage. The main landing gear is a special case: it can be mounted on the wing or on the fuselage. However, it has been found that for stability reasons in the tool it must be kept always for calculations in the fuselage group. To complete the equation, the position of the leading edge of the mean aerodynamic chord of the wing is used as reference point. Thus, equation (3.27), in the x-axe of the plane becomes:

$$(m_{WG} + m_{FG}) \cdot x_{CG,LEMAC} = m_{WG} \cdot x_{WG,LEMAC} + m_{FG} \cdot (x_{FG} - x_{LEMAC}) \quad (3.28)$$

Where m_{WG} and m_{FG} are the mass of the wing and fuselage group, respectively. $x_{CG,LEMAC}$ and $x_{WG,LEMAC}$ are the positions, respect to the leading edge of the mean aerodynamic chord, of the CG of the aircraft and the wing group. x_{FG} is the CG position of the fuselage group, with respect to the nose tip, and x_{LEMAC} is the position of the leading edge of the MAC with respect to the same reference. Reorganize the terms of (3.28) leads to:

$$x_{LEMAC} = x_{FG} - x_{CG,LEMAC} + \frac{m_{WG}}{m_{FG}} \cdot (x_{WG,LEMAC} - x_{CG,LEMAC}) \quad (3.29)$$

The next step that the tool takes is to calculate the terms on the left hand side of equation (3.29). x_{FG} is calculated as an independent body. Thus:

$$\bar{x}_{FG} = \frac{m_F \cdot \bar{x}_F + m_T \cdot \bar{x}_T + m_V \cdot \bar{x}_V + m_{NLG} \cdot \bar{x}_{NLG} + m_{MLG} \cdot \bar{x}_{MLG} + (m_{OI} + m_S) \cdot \bar{x}_S + (m_E \cdot n_E \cdot \bar{x}_E)}{m_F + m_T + m_V + m_{NLG} + m_{MLG} + m_{OI} + m_S + (m_E \cdot n_E)} \quad (3.30)$$

Here is included every part belonging to the fuselage group. The term with the index E corresponds to the engines (engine plus nacelle), and is taken into account only if the engines are selected to be mounted on the aft part of the fuselage. The mass of each component is taken from the mass estimating module. The position of each component CG is now explained.

The fuselage centre of gravity is located at about 45 % of its length, as shown in Figure 3.7. The final value depends on the engine position: if the engines are mounted on the wing, $\bar{x}_{FG} = 0.435$; if they are on the aft fuselage, then is $\bar{x}_{FG} = 0.465$. In addition, the mass of the systems and the operator instruments (m_{OI} and m_S) are located on $\bar{x}_S = 0.45$.

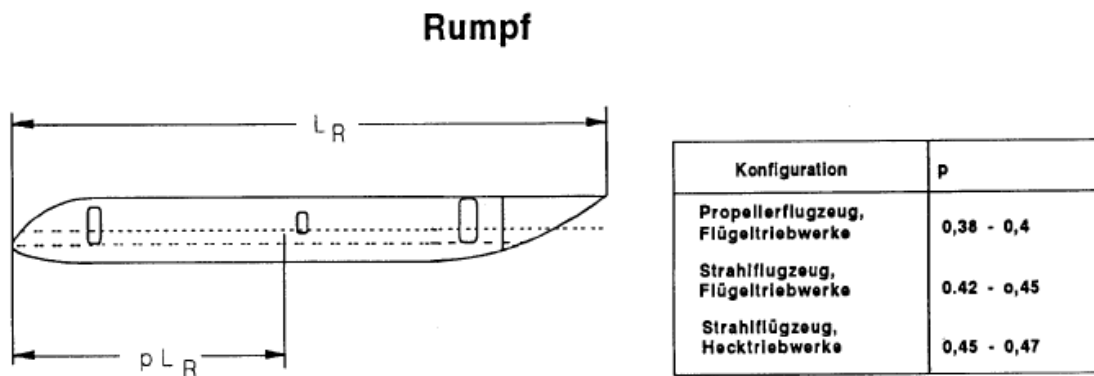
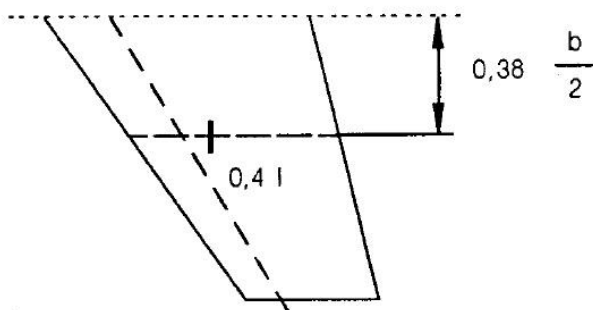


Figure 3.7 Position of the fuselage mass centre depending on engine position (Scholz 1999)

The gravity centre of the tail surfaces is obtained from Figure 3.8. The position of the horizontal tail depends on its position along the vertical tail, z_H/b_V , from $z_H/b_V = 0$ (conventional tail) to $z_H/b_V = 1$ (T-tail). All the values in between correspond to cruciform tail configuration. Obviously, the horizontal tail CG is shifted backwards as long as its position is higher.

Höhen- und Seitenleitwerk



SL bei T- Leitwerk

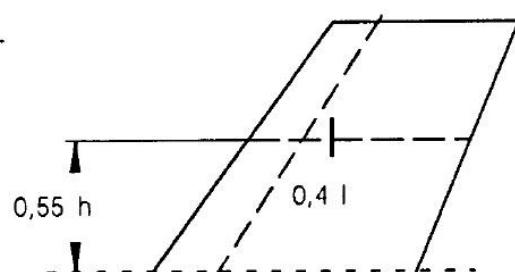


Figure 3.8 Tail surfaces centre of mass (Scholz 1999)

For the horizontal tail mass, the following formulae are used:

$$x_{T,CONV} = l_F - D_{EFVT} - c_{r,H} + \tan(\varphi_{0,H}) \cdot 0.38 \cdot \frac{b_H}{2} + 0.4 \cdot c_{0.38b,H} \quad (3.31)$$

$$x_{T,X} = l_F - D_{EFVT} - \frac{c_{zH}}{b_V} \cdot b_{,v} + \tan(\varphi_{25,V}) \cdot \frac{z_H}{b_V} \cdot b_V + \tan(\varphi_{0,H}) \cdot 0.38 \cdot \frac{b_H}{2} + 0.4 \cdot c_{0.38b,H} \quad (3.32)$$

$$x_{T,T-TAIL} = l_F - D_{EFVT} - c_{r,H} + \tan(\varphi_{25,V}) \cdot b_V + \tan(\varphi_{0,H}) \cdot 0.38 \cdot \frac{b_H}{2} + 0.4 \cdot c_{0.38b,H} \quad (3.33)$$

For the vertical tail fin, the gravity centre is derived by the expression:

$$x_V = l_F - D_{EFVT} - 0.6 \cdot c_{r,V} + \tan(\varphi_{25,V}) \cdot b_V \cdot 0.55 \quad (3.34)$$

Where l_F is the fuselage length and D_{EFVT} is the distance between the end of the fuselage and the end of the vertical tail fin that was taken as a statistical value based on different measures taken from **Jane 92** and **Jane 08**. $\varphi_{i,j}$ is the sweep angle of the different chord lines for both vertical and horizontal tail, b_i is the span of the tail surfaces and $c_{i,j}$ is the chord of different profiles of the vertical and the horizontal tail fins.

The position of the nose landing gear is gotten from the *Mass Estimations* module, because it is already calculated there. For the position of the main landing gear two options are available: when the main landing gear is located on the wing, then its position lies on a certain percentage of the MAC, which is a parameter that the user can set on the optimization controlling module. Then,

$$x_{MLG,W} = x_{LEMAC} + MACfraction \cdot c_{MAC} \quad (3.35)$$

When using this method, the position of the main landing gear must be iterated by the program. If the MLG is chosen to be mounted on the fuselage, then its position, as a percentage of the fuselage length is set as a design parameter that can be set free for optimizations.

If the engines are mounted on the aft fuselage, then they count for x_{FG} , the mass is extracted, as all the other mass data, from the corresponding module, and their position on the fuselage is set as a percentage of the fuselage length with the fuselage end as starting point. This fraction is set as a new design parameter in the *Optimization Set up* module, and is subject to optimizations. Thus,

$$x_E = l_F \cdot (1 - d_{E,FE}) \quad (3.36)$$

Now the wing group will be analyzed. The mass centre of the wing group is measured from the leading edge of the mean aerodynamic chord. The expression to obtain it is basically the same to obtain the position of the wing mass centre, considering when the engines are mounted on the wing or not. When they are not, the expression is obtained from Figure 3.9 and yields:

$$x_{W,LEMAC} = 0.7 \cdot c_{0.35,W} - \left(y_{MAC} - 0.35 \cdot \frac{b}{2} \right) \cdot \tan(\varphi_{0,W}) \quad (3.37)$$

Flügel

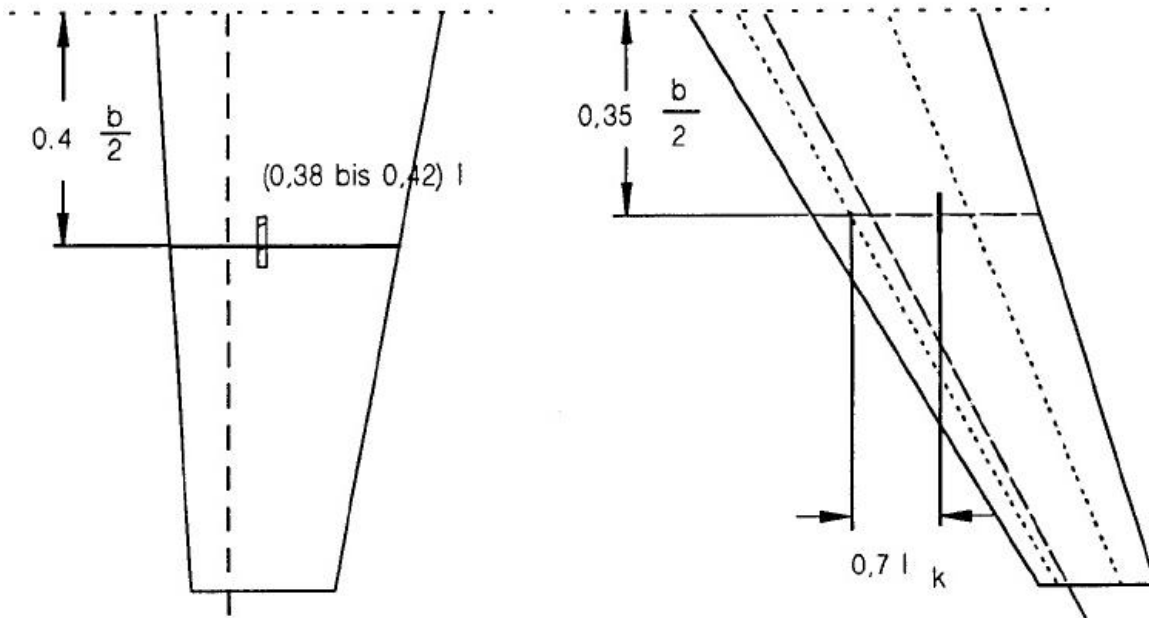


Figure 3.9 Wing centre of mass position (Scholz 1999)

If the engines are mounted on the wing, then their gravity centre with respect to the leading edge of the MAC must be calculated before calculating the gravity centre of the wing group. With that purpose, the scheme showed in Figure 3.10 will be used. The inner engines have the index 2, as the outer engines (when they exist) use the index 1. The expression for both is:

$$x_{CGEi,LEMAC} = (y_{Ei} - y_{MAC}) \cdot \tan(\varphi_{0,W}) - l_E \cdot 0.6 \quad i = 1,2 \quad (3.38)$$

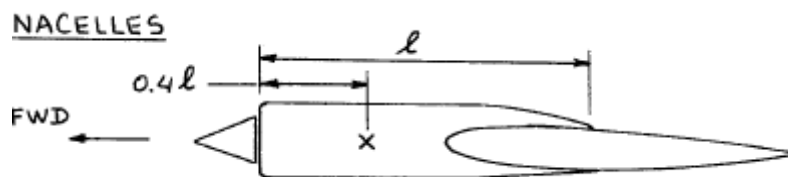


Figure 3.10 Engine and nacelle mass centre position (Scholz 1999)

With the gravity centre of all components of the wing group already calculated, and if the engines are mounted on the wing (otherwise $x_{WG,LEMAC} = x_{W,LEMAC}$), the gravity centre of the wing group is:

$$x_{WG,LEMAC} = \frac{m_W \cdot x_{W,LEMAC} + 2 \cdot m_E \cdot (x_{CGE1,LEMAC} + x_{CGE2,LEMAC})}{m_W + n_E \cdot m_E} \quad (3.39)$$

In equation (3.39) is $x_{CGE1,LEMAC} = 0$ if there are only 2 engines.

The last term to complete the right hand side of equation (3.29) is $x_{CG,LEMAC}$, which can be freely chosen. In OPerA, the method from **Scholz 1999** is followed, and therefore the same value will be taken, being 25 % of the MAC.

Once the position of the MAC leading edge is calculated through equation (3.29), OPerA obtains the position of the gravity centre from the expression:

$$x_{CG} = x_{LEMAC} + x_{CG,LEMAC} \quad (3.40)$$

The loop that OPerA uses to calculate the gravity centre is the following:

1. Once the user presses the button *Find Design Point with CG*, OPerA calculates the geometry of the airplane assuming a tail lever arm of 50 % of the fuselage length for both horizontal and vertical empennage.
2. With the geometry calculated, OPerA calculates the centre of gravity following the method above described.
3. Once the preliminary position of the CG is know, the tool calculates the new lever arm for horizontal and vertical tail as the distance from their respective neutral points to the CG.
4. With the new lever arms, OPerA calculates a new geometry, a new CG and new lever arms. And in the *Gravity Centre* module the percentage difference between the previous and the new lever arm is showed. This process is repeated as many times as the user sets in the *Optimization Set up* module. With 2 iterations is normally enough to achieve a accuracy of less than 1 % in the CG.

The method is also applied for DOE and DE optimizations, by changing the code to calculate the design point and the CG on every iteration.

3.4.3 Folding Wing Technology

It has been already addressed in Section 2 the potential advantage of implementing a supporting strut on the wing of an aircraft and how it allows, among other things, increasing the wingspan by keeping the wing mass constant, or with small increase. However, this project has the goal of delivering the preliminary design sizing of an airplane belonging to ICAO category C. This fact

limits the aircraft wingspan at the airport to 36m, and thus the potential advantage of the SBW configuration may not be fully achieved. Two different ways to go beyond that point and increase the aspect ratio without exceeding 36 meters wingspan are proposed in OPerA:

First, OPerA includes the possibility of adding winglets at the wing tips. **Nita 2012** shows some results in optimizing an Airbus A320 by adding winglets among other things. The winglets are a way to increase the effective aspect ratio of the wing without adding extra wingspan, and thus staying in category C. However, the results of **Nita 2012** show that the increase of effective aspect ratio is less effective than adding the same aspect ratio increase by extending the wingspan. For this reason, a wing folding technology is considered.

The folding wing system will consist on a pair of actuators mounted on the wing that folds it to make the airplane fit into 36m wingspan when landed at the airport. To implement this technology in OPerA the equations included in **Yarygina 2012** are used. These equations are new, and some modifications were done in order to make them suitable to work within OPerA. The paper is written in Russian, a language that the author of this Thesis do not speak, however, thanks to Prof. A. Kretov from Kazan University and Prof. V. Zhuravlev from Moscow Aviation Institute (MAI) for their explanations and the partial translation they provided, it was possible to study the equations provided in the paper. Thus, some equations needed interpretation and adaptation.

Several changes were made on the equations in **Yarygina 2012** during this understanding process: In order to do so, many interpretations and plotted were needed.

The most significant equation of the paper is the one that states the mass of the folded wing:

$$\bar{m}_{FW} = \bar{m}_W \cdot (1 + \bar{m}_J + \bar{m}_{RF} + \bar{m}_{FM}) \quad (3.41)$$

Where \bar{m}_{FM} is the mass of the folded wing divided by m_{MTO} , \bar{m}_W is the dimensionless mass of the unfolded wing, and \bar{m}_J , \bar{m}_{RF} and \bar{m}_{FM} are the masses of the different systems needed to build the folding wing system, namely the mass of the joining system, the mass of the reinforcements, and the mass of the folding mechanism (actuators), divided by the unfolded wing mass. These terms act as increasing weight factors. Figure 3.11 shows the increase mass obtained for different dimensionless wing points, namely $2y/b = 0.32$, $2y/b = 0.48$ and $2y/b = 0.64$. In each one of them, the equations for the different mass addition provided in the reference were used.

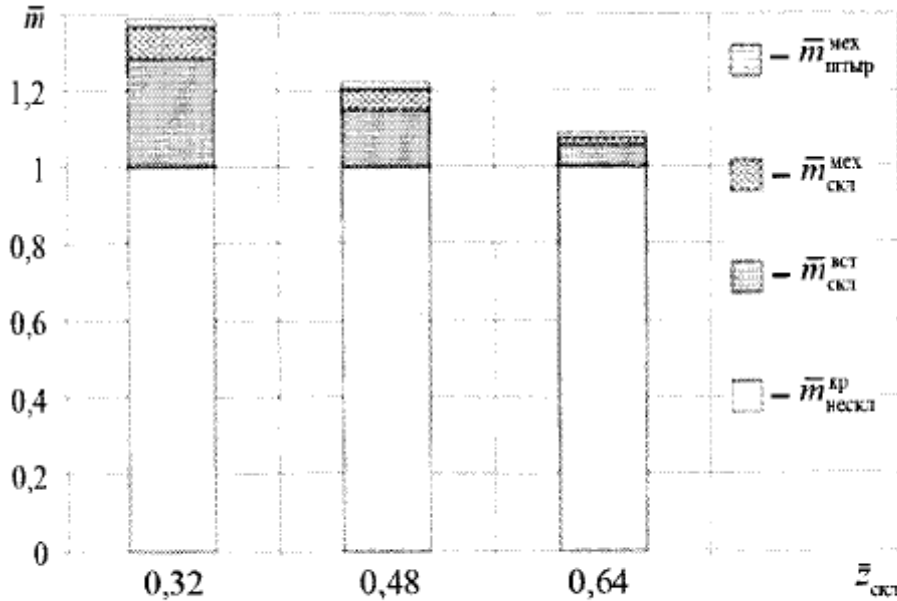


Рис. 5. Изменение прироста относительной массы крыла по размаху

Figure 3.11 Wing mass increase separated with its different parts (Yarygina 2012)

For the mass of the reinforcing system three different equations are available, each one for each point. The equations are:

$$\bar{m}_{RF} = 0.24 \cdot (\bar{m}_F - 0.924)^2 - 0.007 \quad \text{for } \bar{y} = 0.32 \quad (3.42)$$

$$\bar{m}_{RF} = 0.45 \cdot (\bar{m}_F - 0.916)^2 - 0.02 \quad \text{for } \bar{y} = 0.48 \quad (3.43)$$

$$\bar{m}_{RF} = 0.84 \cdot (\bar{m}_F - 0.98)^2 - 0.107 \quad \text{for } \bar{y} = 0.64 \quad (3.44)$$

$$\bar{m}_F = \frac{(c_{YF} + c_T) \cdot (t_{YF} + t_T) \cdot \left(\frac{b}{2} - y_F\right)}{(c_R + c_T) \cdot (t_R + t_T) \cdot b} \quad (3.45)$$

The variable in these equations, \bar{m}_F , is the relative weight of the folded part of the wing, divided by the unfolded wing mass. These three equations were plotted separately on Figure 3.12. In the graphic can be appreciated that the mass of the reinforcing system increases when the folding axis goes to the wingtip, which is not logical. Thus, it was understood that each equation is valid only around the point in which each one was applied (namely $2y/b = 0.32$, $2y/b = 0.48$ and $2y/b = 0.64$). In order to produce a valid equation for the whole y range, a linear interpolation between the three equations was performed. To avoid negative results, a last point for the interpolation was used: the mass of the reinforcing system must be zero at the wingtip, i.e. $\bar{y} = 0$. The resulting plot is shown in Figure 3.13.

For the joining system, as well for the folding mechanism, the equations used were the following:

$$\bar{m}_{FM} = -3.76 \cdot (\bar{m}_F - 0.2)^2 + 0.08 \quad (3.46)$$

$$\bar{m}_J = -0.6 \cdot (\bar{m}_F - 0.2)^2 + 0.02 \quad (3.47)$$

The first one corresponds to the folding mechanism, and the second describes the mass fraction of the joining system. The plot of these equations is shown in Figure 3.14.

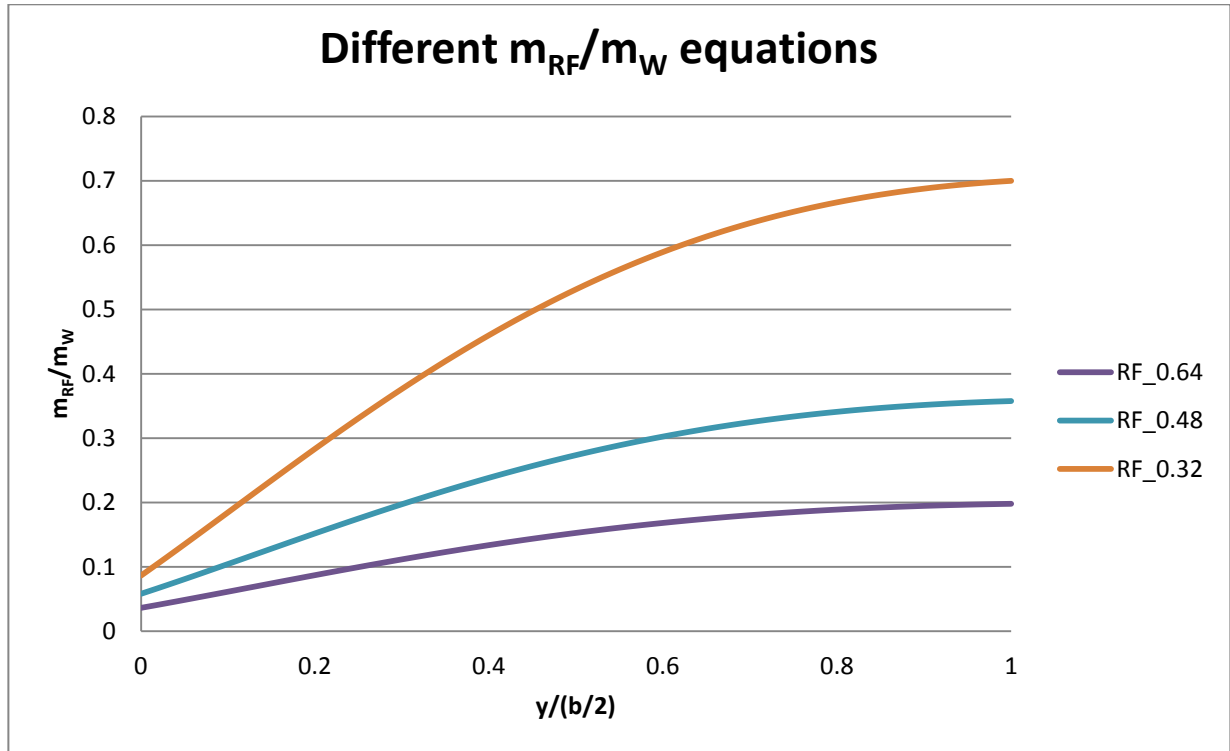


Figure 3.12 Plot of the three equations for the reinforcing system mass

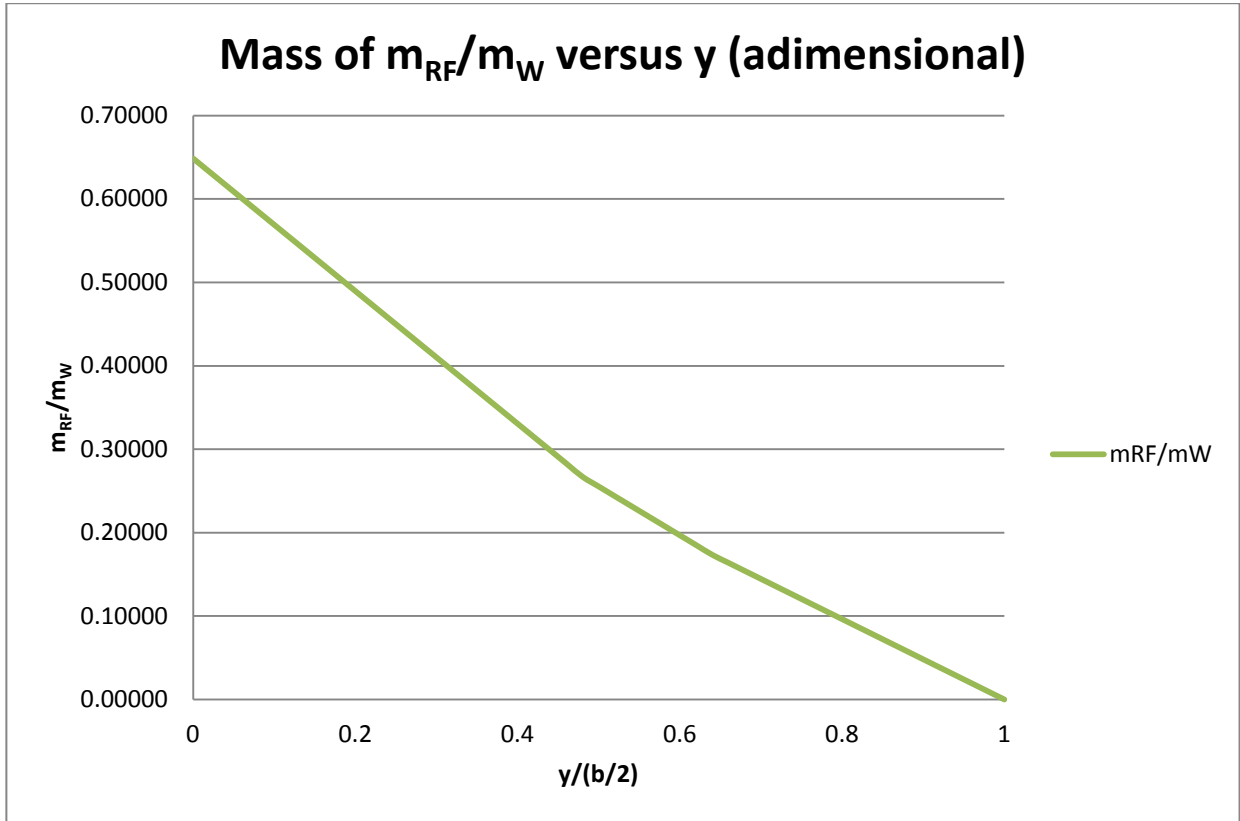


Figure 3.13 Interpolated line for the mass of the reinforcing system

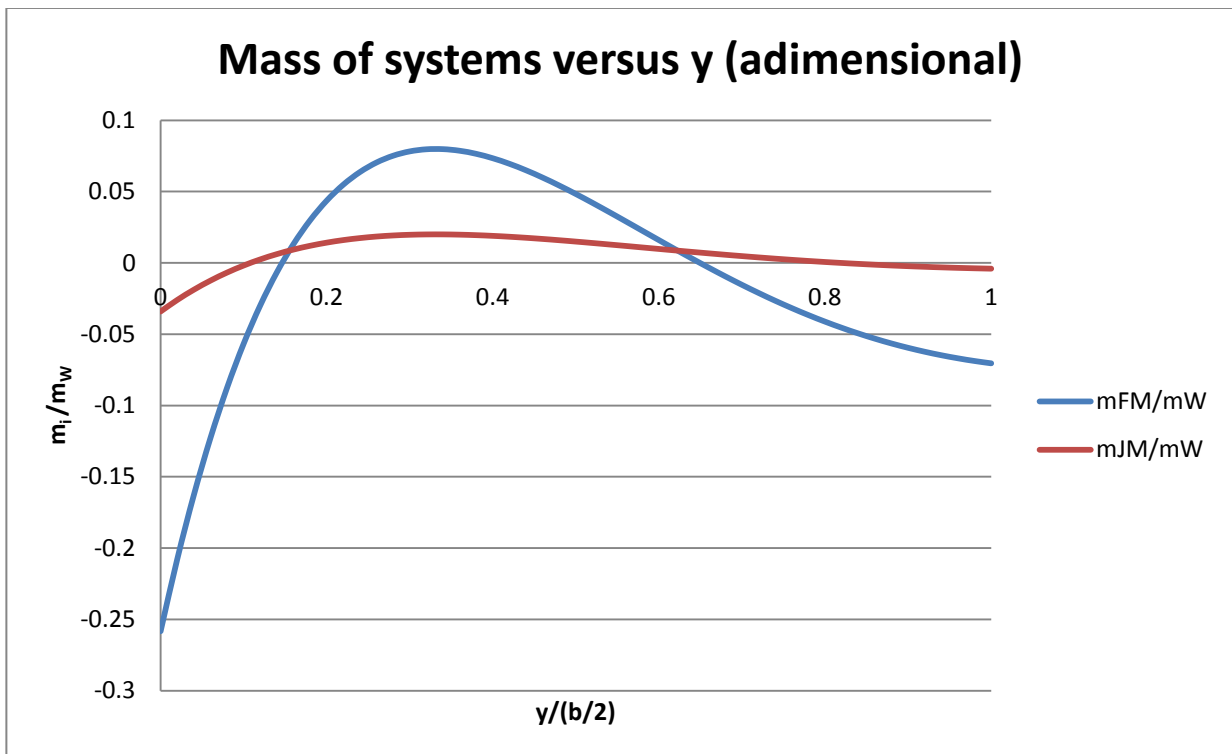


Figure 3.14 Plot of the equations for the folding mechanism and join mechanism masses

Two not logical results can be seen here:

- Both equations go below zero close to the wingtip
- Again, both equations reduce their value and goes below zero close to the wing root.

In order to solve the first one, both equations were slightly shifted upwards, to meet the value zero at the wingtip. This way, the first equation is shifted 0.0704 up, and the second 0.004.

The second result needed more attention: by studying the formula, it can be seen than this is a parabola. Performing a simple derivation and equaling to zero, it is obtained that the highest point in this parabola is $\bar{m}_F = 0.2$, which corresponds to $\bar{y} \cong 0.32$. To avoid the unlogical descent of the results, the equations were modified, so when $\bar{m}_F < 0.2$, the result is constant and equal to the result with $\bar{m}_F = 0.2$. This measure could be named a “patch” since the logic says that the mass of these two systems should increase as the folding axis approaches to the wing root, but no more data was available on the paper, so the constant solution was taken as provisional one. Next revision of the equations should include an increase rate for the mass of these two systems, as they approach to the wing root. However, this does not affect the results of this Thesis, since the folding actuators are never located that close to the wing. Therefore, the plot result is represented in Figure 3.15.

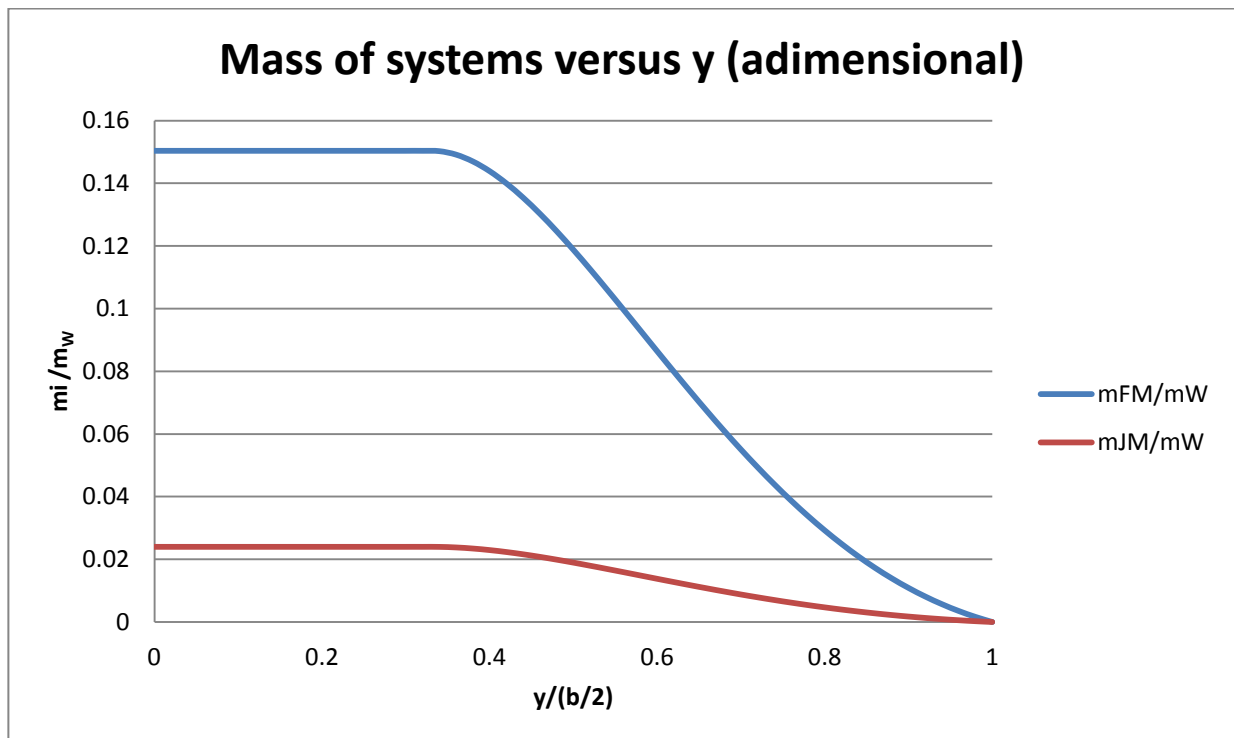


Figure 3.15 Folding system and joining system masses corrected

Finally, the masses of the three systems are plotted together in Figure 3.16, for comparison purposes, and just after it, in Figure 3.17, the results of equation (3.41).

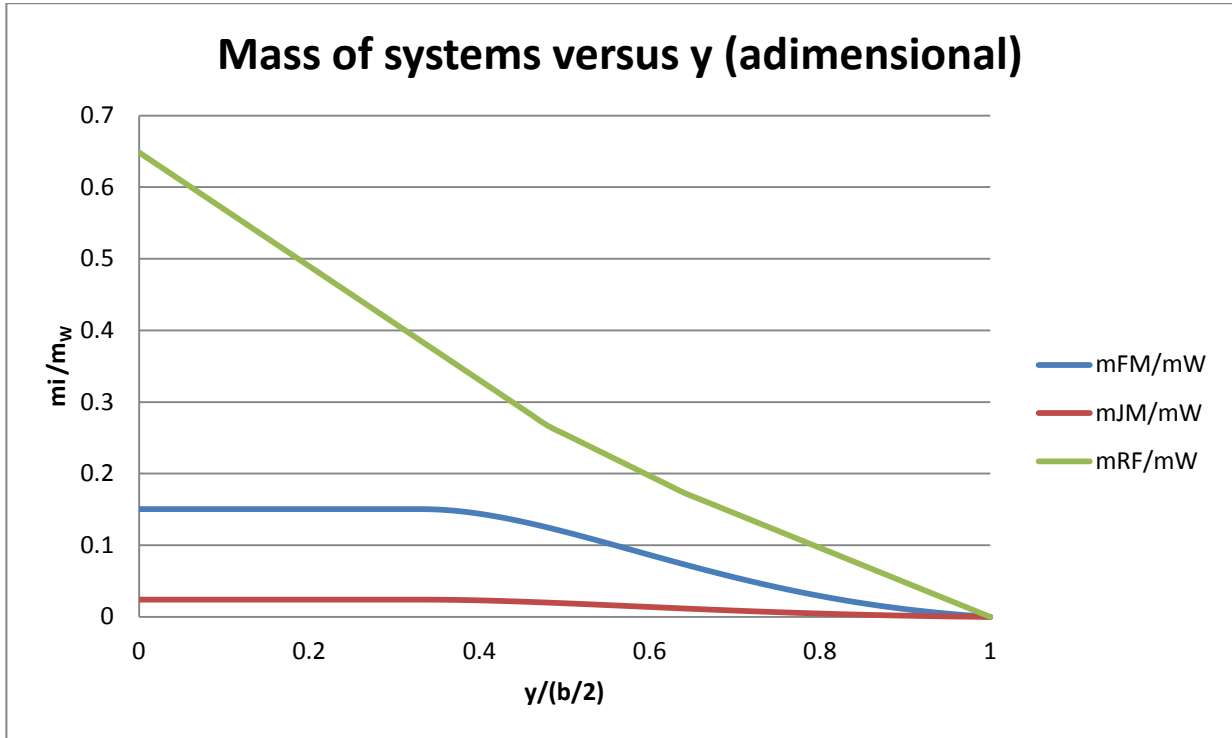


Figure 3.16 Relative mass of the three systems involved in folding wing technology

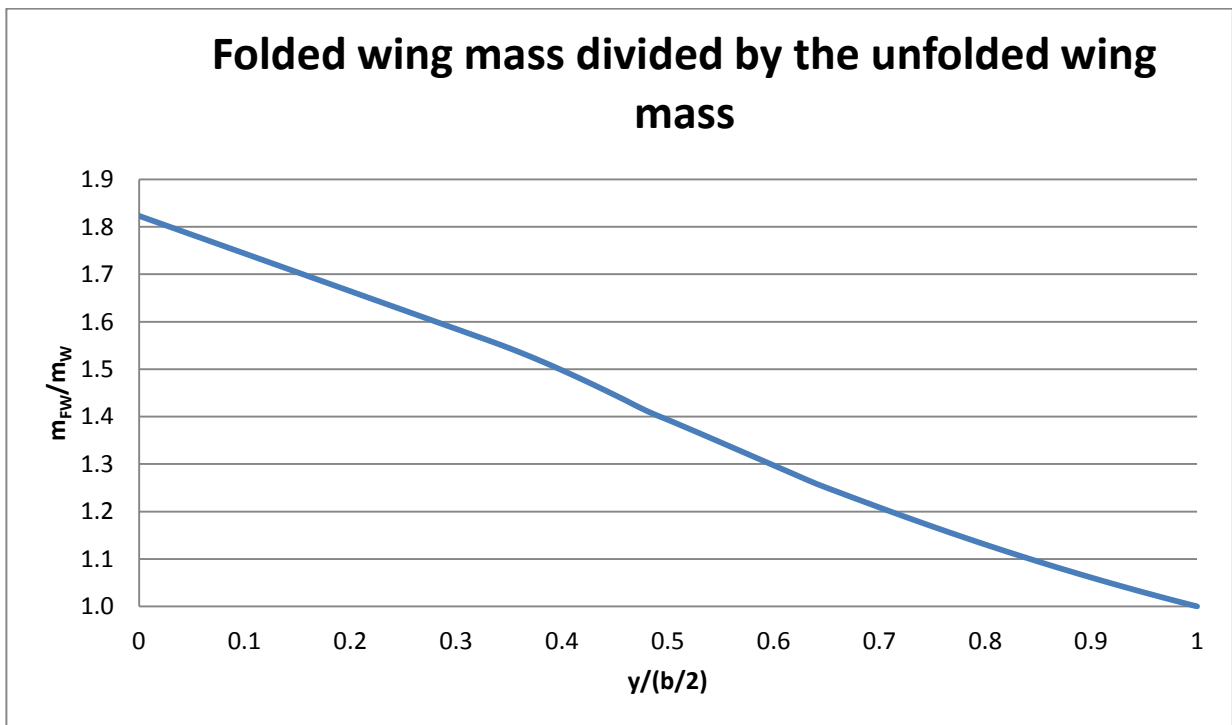


Figure 3.17 Mass increase of the wing with folding wing technology according to actuators position

In addition, it was also considered an interesting case of study the one in which only one half of the wing is folded. The idea came with the consideration that may be beneficial for the wing mass when only one big actuator is used, rather than two small ones. To compare both situations, a new graphic was produced, whose results are shown in Figure 3.18.

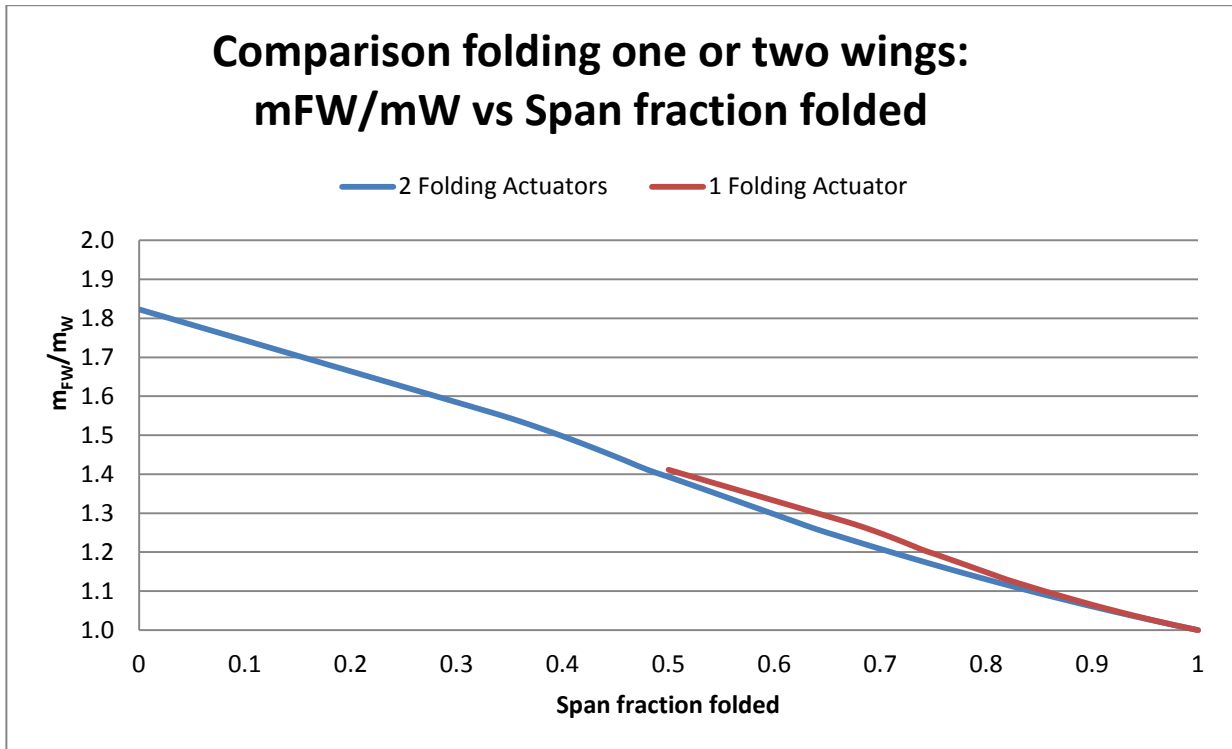


Figure 3.18 Comparison of the wing weight when using one or two folding actuators

As the results show, with the level of accuracy used it is possible to say that the wing mass increase is similar in both cases. However, it seems to be a little bit worse when using two smaller actuators instead of a single bigger one. For the rest of this Thesis, as well as in OPerA, two actuators will be used. In any case, using only one actuator could bring an improvement in maintenance cost, since there is only one actuator to be maintained, and therefore less failure probability. A failure in the actuator would provoke the wing to be unable to fold at the airport, and thus obligate to park on an apron position instead of at the gate. In conclusion, the advantages of folding only one half wing should be considered and evaluated versus disadvantages like the gravity centre shifting to one side, in order to decide whether to include this option in the design or not.

A last point to highlight is that, when this Thesis was almost finished, new bibliography from Yarygina about the folding wing mass was released, with some more details (**Yarygina 2013**). There is it possible to see how the approximation done in the equations for this Thesis was accurate enough. The already mentioned problem with the value of the folding wing system when it is located close to the fuselage is simply solved by not taking into account any folding system closer than $2y/b = 0.3$.



Figure 3.19 Folding system installed on a wing (Yarygina 2013)

3.4.4 New COC Method

On the task of this Thesis it is mentioned that the cost method used in the preliminary design to evaluate and compare different designs will be the so called *Unified Cost Method* proposed by the German space office (DLR). Unfortunately, this method is not yet available when this Project was written, but its basis is already set. The method will combine the philosophies of the method presented in **Scholz 1999**, which is the method developed by the Association of European Airlines (AEA 1989), and the method developed in the Technical University of Berlin (**TUB 2013**). The AEA method is the one which was already implemented in OPerA, ready to calculate Direct Operating Costs (DOC). For this Thesis, AEA method is modified so it also calculates Cash Operation Cost (COC) in both euro and U.S. dollar, and the method developed in TUB is as well included, both for COC and DOC. This way the user is free to choose which method will OPerA use when performing optimizations, as well as which kind of cost (DOC or COC) will be estimated. DOC and COC can be set as objective function, and the user must have a clear idea of which one to use, because due the differences between DOC and COC, it is a big difference optimizing for one or for the other.

3.4.4.1 TUB Cost Method

The following described method starts from the consideration that there are two different elements that determines the Direct Operating Cost of an airplane:

$$\begin{aligned}
 & -C_1: \text{Route independent (fixed) cost} \\
 & -C_2: \text{Route dependent (variable)cost} \\
 & \quad \quad \quad \text{DOC} = C_1 + C_2 \qquad \qquad \qquad (3.48)
 \end{aligned}$$

The route independent cost (C_1) is basically composed of depreciation, interest, insurance and the aircraft crew (flight and cabin crews). In order to simplify calculations, all the independent costs of the aircraft are dependent of the size of the aircraft, and therefore of its Operating Empty Weight (OEW). The main element here is the capital cost of the aircraft, which is assumed as a lineal function of the OEW. The influence of the aircraft market is considered negligible. Thus, the capital cost is:

$$C_{CAP} = [p_{OEW} \cdot (m_{OEW} - m_E) + m_E \cdot n_E \cdot p_E] \cdot (a + f_{INS}) \quad (3.49a)$$

$$\text{with } a = IR \cdot \frac{1 - f_{RV} \cdot \left(\frac{1}{1+IR}\right)^{DP}}{1 - \left(\frac{1}{1+IR}\right)^{DP}} \quad (3.49b)$$

Where $p_{OEW} = 1150 \text{ €/kg}$ is the price per kilogram of OEW, which includes structure, systems and equipment, $p_E = 2500 \text{ €/kg}$ is the engine price based on the engine weight. IR is the interest rate, which is taken here as 5 %. DP is the depreciation period and equals 14 years. $f_{RV} = 10 \%$ is the residual value of the aircraft at the end of the depreciation period, and $f_{ins} = 0.5 \%$ is the insurance rate per year. All this data are used to calculate the annuity factor a . The annuity formula takes both yearly depreciation and interest, and includes the residual aircraft price into the capital cost. It is assumed that an operator is paying an aircraft at a constant price per kilogram and spends the corresponding capital cost constantly per year all over the depreciation period. In addition, insurance costs are also proportional to the aircraft price.

The crew cost is assumed independent of the route because the airline must provide enough number of crews to cover all the operated flights, and thus is dependent of the payload (50 passengers per flight attendant and 100 kg per passenger). This way:

$$C_{CREW} = CC \cdot \left(S_{FA} \cdot \frac{m_{PLMAX}}{5000} + S_{FC} \right) \quad (3.50)$$

The crew complement CC is the number of crews per aircraft. In OPERA is set default as 1, but the user can change it in the module DOC . The annual salary per flight attendant is $S_{FA} = 60000 \text{ €/year}$, and for the flight crew is $S_{FC} = 300000 \text{ €/year}$ for two pilots. Thus:

$$C_1 = C_{CAP} + C_{CREW} \quad (3.51)$$

On the other side, the route dependent cost, C_2 , includes the fuel cost, lubricant, fees and maintenance. However, the lubricant cost is considered to be negligible compared to the fuel cost, and can be addressed as a small correction of this last one. Thus, the route dependent cost comes from the following expression:

$$C_2 = FC \cdot \left(p_F \cdot m_F + p_{PL} \cdot m_{PL} + p_L \cdot m_{MTO} + f(R) \cdot R \cdot \sqrt{\frac{m_{MTO}[to]}{50}} + C_M \right) \quad (3.52)$$

Where $p_{PL} = 0.1 \text{ €/kg}$ are the handling fees, $p_L = 0.01 \text{ €/kg}$ are the landing fees, $f(R)$ is a range dependent ATC price factor (1.0 for domestic Europe, 0.7 for transatlantic flights and 0.6 for Far East flights). R is the flight range, which is taken as 50 % of the design range (the user can change this percentage). C_M is the maintenance cost per flight cycle, and FC is the number of flights per year, taken from the AEA method, so the number used is the same for both methods.

The maintenance cost is calculated following the following method:

$$C_{M,AF,MAT} = m_{OEW}[to] \cdot (0.21 \cdot FT + 13.7) + 57.5 \quad (3.53)$$

$$C_{M,AF,PER} = LR \cdot (1 + Burden) \cdot \{(0.655 + 0.01 \cdot m_{OEW}[to]) \cdot FT + 0.254 + 0.01 \cdot m_{OEW}[to]\} \quad (3.54)$$

$$C_{M,ENG} = n_E \cdot (1.5 \cdot T_{TO,1E}[to] + 30.5 \cdot FT + 10.6) \quad (3.55)$$

$$C_M = C_{M,AF,MAT} + C_{M,AF,PER} + C_{M,ENG} \quad (3.56)$$

Where $C_{M,AF,MAT}$ is the airframe material maintenance cost, which include repair and replacement; $C_{M,AF,PER}$ is the airframe personnel maintenance cost (inspection and repair), and $C_{M,ENG}$ is the engine maintenance cost. FT is the flight time, which is, like the number of flights per year, taken from the AEA calculations. $LR = 50 \text{ €/h}$ is the labour rate, and $Burden$ is the cost burden, which is by default set as 2.

Before the DOC calculation can be finished, the fuel cost must be known. OPerA calculates the fuel cost based on the predictions presented in **Airbus 2012**. The graphic shown on Figure 3.20 delivers a slope used to calculate the future fuel price based in the current price. This way, the user can choose the year for which the fuel price will be estimated. In order to do so, the user must input in the module *Optimization Set up* of the tool the actual year and the actual fuel price, as well as the chosen year for fuel price calculation. In any case, it must be noted that this calculation is merely and estimation, since the future real fuel price cannot be accurately predicted, especially for the far future.

The way in which OPerA calculates the future fuel price is simple: The user must input the current fuel price (in US\$/barrel), the current year, and the year for cost calculation. OPerA then takes the current year fuel price as starting point, and increases it linearly for the cost calculation year using the slope from Figure 3.20 (2.7 \$/barrel/year).

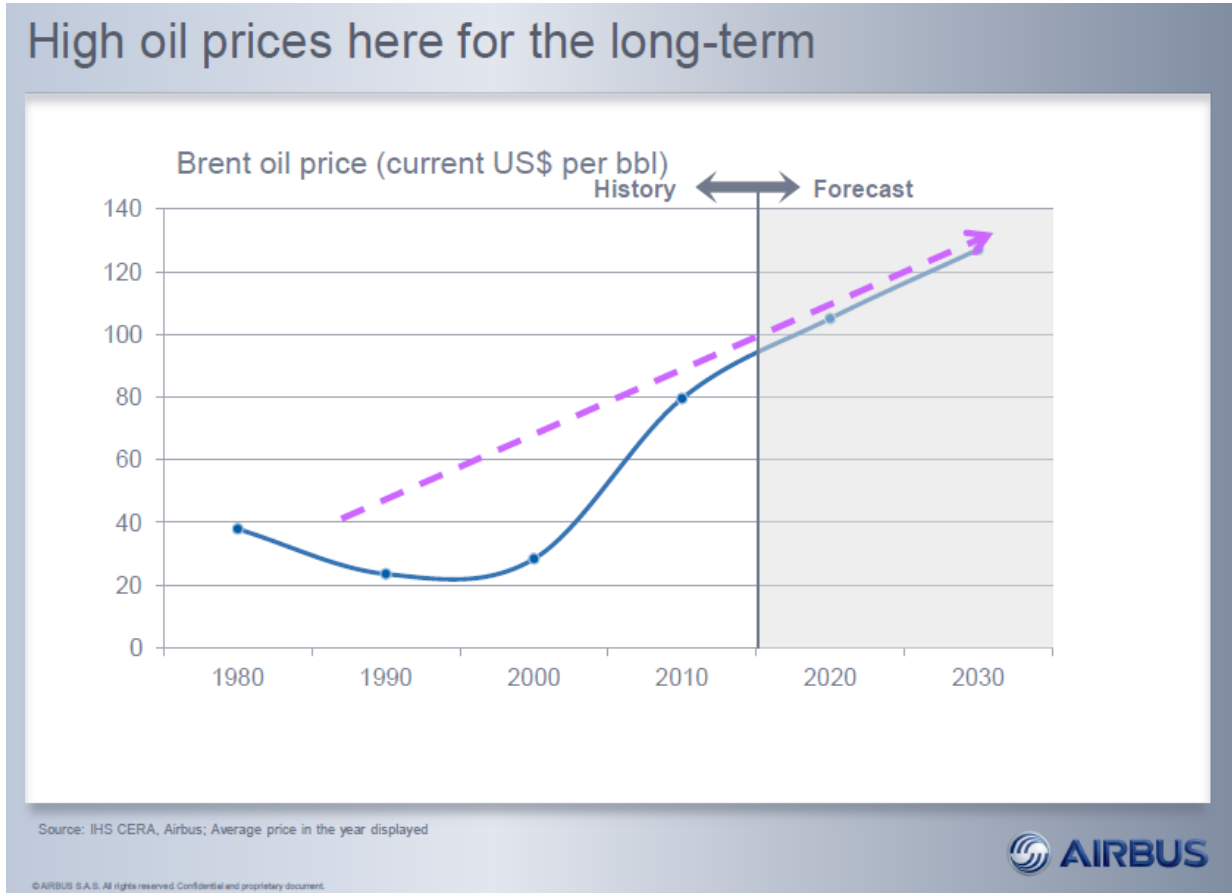


Figure 3.20 Airbus fuel price tendency prediction (Airbus 2012)

4 SBW Design Optimization

Once the modification of the tool was completed, the next step is the design optimization of a strut braced wing aircraft that matches the requirements. The process followed will be as here described:

- The first step will be the identification of the mission and its requirements, providing this way a start point for the design.
- Once the mission is described, the second step consists on identifying the design parameters that will be used for the optimization. After it, a *DOE Diagonal* analysis of all the design parameters will be performed, with the objective of understanding their behaviour and get a rough idea of the tendency that the optimum design might follow.
- Optimization of an Airbus 320 in a few steps, so it will meet the requirements for the design mission and serves as a comparison point to evaluate the potential benefits of the different designs with new technologies applied.
- Set up of OPerA for the calculations. Preliminary evaluation of the possible configurations and selection of the ones that will be selected on the first round.
- Preliminary optimization of the chosen configurations, keeping the requirements fixed to evaluate and find the configurations that have the biggest potential in optimization, savings and results.
- Analysis of the results, commenting them and selecting the most potential configurations for further optimization.
- Set up for optimization of the chosen configurations. Election of objective functions and requirements that will be set free and their boundaries. Second round of optimizations.
- Analysis of the results and selection of the final configuration. Further optimization of the chosen configuration, offering different options with different characteristics.

4.1 Mission Objectives

The first step before getting into the design of an airplane is the identification of the mission that has to be completed. It must be clear which m_{PL} , and which R must be achieved, i.e. the payload

and the range, respectively or, in other words, how many passengers must be carried how far. This way, the requirements can be identified and set. With this data it is also possible to decide which ICAO category suits better to the designed aircraft, so airport requirements can be as well identified. Finally, the certification rules will deliver the Second Segment and Second Approach climb gradients, completing this way the set of requirements needed to start design optimization in OPerA.

For the aircraft designed in this Thesis, it has been chosen to use the requirements proposed by the German Aerospace Centre (DLR) for their *Design Challenge*: Following the current tendency to search for new more economic designs that are at the same time less harmful for the environment (as *Airport2030* does), the German DLR has organized a design challenge, where universities from all over Germany and Europe are invited to participate, producing and exploring new configurations and technologies able to substitute the present aircraft. Currently the participants are working on these configurations (apart from the Strut Braced Wing aircraft, which is object of this Thesis):

- Blended Wing Body:

The Blended Wing Body concept (BWB, Figure 4.1) is an aircraft with divided fuselage and wing structure, unlike the Flying Wing aircraft. However, the wing structure is smoothly blended over the fuselage, making it look like a true flying wing. This type of aircraft has very high lift-to-drag ratio in comparison with present aircraft, with the potential of drastically reduce the fuel consumption or the noise contamination.

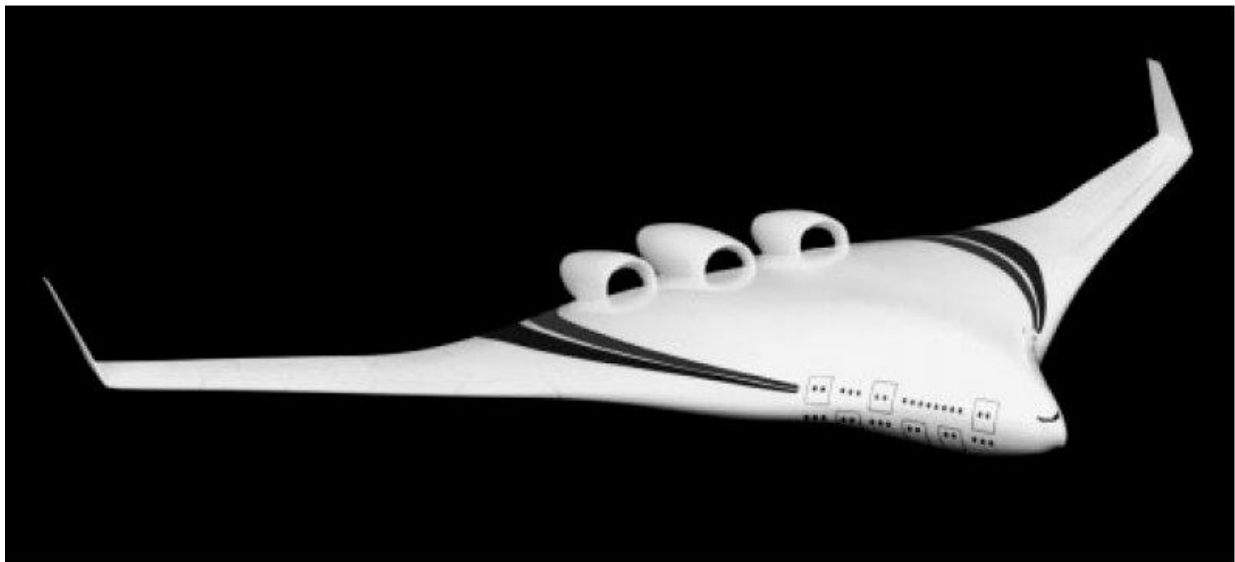


Figure 4.1 Blended Wing Body concept (NASA 1997)

- Box Wing:

Box wing aircraft (Figure 4.2) has two wing planes joined on the tips. This configuration produces less induced drag than conventional configurations and has several structural advantages (bigger structural strength), thus improving its fuel consumption. However, the

structure design might be complicated since the wing is heavier and some problems may appear on the wingtip.

- Cargo less aircraft:

The Cargo Less Concept, as seen in Figure 4.3 is based in the use of a new fuselage shape that is smaller than the conventional aircraft, having this way a smaller wet surface, which means less zero-lift drag and more efficiency. However, this new cabin concept implies that there is no cargo transported or passengers' luggage, which focuses the potential business on short low cost flights.



Figure 4.2 Box wing aircraft concept (Aero 2013)

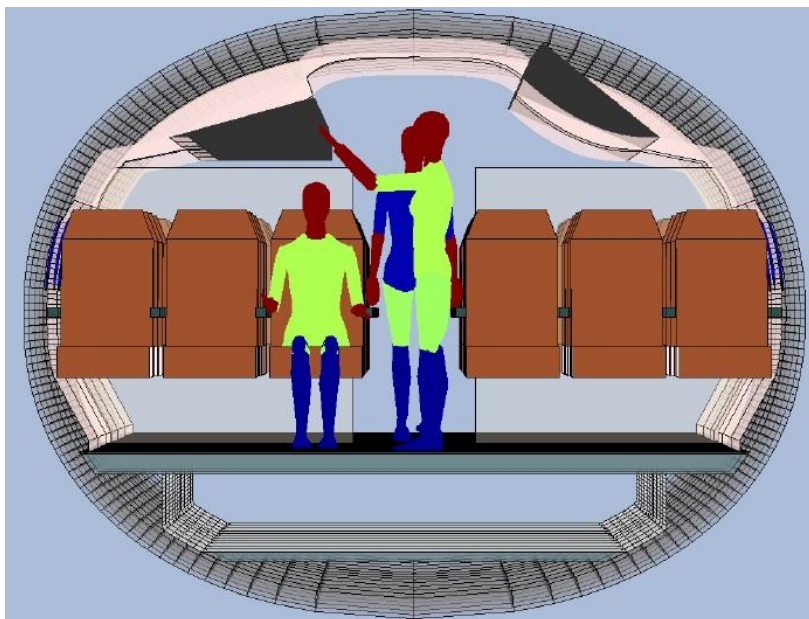


Figure 4.3 Cargo less aircraft concept cabin (DLR 2013)

The mission and the objectives are given by the DLR. They are shown in Table 4.1:

Table 4.1 DLR Design Challenge requirements

Design Requirements	
PAX	190 all economy @30" pitch 100 kg/pax payload capacity for high density layout @28" pitch
Range	2000NM (90 % of flights within Europe and USA < 500NM) Technical means to enable up to 2900NM range
TOFL	2000m, SL, MTOW, ISA + 15 °C
LDGFL	1500m, SL, MLW, ISA +15 °C
Mach	0.79
Initial Climb/Max. Altitude	FL350/FL410
Span	Max. 36 m or technical means to achieve ICAO class C
Noise	-5 dB cum. vs. Chapter 4
Fuel burn	-25 % versus A320 (CFM) 2009
Emissions	Near zero emissions at gate and during taxi
COC	-30 % versus A320 (CFM) 2009

As is it possible to see, the payload ascends up to 190 pax, and the range is 2000 NM. Those will be the fixed requirements of the airplane. It is of interest for the design in OPerA the lengths of the takeoff and landing fields, which is 2000 m and 1500 m respectively. The Mach number is specified as well, taking a value of 0.79, and the requisite of the Second Segment and Missed Approach are already set into OPerA, based on certification rules. It is important to note that OPerA does not perform calculations of noise nor emissions, so those requirements will be not considered here, and they would be later taken into account in future design phases. However, aiming for low fuel consumption or higher by-pass ratio engines will derive less noisy engines with low fuel consumption, which means low emissions. In addition, it is possible to see that one of the requirements is a 30 % savings in COC with respect to the Airbus 320 with CFM engine of 2009. This requirement is seen more as a hypothetical goal, since it means huge savings that

are very difficult to achieve without changing the whole concept of an aircraft. However, and taking into account the results shown in **Nita 2012** with the SBW and the NFL technologies, the -25 % in fuel burn goal respect to A320 seems possible to complete.

All this DLR indications are enough to identify the requirements and design parameters that will be used in OPerA, by setting them free, limited or fixed in the *Optimization Set up* module. They are shown in Table 4.2.

Table 4.2 List of requirements, fixed parameters and design parameters for the design

Requirement/ Fixed parameter	Value	Design parameter	Low limit	High limit
Takeoff field length $TOFL$	2000 m	$C_{L,max,TO}$	2.5	3.14
Landing field length LFL	1500 m	$C_{L,max,L}$	2.5	3.14
Number of passengers n_{PAX}	190	m_{ML}/m_{MTO}	0.86	1
Cruise Mach number M_{CR}	0.79	AR (depends on span limit)		
Number of engines n_E	2	φ_{25}	0°	35°
		λ	0.01	0.5
		z_H/b_V (when cruciform tail)	0.01	0.99
		h_P/D_N	0.1	0.3
		BPR	6	15
		$d_{ENG,F}$ (when engines on fuselage)	0.2	0.5
		$l_{F,MLG}$ (when MLG on fuselage)	0.5	0.7

With respect to the cabin configuration, the cabin of the new aircraft will use the same parameters as the A320: these will not be varied. The parameters are:

Table 4.3 Cabin parameters

Parameter	Value
Seat abreast n_{SA}	6
Seat pitch SP	0.7366 m
Aisle width w_{AISLE}	0.508 m
Seat width w_{SEAT}	0.508 m
Armrest width $w_{ARMREST}$	0.0508 m
Side clearance $s_{CLEARANCE}$	0.015 m

4.2 Single Parameter Study

Before starting with the design optimization of the new aircraft, it is recommended to perform a preliminary study of all the design parameters that will modify the new aircraft. This is done because the use of the tool must be supervised by the designer, and thus he needs to understand how the tool works and how the variables behave, in order to be able to detect possible failures or inconsistent results, as well as being able to predict the tendency that the optimum will presumably follow.

In this study all the design parameters will be varied one by one, checking and commenting the results, if they are within the expected, and previewing possible optimum configurations. For the study the reference A320 included in OPerA will be used, with the fuel price of 2009, and the objective function will be COC calculated with the TUB method. The parameters used for the reference A320 and their corresponding result when executing the order *Find Design Point with CG* in OPerA are the following:

Table 4.4 OPerA results for reference standard A320 (CFM) 2009

Parameter	Value	COC €/ton/mile	MTO kg	OEW kg	MF Kg
<i>TOFL</i>	1447.8 m	0.731470	72648	40000	13033
<i>LFL</i>	1767.83 m				
$C_{L,max,L}$	3.14				
$C_{L,max;TO}$	2.82				
m_{ML}/m_{MTO}	0.8776				
<i>AR</i>	9.5				
n_E	2				
n_{PAX}	180				
n_{SA}	6				
φ_{25}	25°				
λ	0.213				
h_p/D_N	0.1524				
<i>BPR</i>	6				
M_{CR}	0.76				
<i>SP</i>	0.7366 m				
w_{AISLE}	0.508 m				
w_{SEAT}	0.508 m				
$w_{ARMREST}$	0.0508 m				
$s_{CLEARANCE}$	0.015 m				

4.2.1 m_{ML}/m_{MTO}

This parameter indicates the quantity of fuel spent during the flight, in the form of the ratio between the maximum takeoff mass and the maximum landing mass. When this parameter is set free and travels between the boundaries, the result is the following (Figure 4.4):

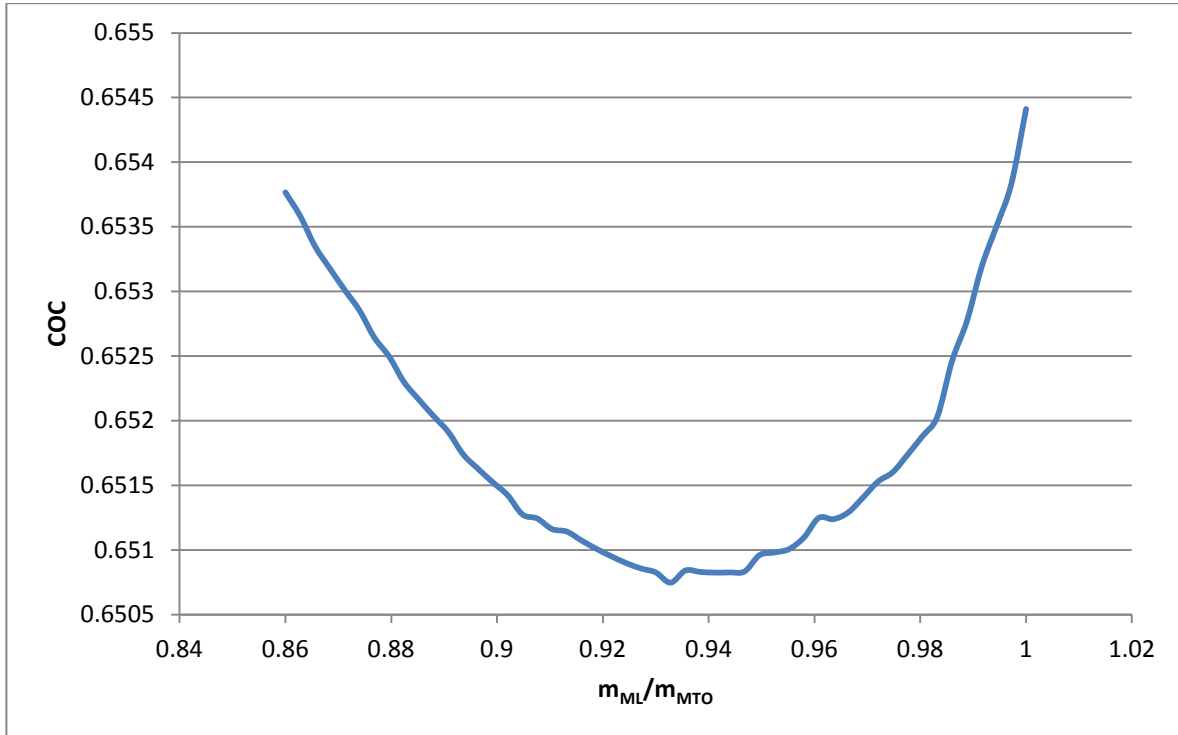


Figure 4.4 COC variations with m_{ML}/m_{MTO}

As it can be observed, increasing the ratio of m_{ML}/m_{MTO} reduces the COC because this reduces the fuel mass as well and the maximum take of mass, this means that the aircraft uses less fuel. However, when the minimum is achieved, the total takeoff mass starts to increase, which means that, even when the fuel mass ratio can be smaller, the total weight is increasing, as can be appreciated on Figure 4.5, where the evolution of the fuel mass and the takeoff mass is represented, divided each by its respective minimum, so the smallest value that both curves achieve is 1 (done this way to show the tendency and not the absolute values):

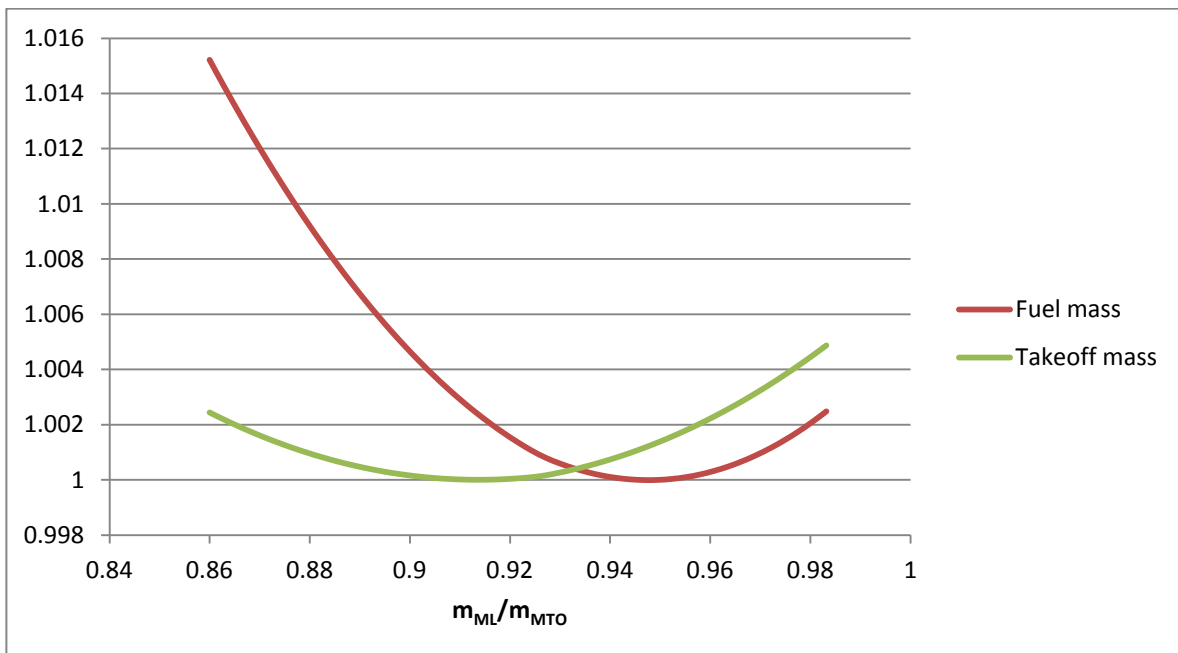


Figure 4.5 Evolution of fuel mass and takeoff mass with m_{ML}/m_{MTO}

From Figures 4.4 and 4.5 is it logical to expect the optimum being a little bit higher than the original 0.87 of the reference A320 aircraft. However, this experiment varies only m_{ML}/m_{MTO} and is only valid to understand the behaviour and influence of the variable, so it is possible that when performing the real optimizations different results occur due to the influence of other variables.

4.2.2 Aspect Ratio

The aspect ratio comes from the following expression:

$$AR = \frac{b^2}{S_W} \quad (4.1)$$

The aspect ratio is basically a measure of how narrow the wing is, by relating the wing span with the wing surface. It has great influence on the aircraft aerodynamic efficiency, i.e. the lift-to-drag-ratio, since the drag depends directly of it in the polar expression:

$$C_D = C_{D,0} + \frac{C_L^2}{\pi \cdot A \cdot e} \quad (4.2)$$

From (4.2) is easy to see that, the bigger the wingspan, the smaller the drag. However, increasing the wingspan increases the wing size as well, and thus increases the zero-lift drag, which depends on the wet surfaces of the aircraft. Performing the experiment gave the following result (Figure 4.6):

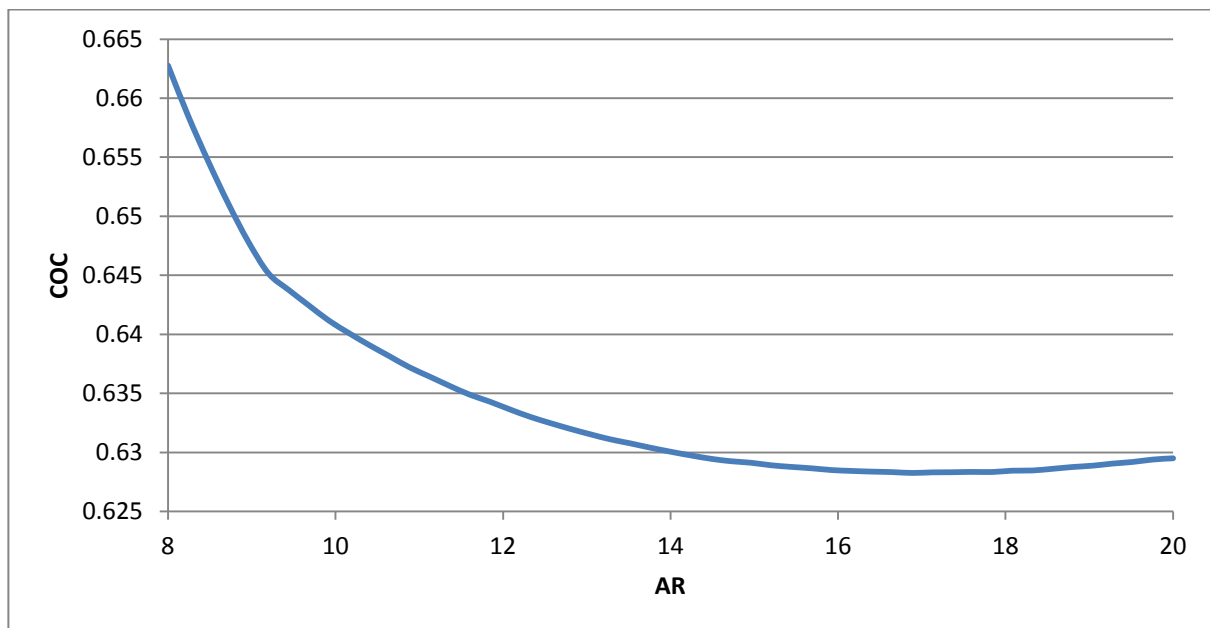


Figure 4.6 Results of experiment varying the wing aspect ratio

As expected, increasing the aspect ratio reduces the COC, for the aircraft becomes more efficient and burns less fuel. However, there is a minimum, and after it, the increase in wing span makes the wing heavier, because the wing bending moment becomes higher. Results shown in Figure 4.6 are done on a cantilever wing, and it is expected that installing supporting struts under the wing will shift the minimum to the right, so higher spans are achievable, and thus bigger wing efficiency.

4.2.3 Sweep Angle (φ_{25})

φ_{25} is the sweep angle of the 25 % chord line of the wing. Increasing the sweep angle of the wing is necessary to wing at higher speeds that go to close the speed of sound, This is because on swept wings the air flow can be divided in two components (Figure 4.7): on one side, the flow from the leading edge to the trailing edge of the wing, and on the other hand the flow perpendicular to that one, from the wing root to the wing tip. By building a wing like this, the flow from leading to trailing edge is approximately reduced by:

$$M' = M \cdot \cos (\varphi_{25}) \quad (4.3)$$

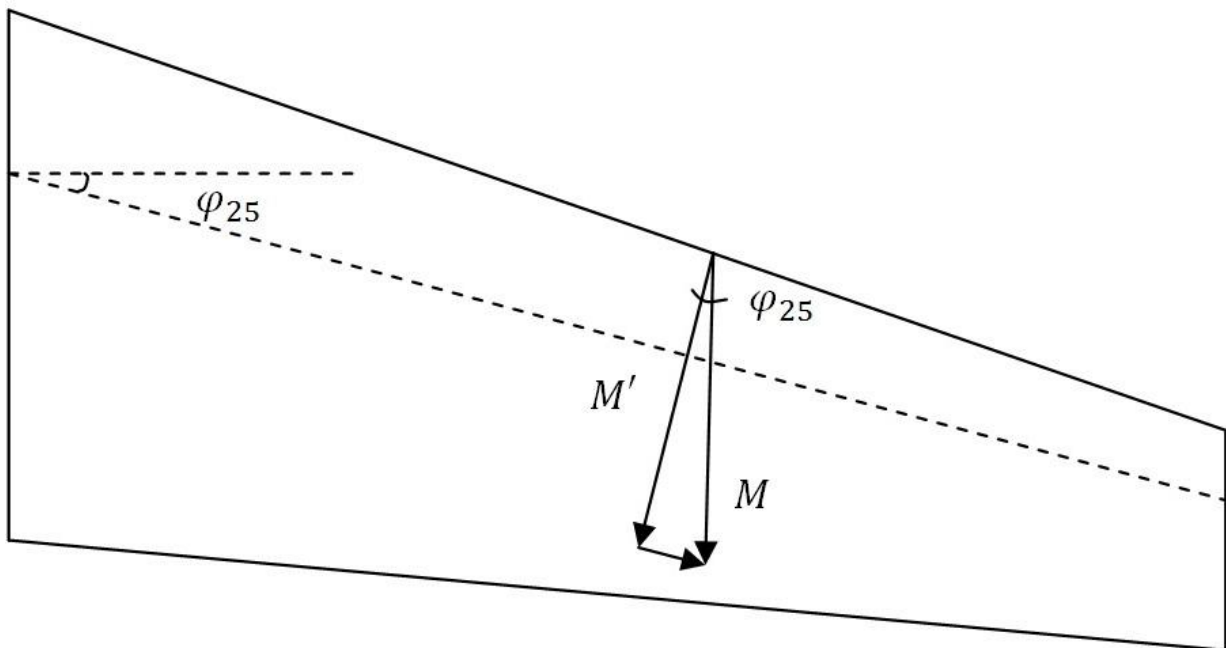


Figure 4.7 Flow over a swept wing

This reduction of the speed delays the compressibility effects derived from flying at transonic speeds. However, increasing too much the sweep angle can make the wing weight grow too much, and it can as well increase the drag, since the air runs longer over the wing surface, making the boundary layer thicker and eager to turn turbulent. Low sweep angles allow the use

of *Natural Laminar Flow* technology (NLF), a way to reduce the wing drag and make the wing more efficient. Figure 4.8 shows the result of varying the sweep angle for different speeds:

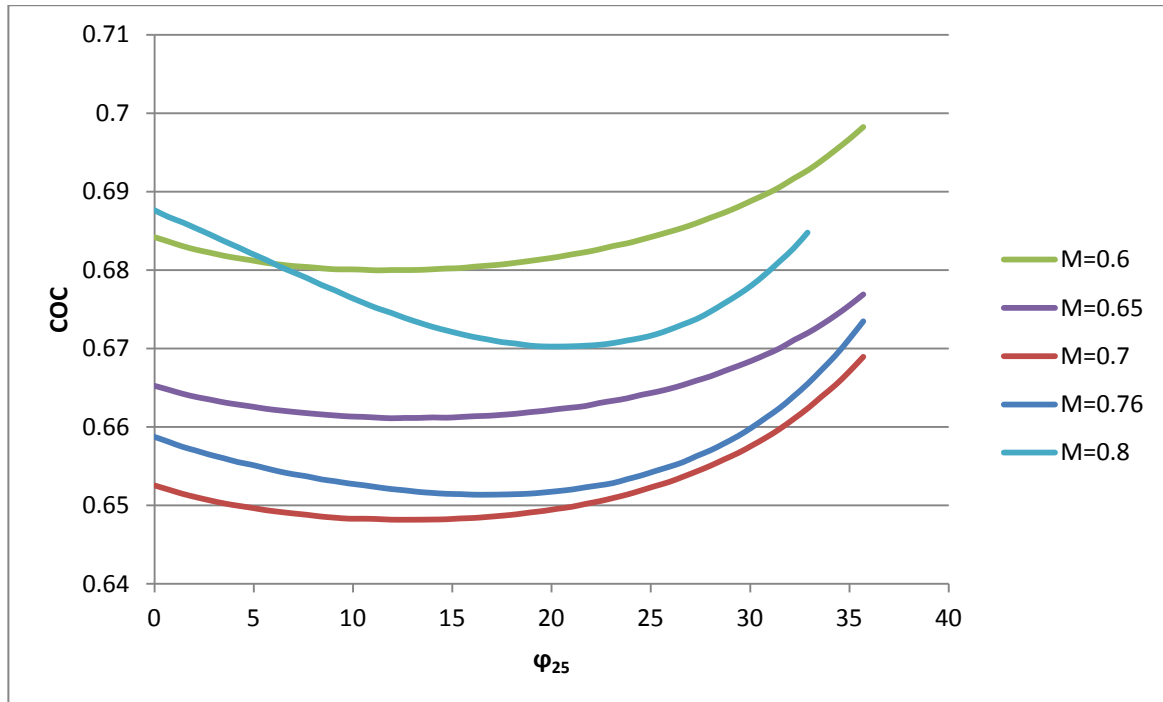


Figure 4.8 Results of varying the sweep angle for different cruise Mach numbers

Is it possible to observe that reducing the sweep angle from the original 25° has a positive effect on the overall result, no matter what the speed are. However, is it also possible to observe how the COC goes down as the speed goes down as well, but it increases again for $M = 0.65$, the explanation of this comes with the speed itself: flying slower means flying less, and that increases the cash operating cost. It is possible to see as well that the optimum sweep angle is smaller with slower speeds as expected, because of the compressibility effects (or the lack of them) at lower speeds. The overall optimum it is expected here as a compromise between speed and efficiency, and an increased effect when using the NLF technology.

Another interesting result is the influence of the sweep angle on the wing mass depending on the speed (Figure 4.9). At lower speeds, low sweep angle makes the wing lighter. However, increasing the speed not only gives a heavier wing, but also, as expected, eliminates the advantages of having lower sweep, being the wing heavier at lower sweep angles as well. This would help understand, for example, the different tendency that the optimizer can get when setting as objective function other function that is not COC, such as wing mass, or takeoff mass.

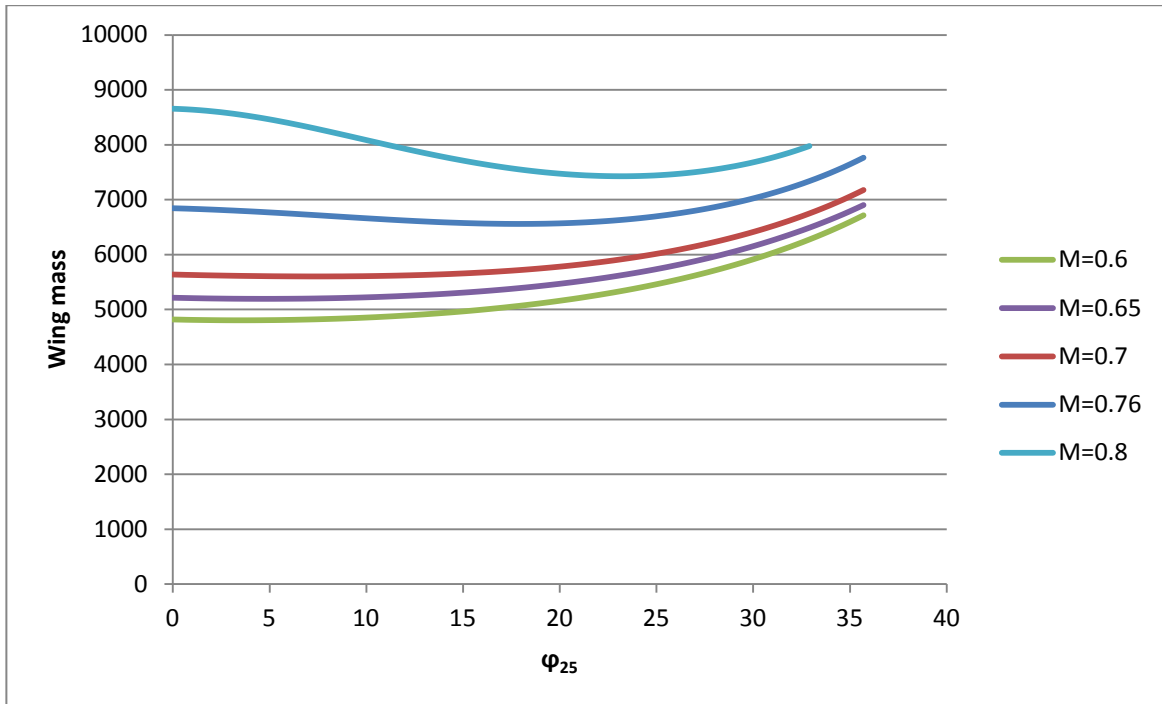


Figure 4.9 Wing mass variations with the sweep angle for various speeds.

Finally, the last experiment with the sweep angle is the influence that this has on the wing thickness. Figure 4.10 shows how t/c varies with the sweep angle. As seen, lower wing sweep and thinner wings come together, which means less aerodynamic drag. This is an advantage used by the strut braced wing technology: by using struts, the wing can be thinner, and thus smaller sweeps can be used. It is also possible to see that higher speeds get smaller thickness ratios: this is because thinner wings are needed to fly at higher speeds to reduce the aerodynamic drag.

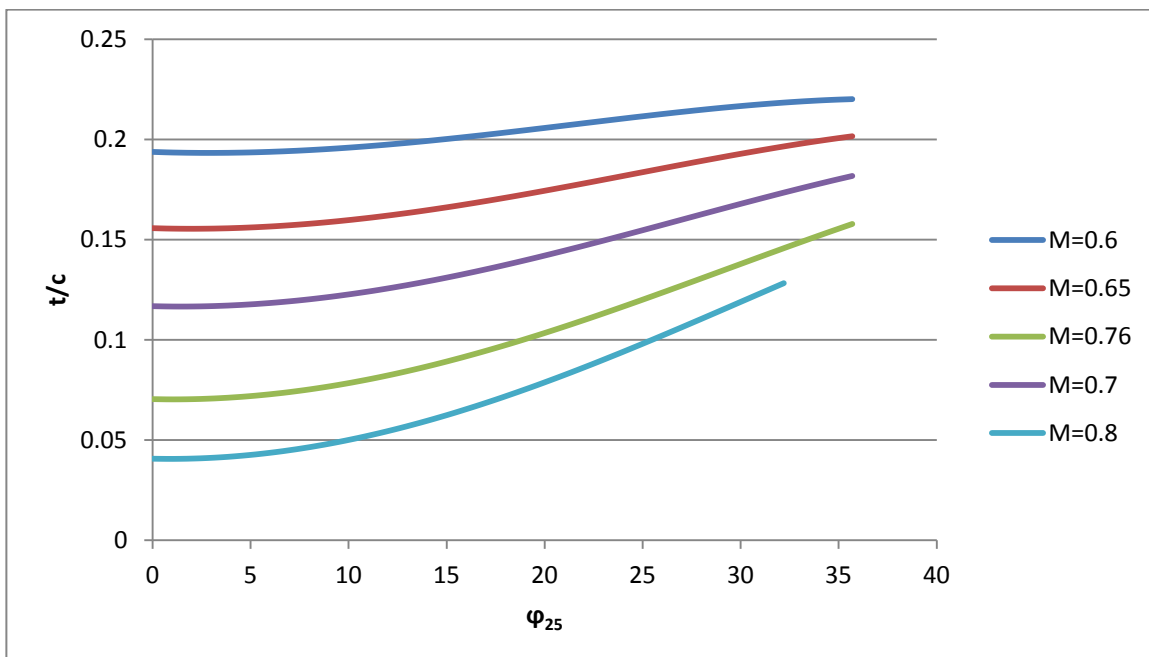


Figure 4.10 Thickness ratio variations versus sweep angle

4.2.4 Taper Ratio

Taper ratio is defined as the ratio between the wingtip chord and the wing root chord:

$$\lambda = \frac{c_T}{c_R} \quad (4.4)$$

The information that the taper ratio is giving is the planform shape of the wing. For the wing aerodynamic efficiency to be the biggest possible, the planform shape of the wing must be as similar as possible to the elliptical wing, which is reflected on the equations with the Oswald efficiency factor. This factor depends as well of the taper ratio of the wing, which means that the taper ratio has an important influence on the wing aerodynamic efficiency. However, it must be considered that a high wing taper ratio affects negatively to the wing weight, as can be seen on Figure 4.11, by shifting the half wing centre of mass outboard, creating bigger wing root bending moments. On the other side, with too low taper ratio may become hard to hold the main landing gear on the wing (a factor that would not be a problem if a high wing configuration is selected), and can bring aerodynamic problems on the wing tip. As shown in Figure 4.12, reducing the wing taper ratio helps reducing the COC, so it is expected that the optimum design follows this tendency, both when COC, fuel mass and takeoff mass are selected.

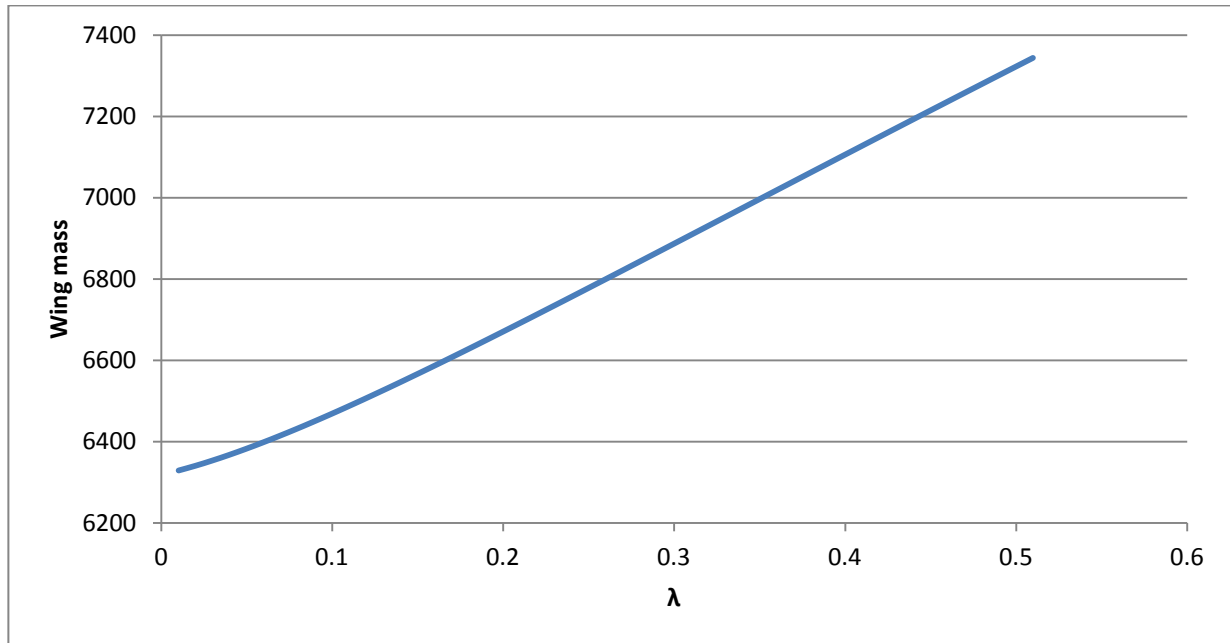


Figure 4.11 Wing mass variation with the taper ratio ($M = 0.76$)

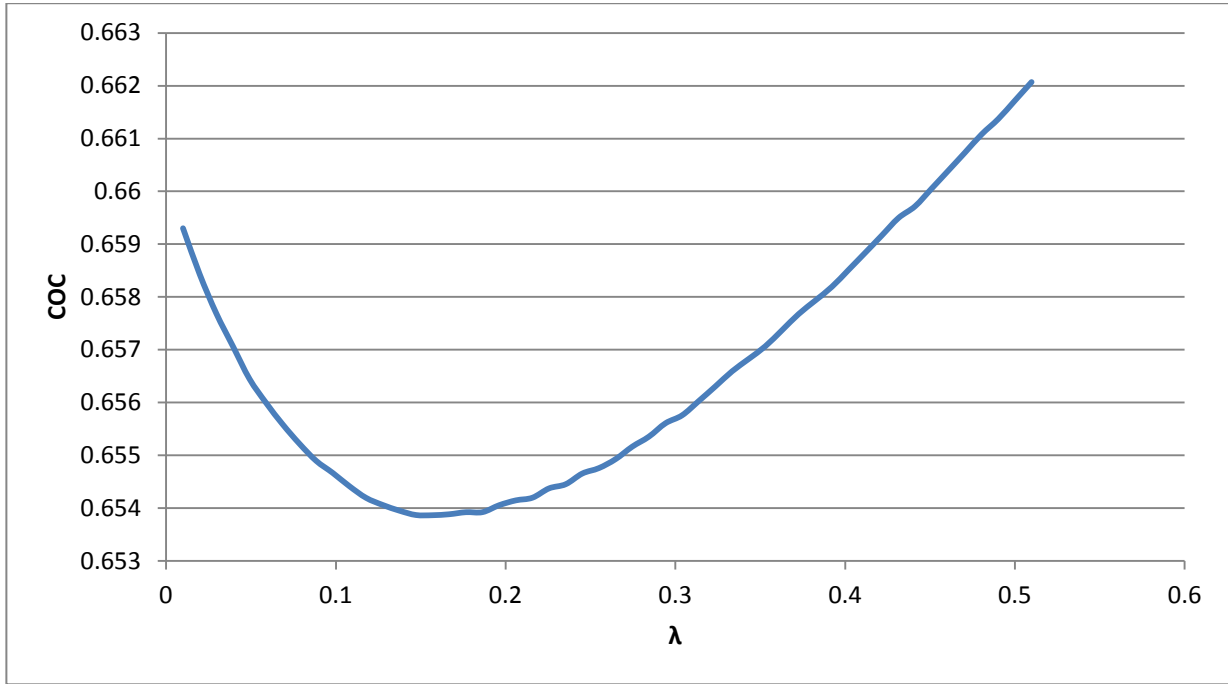


Figure 4.12 COC variation with taper ratio ($M = 0.76$)

4.2.5 By-pass Ratio

Engines nowadays are designed in a way that they divide the air flow in two different streams: one of them flows inside the engine turbine, and is burned, and the other goes around (Figure 4.13). The by-pass ratio is defined as the ratio between the air mass that flows through the ducted fan and the mass flowing inside the turbine and the combustion chamber. A bigger by-pass ratio means smaller thrust specific fuel consumption, especially at low altitudes, although this way the engine size and weight increases. Another advantage from the higher by-pass ratio engine is that they produce less noise, which is good for the requirements that new aircraft must meet. Analyzing this parameter with OPerA delivers the result for COC shown in Figure 4.14.

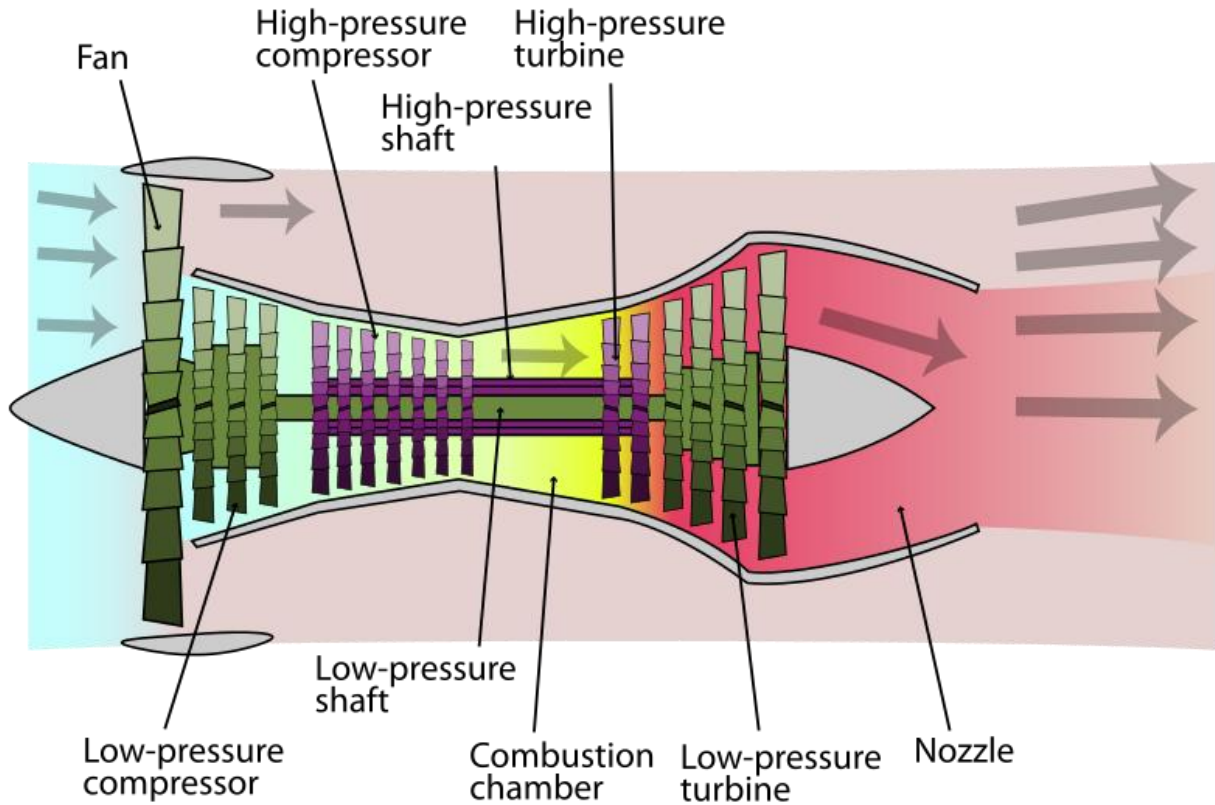


Figure 4.13 Engine with high by-pass ratio (Wikipedia 2013)

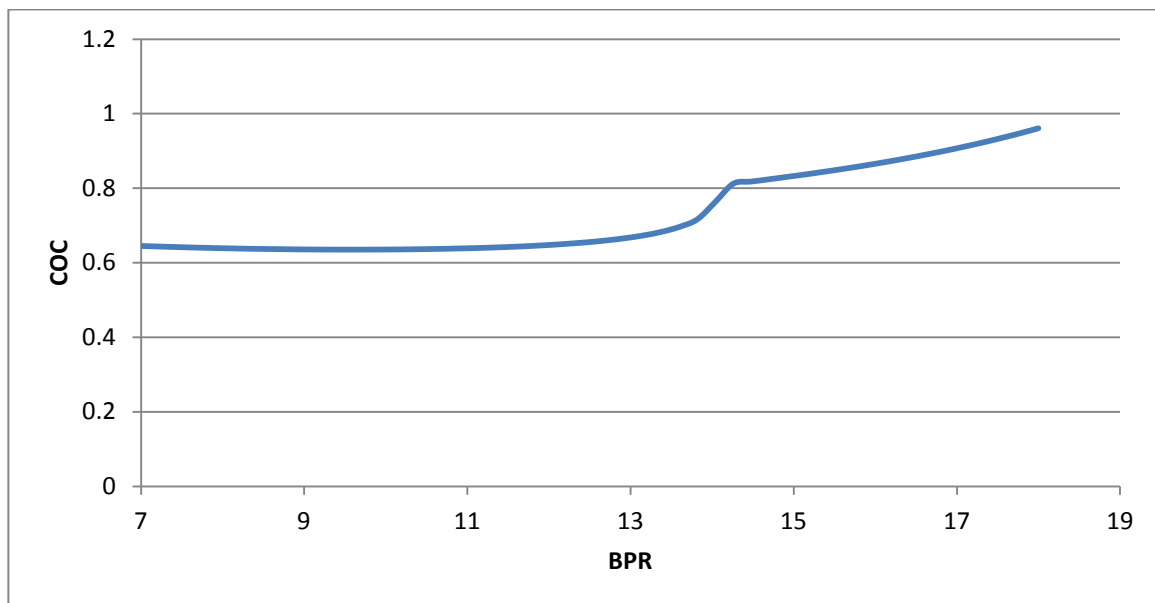


Figure 4.14 BPR variations versus COC

As it can be seen in the results, increasing the by-pass ratio of the engine is beneficial, because the increase on the by-pass ratio means a decrease in the thrust to weight ratio. However, when the by-pass gets too high, the weight of the engines gets high as well, which is bad for the COC. In addition, the zero-lift drag of the airplane increases as well when this happens, because the size of the engine comes with an increase of its wetted area.

It is also of interest to consider the flight altitude when the by-pass ratio is analyzed. This is because the advantages of higher by-pass ratios are more noticeable at lower altitudes. OPerA gives the flight altitude depending on the design point with the cruise speed line. Figure 4.15 shows the flight altitude versus the by-pass ratio. As it can be seen there, higher by-pass ratios are better in lower altitudes, up to the point where the kink on the line appears: there the Cruise line of the Matching Chart is not dimensioning anymore, but the Second Segment Climb line, and thus the design point altitude varies much less, being almost constant. This kink is also visible in Figure 4.14. What is it possible to extract from here is that the by-pass ratio of the optimum configuration will grow depending on the flight altitude, so if the optimum aircraft flies lower is it expected to find higher by-pass ratio.

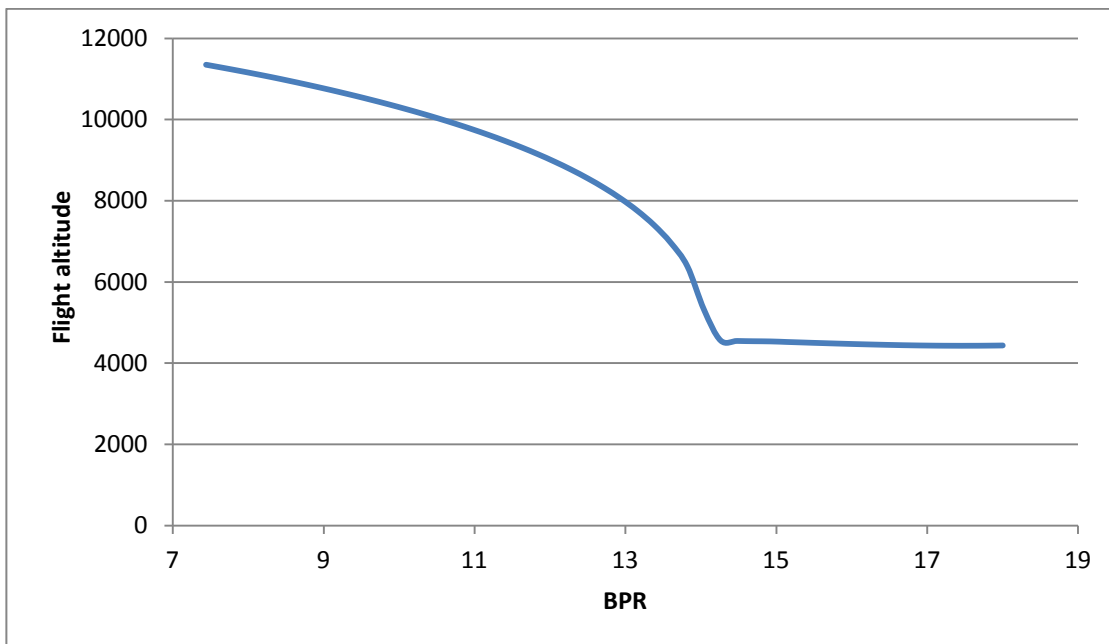


Figure 4.15 By-pass ratio versus flight altitude

4.2.6 Relative Distance between Engine and Wing

This parameter represents the vertical distance between the wing and the engine divided by nacelle diameter. Basically it has an impact on the wetted area of the pylon, increasing the zero-lift drag produced by it when it increases. It has as well an impact on the length of the main landing gear; this means that, the further is the engine from the wing, the longer the landing gear gets, because the engine not only must not touch the ground, but as well have a certain clearance to avoid impacts on landing. The longer the main landing gear is, the heavier it gets. This parameter, when acting together with BPR, can make the landing gear too long, and thus too heavy. Figure 4.16 shows the impact of h_V/D_N on the main landing gear length for different values of BPR. From the results it is noted that the distance between the engine and the wing should be as small as possible, but taking into account that the closer it gets to the wing, the bigger aerodynamic interference produces, and then reduces the lift-to-drag ratio.

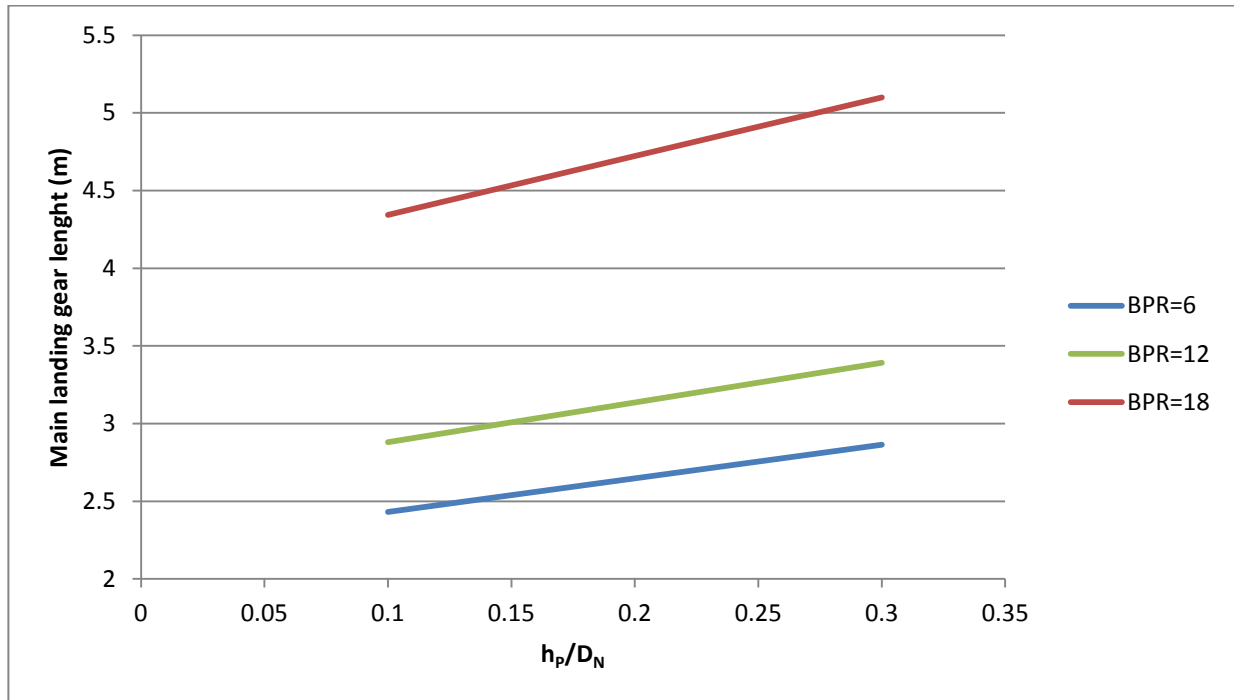


Figure 4.16 h_p/D_N versus main landing gear length, for various *BPR*

4.2.7 Horizontal Tail Position

One of the most important aspects of the aircraft configuration is the empennage position. The tail can be shaped in many different ways (Figure 4.17), each one of them having different advantages and disadvantages. OPerA offers full support for three of this configurations: the lower (conventional) tail, the cruciform tail, and the T-tail. The difference between these three configurations is basically the position on which the horizontal tail lies along the span of the vertical tail fin. This is measured with the parameter z_H/b_V , which is the height of the horizontal tail divided by the total vertical tail span. In order to activate this parameter in OPerA, the tail must be set as cruciform. Otherwise, when telling OPerA that the tail is either conventional or T-tail, this parameter will be fixed on the value zero or one, respectively.

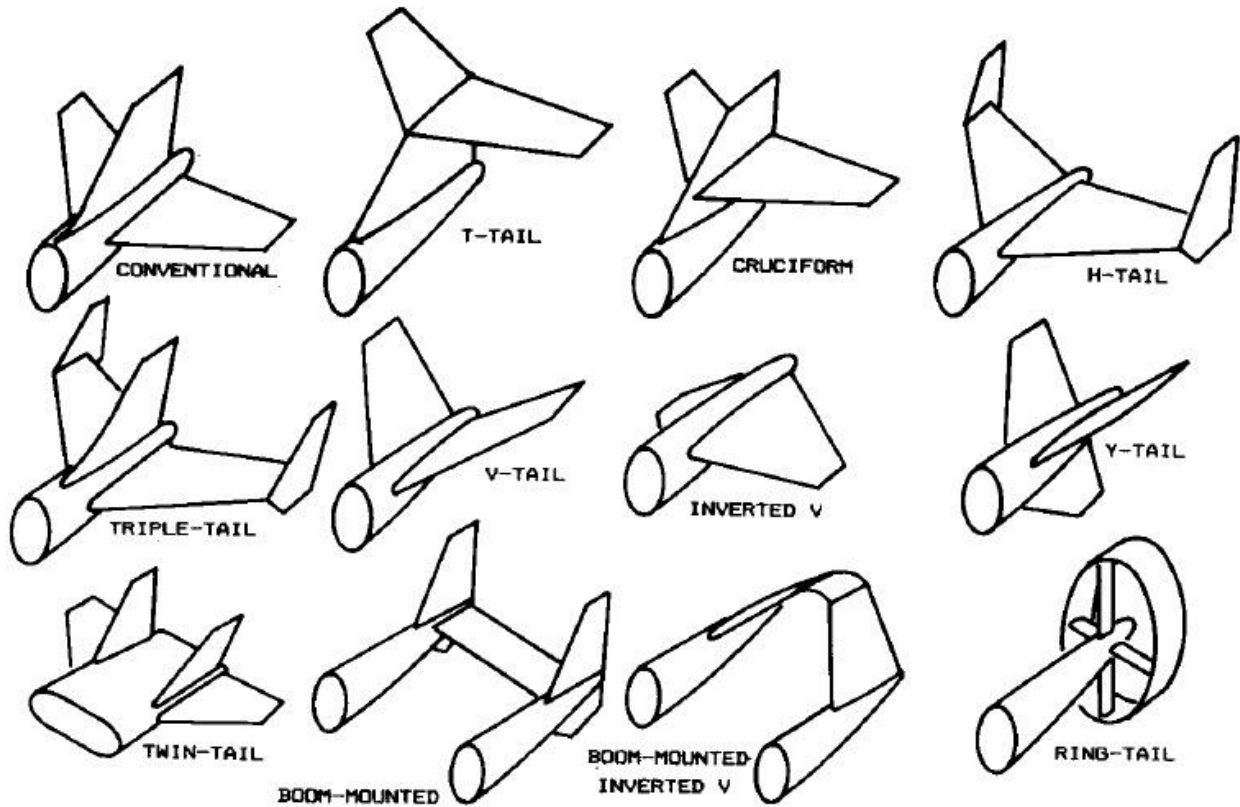


Figure 4.17 Different tail configurations (Raymer 2006)

By setting the tail as cruciform, the parameter z_H/b_V can vary freely from zero to one, moving the horizontal tail plane upwards from conventional tail to T-tail. Moving the tail upwards have aerodynamic benefits, because the tail gets out of the influence of the wing wake, and thus the dynamic pressure over it is bigger, being the tail this way more effective and therefore smaller. However, aerodynamic improvement is not the only effect that appears when shifting the horizontal tail plane upwards. Another effect, that proved to be very important, is the influence of the tail position on the centre of gravity: The previous version of OPerA did not take gravity centre into account. That means that the tail lever arm, one important part of tail size calculation, was estimated as half of the fuselage length. The horizontal and vertical tail surfaces are estimated with the expression for the tail volume coefficient:

$$S_T = \frac{C_H \cdot S_W \cdot c_{MAC}}{l_H} \quad (4.5)$$

$$S_V = \frac{C_V \cdot S_W \cdot b}{l_V} \quad (4.6)$$

As it can be seen, the bigger the lever arms are, the smaller the tail surfaces are. When the lever arms were estimated as half of the fuselage length, this parameter had no big influence on the surface because it was constant. Now, taking into account the gravity centre of the wing means that the tail arm is variable, and thus the tail surface and mass. Moving the tail upwards initially means that the horizontal tail surface gets smaller, but the vertical tail fin gets heavier (it must support the horizontal tail). This shifts the gravity centre backwards of the plane, reducing the

lever arm and therefore increasing the tail surfaces. This process converges to the corresponding centre of gravity of the design point, giving the final result. It was noted that the difference of including or not mass centre calculation was quite important, as shown in Figure 4.18. There is possible to see how the COC goes down with upper horizontal tail if the gravity is not considered, and up if it is. This result reflects that the influence of the gravity centre position is very important for tail sizing. In addition, it must be considered as well that, when shifting the horizontal tail upwards, there is a possibility to position it in the forbidden area marked on **Raymer 2006** which risks the airplane to enter in deep stall. Figure 4.19 shows how the mass of the vertical and the horizontal tail are affected by the tail position: the horizontal tail gets lighter, while the vertical tail gets heavier.

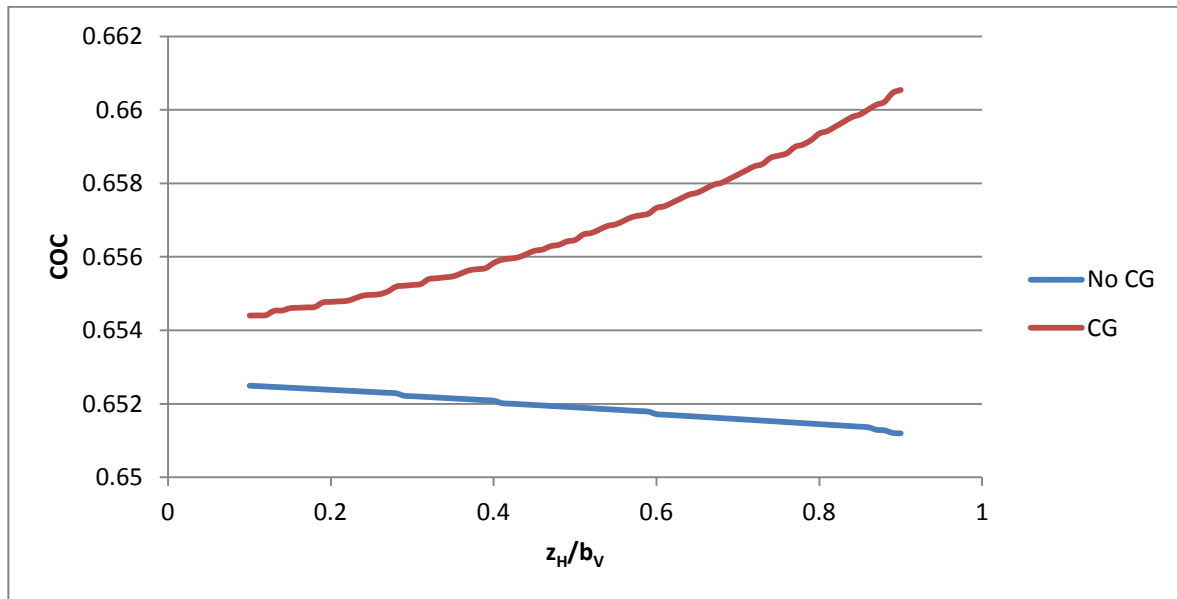


Figure 4.18 Comparison of the effect of centre of gravity calculation in tail position

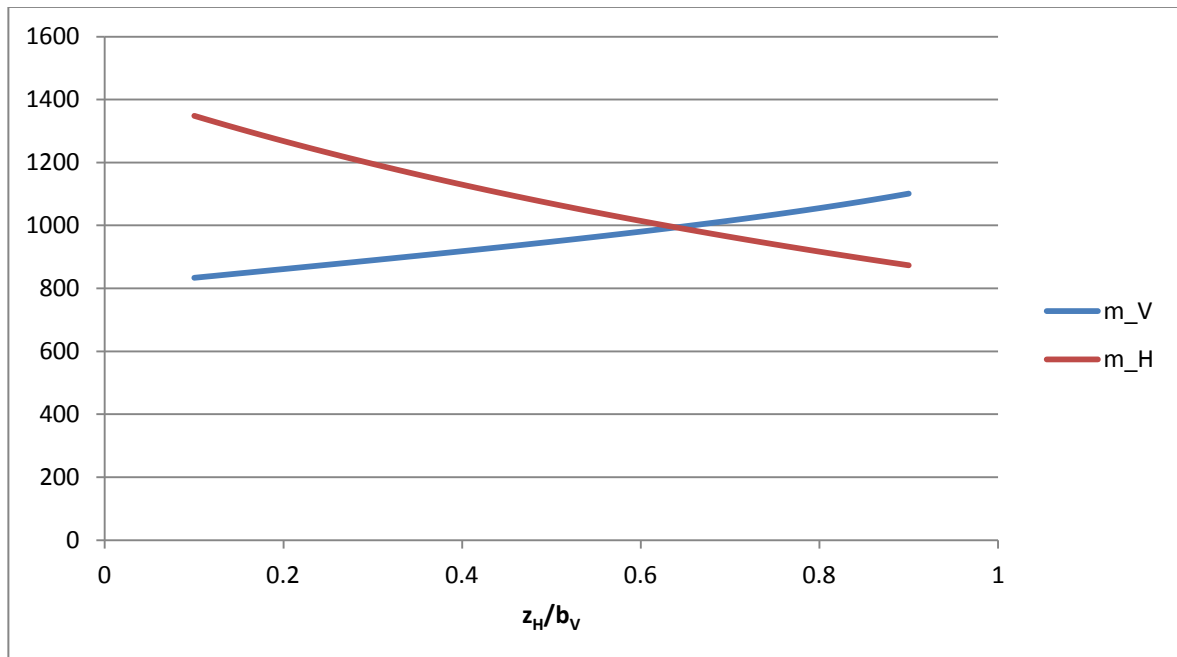


Figure 4.19 Effect of tail position in tail mass

4.2.8 Engine Position on Fuselage

As said before, it has been included in OPerA a new module that gives the tool the ability to estimate the position of the centre of gravity. As a consequence of this a more realistic estimation becomes possible, when the aircraft is configured to have engines mounted on the fuselage. Therefore, a new design variable has been added to OPerA. This new variable is the position of the engines on the fuselage. The variable ($d_{ENG,F}$) represents the distance between the engine centre of gravity and the aft end of the fuselage, divided by the total length of the fuselage. It was chosen this way, because OPerA offers also the option to situate the engines in an average position taken from statistical values (reflected in the module *Other Sources*), and this values were measured from the aft fuselage. Figure 4.20 shows the effect of varying the position of the engines on the fuselage (the engines were set as mounted on the fuselage).

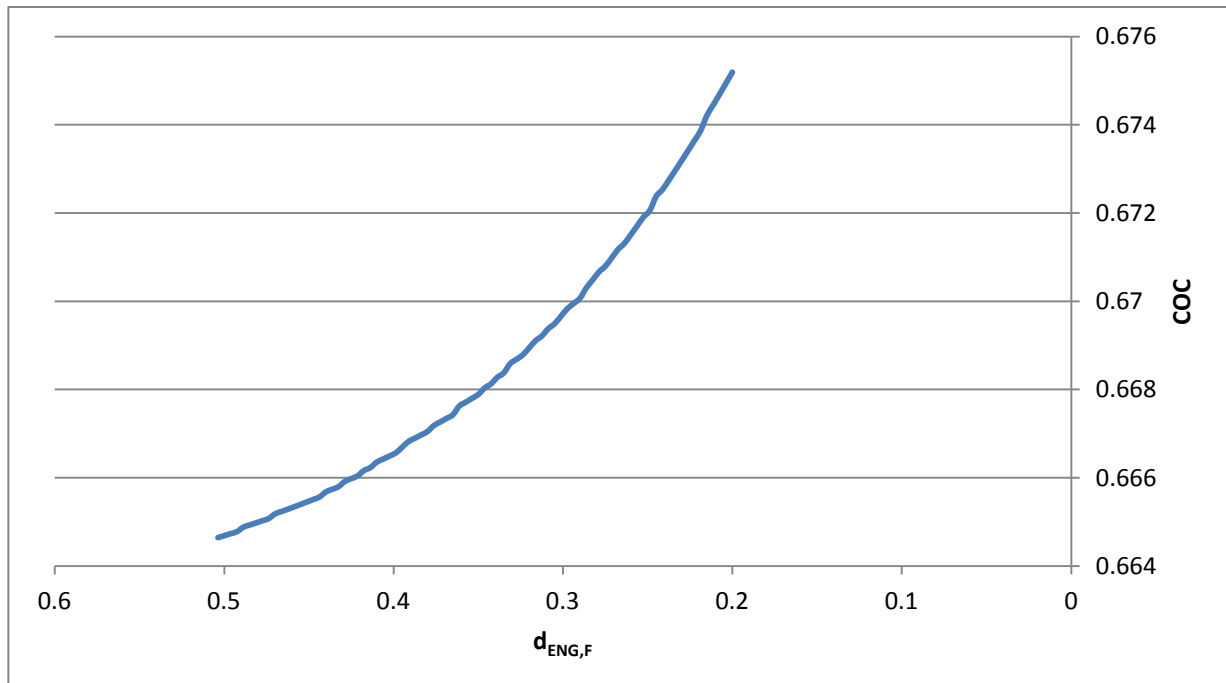


Figure 4.20 Variation of engine position over the fuselage

After performing the single parameter analysis in OPerA, the results are the expected ones: Shifting the engine to the aft part of the fuselage makes the COC increase, because the centre of gravity travels backwards as well, making the aircraft heavier. This effect is worse when the bypass ratio increases, since the engine weight is bigger the bigger *BPR* is. In addition, mounting the engines on the fuselage forces to use cruciform or T-tail, and that contributes even more to this effect.

4.2.9 Main Landing Gear Position

Another design parameter added in OPerA when working on this project is the position of the main landing gear, when this is mounted on the fuselage. This is done because the strut braced wing configuration uses high wing, and therefore is better to install the main landing gear on the fuselage rather than on the wing. The parameter is set as the distance of between the aircraft nose and the mass centre of the main landing gear, divided by the fuselage length. As shown in Figure 4.21, this parameter has similar influence than the position of the engines, because what is done is basically the same: moving a mass along the x-axe of the aircraft. However, its influence is smaller than the engine position, since the mass of the main landing gear is obviously smaller. The conclusion is that the closer the main landing gear gets to the gravity centre, the less influence it has in the rest components, and thus is more beneficial for the aircraft COC.

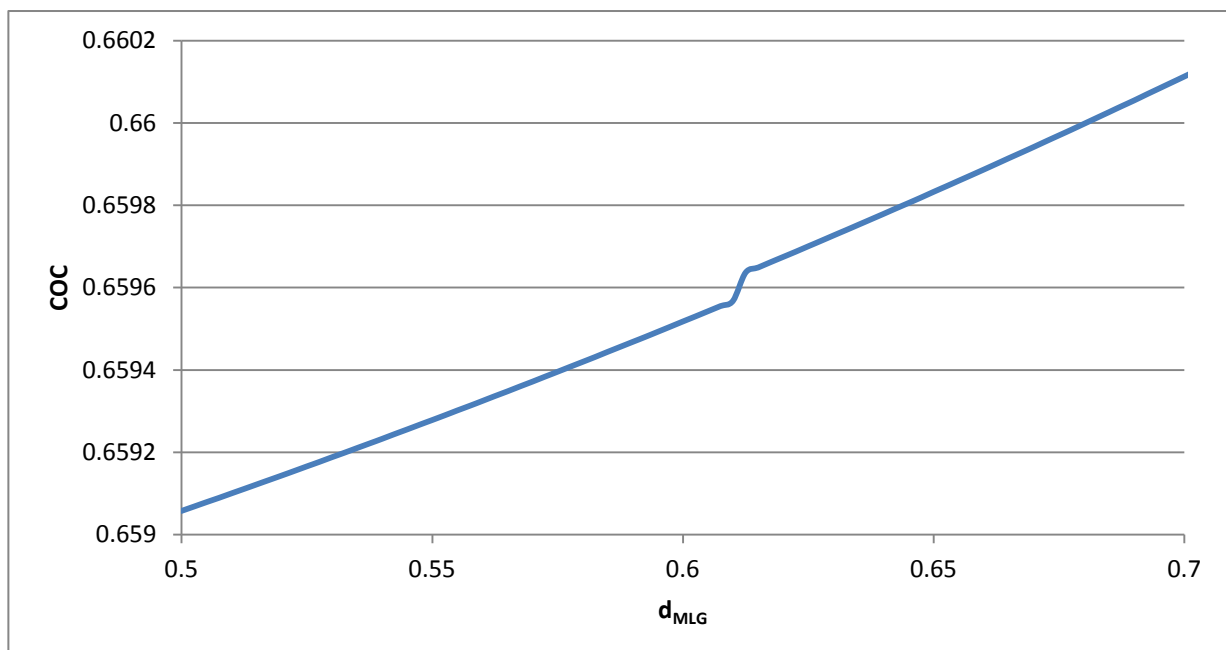


Figure 4.21 Influence of the main landing gear position over the COC

4.2.10 $C_{L,max,TO}$ and $C_{L,max,L}$

These two parameters were left to the end because they must be varied together. This means that the analysis performed for evaluate their influence was not DOE but DE evolution. The parameters were set free with COC as objective function. The results showed in Figure 4.22 show that the minimum COC comes when both parameters grow and become similar in value. When the two maximum lift coefficients grow higher, more lift is produced, and therefore taking off and landing can be performed at slower speeds. In equations (3.5) and (3.6) is it possible to see that, the bigger the lift coefficients are, the less restrictive their lines on the Matching Chart

are, therefore shifting the design point to another with less thrust-to-weight ratio and bigger wing loading, both of them conditions that lead to more optimum design points. $C_{L,max,L}$ and $C_{L,max,TO}$ have also an influence in the maximum lift-to drag ratio on the Second Segment And Miss Approach lines, modifying them as well and changing the optimum design points.

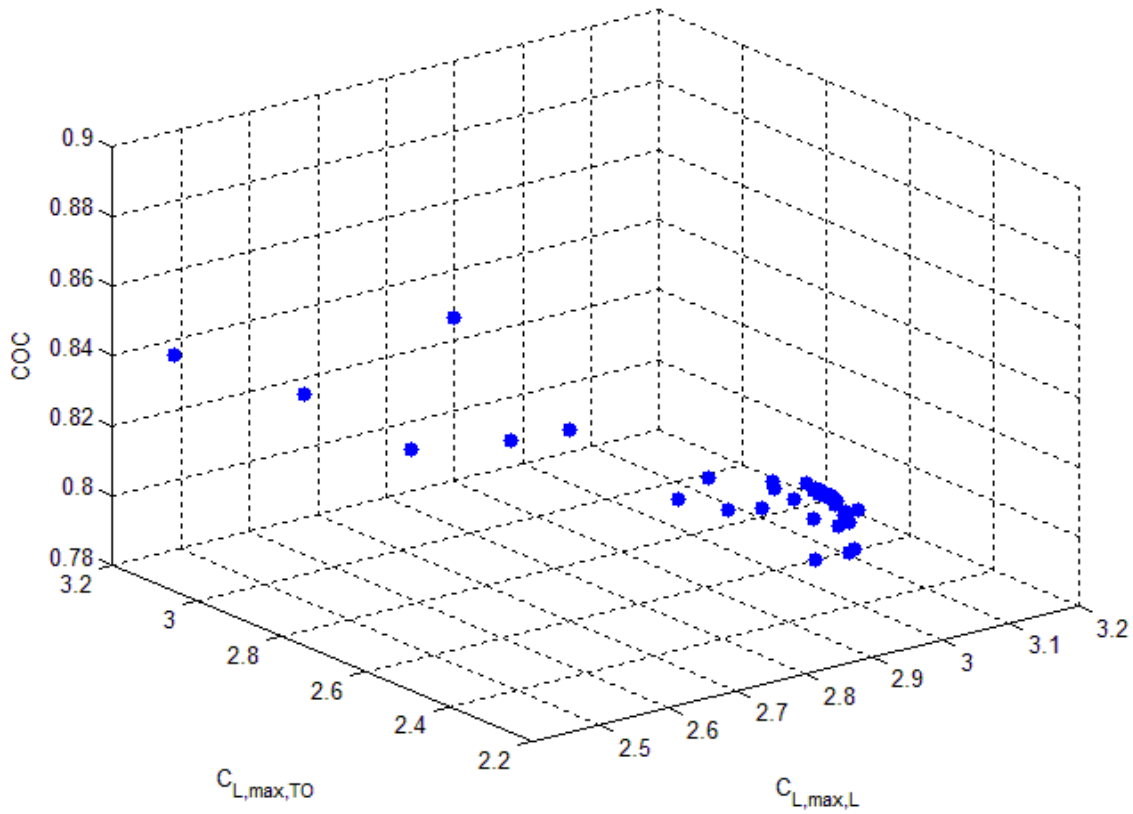


Figure 4.22 Influence of the maximum lift coefficients on the COC

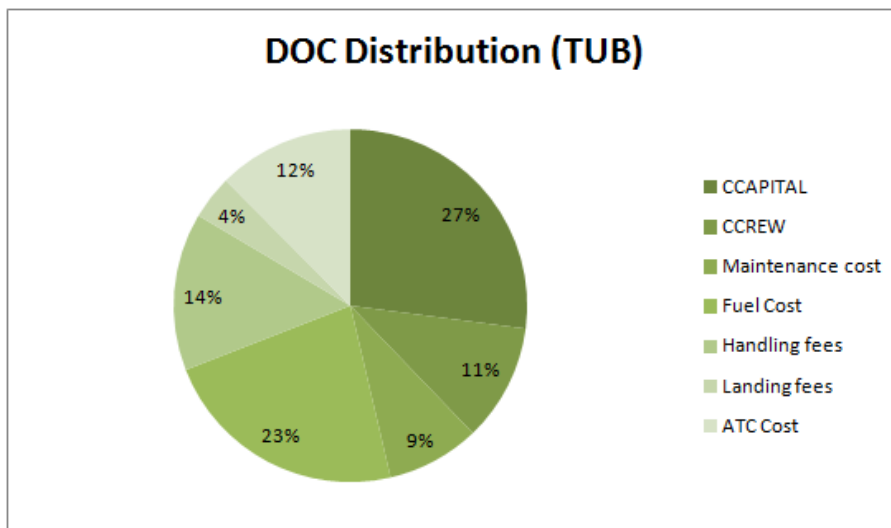
4.3 A320 Optimization

When designing a new aircraft, is it important to have a reference point to refer to. This way, is it possible to compare results and determine the advantages and disadvantages that the new design can bring along. For this specific design, the requirements of the DLR *Design Challenge* are followed, and some of the goals to achieve are set in comparison with the current A320 (CFM) 2009. For this reason, the logic says that the best reference to be used is the mentioned Airbus 320. In addition, OPerA was designed and tested on the first place using A320 as reference aircraft, so it is expected to work well with it. However, the aircraft being designed for this Thesis is planned to be on service on the year 2025. This means that some results, such as the cash operating cost, are no longer comparable. For example, Table 4.5 shows how the A320 cost parameters change just by changing the design year.

Table 4.5 Variation of A320 cost through years (€/ton/mile)

	A320 (CFM) 2009	A320 (CFM) 2025
COC (TUB method)	0.731470	0.891686 (+22 %)
COC (AEA method)	0.813061	0.973276 (+20 %)
DOC (TUB method)	1.002917	1.163133 (+16 %)
DOC (AEA method)	1.128452	1.288668 (+14 %)

Is it possible to see how the price increases because of the increment on the fuel price. An interesting result is to observe how the increment is bigger in COC than in DOC. This is due to the definition of COC and DOC: COC is basically the same as DOC only without the aircraft price. This is clearly visible on Figures 4.23 and 4.24, where the pie charts for DOC and COC estimated with the TUB method are plotted for the A320 (CFM) 2009. Is it possible to see how the area corresponding to the fuel cost is lower in DOC than in COC. In addition, this also tells the most important factors for each method. This way is it possible to say that when optimizing with DOC as objective function, what OPerA will try to find is a compromise between aircraft mass and fuel mass, focusing more in smaller aircraft mass rather than fuel saving, for the mass is the main factor that determines the aircraft price and fees; for COC is the contrary: fuel gets priority over aircraft mass.

**Figure 4.23** DOC pie chart for A320 (CFM) 2009

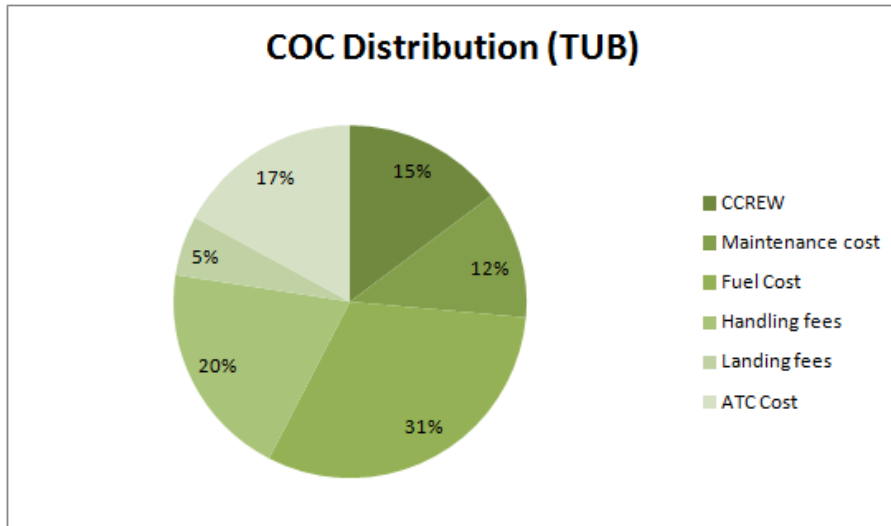


Figure 4.24 COC pie chart for A320 (CFM) 2009

4.3.1 First A320 Optimization

The first step that will be taken in an optimization on the standard A320, with its original requirements fixed. The year for calculation objective will be 2025. This way the optimization potential of the tool can be analyzed, as well as appreciate how will affect the fuel price rise on the characteristics of the airplane. The requirements are (Table 4.6):

Table 4.6 Requirements of standard A320

Requirement	Value
Landing field length LFL	1447.8 m
Takeoff field length TOFL	1767.83 m
Number of passengers n_{PAX}	180
Cruise Mach number M_{CR}	0.76
Design Range R	1510 NM

As it can be seen, the number of passengers, the cruise speed and the design range are smaller than the ones for the Design Challenge. For the optimization, the cabin parameters were kept fixed after performing the optimization, the results are (Table 4.7):

Table 4.7 Optimization results with original A320 requirements

Parameter	Value	COC €/ton/mile	MTO kg	OEW kg	MF Kg
$C_{L,max,L}$	3.041	0.8521	71335	40113	11606
$C_{L,max;TO}$	2.791				
m_{ML}/m_{MTO}	0.8719				
AR	10.74				
φ_{25}	13.82°				
λ	0.1797				
h_p/D_N	0.2597				
BPR	10.27				

The COC has increased, as expected due to the fuel price increase. However, the tool reduced the fuel mass, and now the airplane uses less fuel than in the 2009 version. The maximum take off mass has been as well reduced, in an attempt to reduce the costs related with this parameter. This optimization can be considered a good starting point, but it is not yet suitable for direct comparison with the new aircraft created, since its mission is clearly different to the one that will be studied (190pax and 2000NM range). However, it has been seen that the tool is doing what it is expected: the fuel mass and the takeoff mass were reduced. It is also interesting to highlight how the by-pass ratio and the aspect ratio tend to increase, as expected, having a good effect on aerodynamic efficiency and fuel consumption, and are the main reasons for the fuel mass descent, along with the descent on the sweep angle.

4.3.2 Second A320 Optimization

The next step to take is to adapt the optimized A320 to the requirements for the Design Challenge. The procedure will be similar as done before: the requirements will be identified, and then set in the tool. Finally, the optimization is run and the results briefly discussed.

The new requirements are shown in Table 4.8:

Table 4.8 Requirements for Design Challenge

Requirement	A320 standard	Design challenge
Landing field length LFL	1447.8	1500 m
Takeoff field length TOFL	1767.83	2000 m
Number of passengers n_{PAX}	180	190
Cruise Mach number M_{CR}	0.76	0.79
Design Range	1510 NM	2000 NM

Once the requirements are set, the optimization is started with objective function the cash operating cost. Results are shown in Table 4.9.

The results show how the overall mass of the aircraft has increased. This was expected because now the aircraft flies longer and carries more payload. The fuselage must be adapted to this new situation, as well as the aircraft must carry more fuel in order to achieve longer distances. The COC, however, has been reduced. This is basically due to the new mission: the aircraft flies longer and faster, that means that it can cover the longer distances in the same, or fly more times the same distance during the year. This has a positive impact in the COC that is reflected in the final result.

This new optimized aircraft will be the reference point for the following results, and all of them will be compared to it to evaluate the potential savings in fuel and COC. This way will be possible to estimate the achievement of the goals imposed for the Design Challenge.

Table 4.9 A320 optimized for Design Challenge requirements

Parameter	Value	COC €/ton/mile	MTO kg	OEW kg	MF Kg
$C_{L,max,L}$	3.089	0.7537	79057	43826	15044
$C_{L,max;TO}$	2.741				
m_{ML}/m_{MTO}	0.870				
AR	11.93				
φ_{25}	16.77°				
λ	0.226				
h_p/D_N	0.1504				
BPR	9.469				

4.4 Preliminary Evaluation of Possible Configurations

This Thesis has the goal of designing a suitable aircraft to participate in the DLR Design Challenge for finding the future aircraft. To complete this objective, the tool OPerA will be used. This way, this Thesis is a way to prove that OPerA is a competent tool, able to perform the task it was designed for: optimization of preliminary design aircraft.

As mentioned before (see section 4.1), there are different aircraft configurations currently tested and designed by the participants: the Blended Wing Body aircraft, the Box Wing aircraft (currently developed as well in the AERO Group of the Hamburg University of Applied Sciences where this Thesis was written), and the Cargo Less aircraft. The fourth configuration is the one subject to this study: the Strut Braced Wing aircraft (SBW). Section 2 gives an overview of this kind of aircraft and what to expect from it. In this section the process to find and optimize a suitable design that matches the Design Challenge requirements will be explained. The first step is to analyze and pick the different configurations that will be tested.

4.4.1 Identifying Configurations to Test

In order to start optimizing, the first necessary condition is to decide which configurations are potential for design, optimization and compare. This project intends to introduce two new technologies: the strut braced wing and the folding wing. The first, as already said, has the advantage of reducing significantly the mass of the wing, or conversely, allowing to increase the size of the wing keeping its mass constant. Increased aspect ratios achieve higher lift-to-drag ratios, which means that the fuel consumption goes down, and so does the COC. The second technology is applied as a support for increased aspect ratio: aircraft that include folding wing systems are allowed to stay in ICAO category C (required in the challenge) while increasing its wingspan further than 36 m. In addition, braced wing technology makes possible to use natural laminar flow (NLF) technology on the wing. This technology increases the size of the laminar boundary layer over the wing, thus reducing the zero-lift drag and therefore increasing the lift-to-drag ratio. This technology is applied as a support of the braced wing technology, in order to improve the results obtained with it.

As said, the first step in this process is to identify the different possible configurations, and choosing which ones should be studied to find the potential optimum. In order to so, all the different configurations will be divided in 4 groups: each group contains all the possible configurations using each of the mentioned new technologies, or a combination of them. This way, the four groups or cases of study are:

- Group 1: No new technologies applied.
- Group 2: Braced wing technology.
- Group 3: Folding wing technology.
- Group 4: Braced wing technology plus folding wing technology.

Each one of these groups contains a series of possible configurations that should be tested. These configurations vary from each other in aspects like the position of the wing or the tail, for example. The possible options are the following:

- Wing position: OPerA lets the user select between low wing, medium wing and high wing. However, the medium wing is not used because is used for small airplanes or military airplanes. A medium wing reduces the cabin volume, and this is something not interesting for passenger aircraft. In addition, when using strut braced wing, the low wing is automatically discarded. In this case the strut would act in compression instead of traction, and this comes with a weight penalty for the strut, and the possibility of buckling.
- Tail position: Again, OPerA lets the user choose between three different options, namely conventional (low) tail, cruciform tail, and T-tail. These three options will be checked in all the groups.

- Engine position: There are two possibilities to mount the engines. They can be either on the aft fuselage or under the wing. However, it makes no sense to test aft mounted engines when using conventional tail, because the tail would be right on the engine wake, and that is not allowed. Therefore, combination of conventional tail and aft engines is not tested.
- Wingspan limitation: Here are two possibilities considered for this study: 36 m and 52 m. The first has the goal of making an airplane that fits into category C with no need of using folding wing technology, allowing the use of winglets. This means that folding wing technology will not be tested for 36 m span limitation, as it makes no sense. On the other side, 52 m wingspan limitation is intended to obtain aircraft with high aspect ratio that either fit on the ICAO category D, or in the category C with the use of folding wing system.

Table 4.10 summarizes all the tested configurations. The nomenclature used is the following: the first letter is the wing position, either low (L) or high (H). The second letter is the tail position. It can be conventional (C), cruciform (X) or T-tail (T). The third letter corresponds to the engine position, on wing (W) or fuselage (F) and, finally, the last number indicates the span limit (36 or 52 m).

Table 4.10 Summary of all tested configurations

Configuration	Normal	Braced	Folded	Braced+Folded
LCW36	✓	X	X	X
LCW52	✓	X	✓	X
LXW36	✓	X	X	X
LXW52	✓	X	✓	X
LXF36	✓	X	X	X
LXF52	✓	X	✓	X
LTW36	✓	X	X	X
LTW52	✓	X	✓	X
LTF36	✓	X	X	X
LTF52	✓	X	✓	X
HCW36	✓	✓	X	X
HCW52	✓	✓	✓	✓
HXW36	✓	✓	X	X
HXW52	✓	✓	✓	✓
HXF36	✓	✓	X	X
HXF52	✓	✓	✓	✓
HTW36	✓	✓	X	X
HTW52	✓	✓	✓	✓
HTF36	✓	✓	X	X
HTF52	✓	✓	✓	✓

4.4.2 Preliminary Test Results

Once the different configurations are set, they were tested with OPerA. Each configuration was set as input in OPerA, and the requirements were fixed to those already shown for the Design Challenge. The objective function was in every case the cash operating cost: this way is it possible to analyze and find the best configuration for further optimization, as well as compare it to the reference A320 aircraft. Table 4.11 shows the COC results for each group in absolute values, Table 4.12 shows the same results compared to the optimized A320.

Table 4.11 Preliminary test round best results (separated on groups)

Configuration	Normal	Braced	Folded	B+F
LCW36	0.7537	/	/	/
LCW52	0.7379	/	0.7537	/
LXW36	0.7602	/	/	/
LXW52	0.7490	/	0.7593	/
LXF36	0.7786	/	/	/
LXF52	0.7586	/	0.7719	/
LTW36	0.7648	/	/	/
LTW52	0.7546	/	0.7619	/
LTF36	0.7793	/	/	/
LTF52	0.7676	/	0.7820	/
HCW36	0.7673	0.7462	/	/
HCW52	0.7439	0.7104	0.7612	0.7122
HXW36	0.7729	0.7389	/	/
HXW52	0.7516	0.7096	0.7649	0.7264
HXF36	0.7844	0.7480	/	/
HXF52	0.7746	0.7271	0.7848	0.7521
HTW36	0.7721	0.7463	/	/
HTW52	0.7646	0.7208	0.7703	0.7316
HTF36	0.7823	0.7492	/	/
HTF52	0.7731	0.7508	0.7850	0.7448

Table 4.12 COC results of preliminary test round compared with optimized A320

Comparison	Normal	Braced	Folded	B+F
LCW36	0.00 %	/	/	/
LCW52	-2.10 %	/	-0.01 %	/
LXW36	0.85 %	/	/	/
LXW52	-0.62 %	/	0.74 %	/
LXF36	3.30 %	/	/	/
LXF52	0.65 %	/	2.41 %	/
LTW36	1.47 %	/	/	/
LTW52	0.11 %	/	1.09 %	/
LTF36	3.40 %	/	/	/
LTF52	1.84 %	/	3.75 %	/
HCW36	1.81 %	-1.00 %	/	/
HCW52	-1.30 %	-5.75 %	1.00 %	-5.50 %
HXW36	2.54 %	-1.96 %	/	/
HXW52	-0.27 %	-5.85 %	1.49 %	-3.62 %
HXF36	4.07 %	-0.76 %	/	/
HXF52	2.77 %	-3.53 %	4.12 %	-0.21 %
HTW36	2.43 %	-0.98 %	/	/
HTW52	1.45 %	-4.36 %	2.20 %	-2.93 %
HTF36	3.79 %	-0.60 %	/	/
HTF52	2.57 %	-0.39 %	4.15 %	-1.19 %

The analysis of the results brings different conclusions. For example, the use of the folding technology, as expected, means always an increment in COC. This is because new actuators are being implemented on the aircraft, adding weight and complexity to the design. Comparing the folded results with the normal configuration results, it is clear that folding wing is always worse in COC than an aircraft not including it. The real advantage that the folding wing gives is the possibility to fit in a smaller category despite the wingspan is actually bigger than the allowed one. This way, the folding wing system can be seen as a small penalty in COC that comes with the great advantage of being able to use high aspect ratio wings and still fit in ICAO category C.

Another interesting result comes when checking the braced wing results. They are always better than the reference aircraft, due to a bigger efficiency that is translated in less fuel consumption and smaller takeoff weight than the normal equivalent. It is possible to see an improvement up to 5.85 % on the COC, even in these preliminary results. These are promising results that suggest that it is possible to get even better results in further optimization steps. In addition, results for braced and folded technology together confirm what was already suggested: adding a folding system is equivalent to higher cost, but it comes with the airport advantages.

For the next step, it is necessary to select the configurations that will be object of further optimizations. In order to do so, the best results for each group are gathered together in Table 4.13 and commented later.

Table 4.13 Preliminary optimization round best results separated in groups

Group	Best configuration	COC (€/ton/NM)	MTO (kg)	MF (kg)	OEW (kg)
Normal	LCW52	0.7379	80863	13792	46885
Braced (36 m)	HXW36	0.7389	75547	14789	40572
Braced (52 m)	HXW52	0.7096	76274	12959	43169
Folded	LCW52	0.7537	81263	14629	46448
Braced + Folded	HCW52	0.7122	75836	13143	42506

The most interesting result to comment here is how the T-tail configurations do not appear at all in any of the best results for any group. The fuselage mounted engines neither appear, but that was an expecting result, especially when seeing the results from Table 4.12, where is it possible to see that, except for the braced HXF52 configuration, the rest of the fuselage mounted airplanes have poor results. It is possible to see as well in Table 4.13 how the configurations with 52 m span limitation get better results in every case, and how they are better as well in fuel consumption: the biggest fuel mass in Table 4.13 is the one corresponding to the only 36 m configuration on the table, this proves that a higher aspect ratio is indeed more efficient, and has the biggest potential. Conversely, this 36 m limited version is as well the lightest one, as being able to combine a smaller size with the strut advantages in fuel reduction.

It is interesting to see how the best results in 52 m limited braced and braced plus folded groups exchange their positions: while HXW52 is the best and HCW52 is the second best braced configuration, they are second and first braced and folded configurations, respectively. This is because both configurations are similar in results. However, the configuration including a cruciform tail has a small disadvantage: when checking its design point position on Raymer suggestion graphic (Figure 4.25), it is clearly visible that it is right inside the forbidden area, where there is risk of tail blanketing when the plane stalls. This makes this configuration sensible to deep stall, and some technical measures to avoid it are needed. Since this would mean more complexity and probably more cost, this configuration is discarded. In addition, the best configuration in the braced plus folded group is HCW52, being HXW52 the second one, and, since the final configuration will be braced plus folded, this acts as a confirmation that is a good option to take HCW52 and HCW36 as the configurations that will go under further optimization. More results of this first round of iterations are found on the appendix of this Thesis, and the complete results are included in the CD-Rom coming with this Thesis, in the file "First Optimization Results.xls".

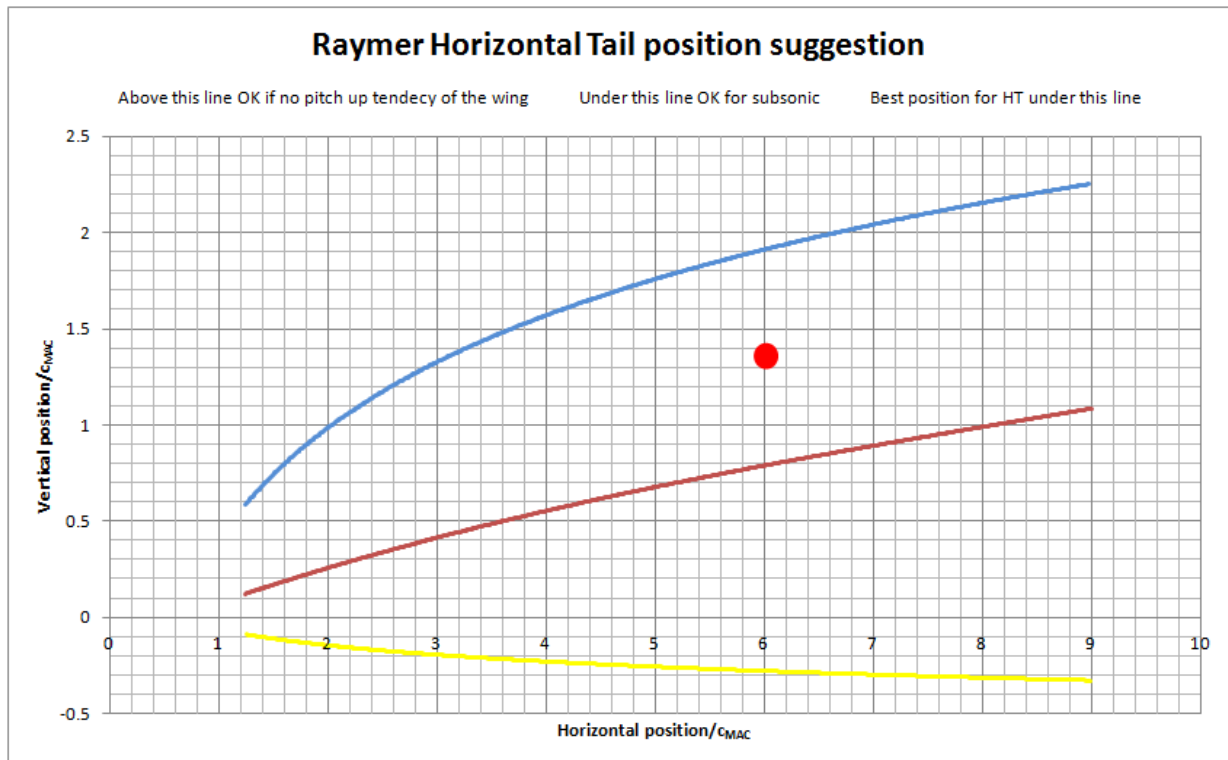


Figure 4.25 Design point of braced HXW52 in Raymer suggestion plot

4.5 Further Optimization of Chosen Configurations

In the previous section (4.4) all the possible configurations were tested and filtered. This process gave as result two configurations that have more potential than the others: High wing with conventional (low) tail and engines on wing, for both 36 m and 52 m meters of span limitation. This is: HCW36 and HCW52, using the configuration nomenclature presented in this Thesis.

These two configurations will be now tested and further optimized in an attempt of how far it is possible to go with the optimizations and how much the benefits can be. In order to do so, first it must be clear where the further optimization is possible, and what is necessary to do to obtain better results. Obviously, all the design parameters were already set free, which means that no better results can appear by just running the optimizations again. However, there is a set of parameters that has not yet being optimized: the requirements. When further optimization is to be achieved, the requirements must be optimized. This must be done carefully, as the requirements are given fixed for the Design Challenge, and should be broken only for a good reason. This is why the requirements will be set free in this second optimization round: the objective is to evaluate the full potential of the chosen configurations and, if the results are positive enough, propose a change in the requirements.

However, not every requirement can be varied. This means that before any new optimization, the requirements fixed and the requirements free, as well as the limits of these last ones, must be clearly detailed.

The most important requirements are the mission requirements, i.e. the payload and the range. Those requirements define the mission that the airplane must complete and are completely fixed. These requirements will not be set free at any moment and will prevail with their current value. As a remembering, say that these values are 190 passengers of payload and 2000 NM design range.

The other requirements that OPerA uses are the landing and takeoff field lengths, and the cruise Mach number, as well as the Second Segment and Missed Approach climb rates. However, these two last are fixed due to certification reasons. Therefore, the only freed parameters for further optimizations will be the field lengths and the cruise Mach number, as shown in Table 4.14.

Table 4.14 Second round optimizations requirements and limits

Requirement	Low limit	Top limit
Payload	190pax, 100 kg/pax	Fixed
Design range	2000 NM	Fixed
Takeoff field length	1500 m	2700 m
Landing field length	1500 m	2700 m
Cruise Mach number (m_{CR})	0.55	0.85

As seen in the table, now the field distances are limited up to 2700 m, this can be a little too high, but the idea behind this second optimization round is to evaluate the real potential of the chosen configurations, and it is expected to find the optimum points beyond the 2000 m limit. The Mach number is set free as well, and it is expected to go lower than the required 0.79.

The optimizations will be this time run to different objective functions, such as minimum fuel of minimum take of mass, as well as the original minimum COC. A couple of optimizations will be performed as well with the DOC as the objective function, to understand the difference between optimizing for COC and DOC.

The first optimized configuration was HCW36 braced. The optimization was run for all the already mentioned objective functions, as well as for minimum DOC. The minimum results are the following (Table 4.15):

Table 4.15 Best results obtained for HCW36 SBW with free parameters

Minimum result	Value	Difference with A320
Minimum COC	0.7051 €/ton/mile	-6.45 %
Minimum MF	12947 kg	-13.94 %
Minimum MTO	68559 kg	-13.27 %
Minimum OEW	35163 kg	-19.77 %
Minimum DOC (TUB)	0.9123 €/ton/mile	-8.21 %

As it is possible to see, results are now better, with a COC reduction up to 6.45 %, and an interesting 13.94 % improvement in takeoff fuel mass. As expected, the varied requirements had a great impact in the results. The Mach number is reduced to 0.64 ... 0.66, depending on the optimization run, and the takeoff field length grew to a maximum of 2670 m when optimizing for DOC. It was observed that optimizing for DOC as an objective function gave better results in takeoff mass, while COC gives lower fuel masses. Therefore, since DOC includes the aircraft price that is mass dependent, and delivers as well good results for fuel mass, the result is that the DOC reduction is higher than COC reduction. This is especially important for airlines that prefer to buy their own aircraft, instead of lease them.

The next tested aircraft configuration was HCW52, with braced wing but without folding wing system. This configuration is expected to deliver the best possible results for braced wing technology, since the span now is free to grow up to 52 m, and there is no extra weight coming from the folding wing actuators. The results obtained are shown in Table 4.16:

Table 4.16 Best results obtained for HCW52 SBW with free parameters

Minimum result	Value	Difference with A320
Minimum COC	0.6507 €/ton/mile	-13.67 %
Minimum MF	10005 kg	-33.5 %
Minimum MTO	65145 kg	-17.6 %
Minimum OEW	33217 kg	-24.21 %
Maximum lift-to-drag ratio	24.26	+29.73 %
Maximum Wingspan	47.44 m	/

The results show a very important improvement when compared to the optimized A320. The reason for them is the almost 30 % increase in lift-to-drag ratio that is obtained when span can grow free up to 52 m, allowing this way the aspect ratio to reach values up to 25. It was

interesting to notice that optimizing for MTO however delivered an optimum aspect ratio of just 17.12. This is because increasing the aspect ratio means increase the wing mass, and therefore the tool found a compromise between wing efficiency and wing weight. However this reduction, as well as the fuel mass reduction, comes along with a decrease of cruise speed, achieving a minimum of 0.554 for the MTO objective optimization. COC optimization gave a cruise Mach number of 0.64, similar to those obtained for the 36 m span limited aircraft. The field lengths, on the other hand, grow up as well as expected, reaching a maximum of 2654 m when optimizing for take of mass. However, minimum COC optimization gave a more acceptable 2374 m, and minimum fuel optimization delivered the minimum takeoff landing field distance: 2048 m, very close to the Design Challenge requirements.

After the HCW52 SBW aircraft was calculated, the differences when adding the folding wing technology must be checked, to determine whether the benefits of the higher wingspan can be used without outfitting the C category (limited to 36 m) without great penalty. The optimization runs where the same as for the HCW52 SBW without folding wings and the results are shown in Table 4.17:

Table 4.17 Best results obtained for HCW52 SBW + Folding wing with free parameters

Minimum result	Value	Difference with A320	Diff. with HCW52 SBW
Minimum COC	0.6633 €/ton/mile	-11.99 %	+1.94 %
Minimum MF	10094 kg	-32.91 %	+0.89 %
Minimum MTO	65664 kg	-16.94 %	+0.79 %
Minimum OEW	33653 kg	-23.21 %	+1.31 %
Maximum lift-to-drag ratio	23.84	+27.49 %	-1.73 %
Maximum wingspan	47.74 m	/	+0.63 %

As expected, the difference is not big enough to justify going for an unfolded wing and a D category aircraft. All the results obtained for the folded HCW52 SBW were similar to the unfolded ones, with small differences like the ones showed in Table 4.17. This means that is more interesting for the airline point of view to choose a folded wing configuration over an unfolded one, since the aircraft will fit in more boarding gates at the airport, and, if the folding wing system fails there will be always the possibility to park the plane in an apron position.

However, folding wing is not the only possible improvement for the braced HCW52. Another technology that is going to be added and was already mentioned is Natural Laminar Flow, a technology that controls the boundary layer over the wing, achieving bigger laminar flow areas, decreasing this way the zero-lift drag and therefore incrementing the maximum lift-to-drag ratio. This technology is expected to bring more COC reductions and fuel mass reductions when

summed up with the braced wing. In addition, the folding wing system, as already seen, allows a 52m span limited aircraft to fit into category C in exchange for a small COC penalty. Thus, the last optimized aircraft for the second round is HCW52 SBW with Folding Wing system and Natural Laminar Flow. Results are shown in Table 4.18:

Table 4.18 Best results obtained for HCW52 SBW+FWS+NLF with free parameters

Minimum result	Value	Difference with A320	Diff. with HCW52 SBW FWS
Minimum COC	0.6448 €/ton/mile	-14.45 %	-2.79 %
Minimum MF	9550 kg	-36.52 %	-5.39 %
Minimum MTO	64806 kg	-18.03 %	-1.31 %
Minimum OEW	33516 kg	-23.52 %	-0.41 %
Maximum lift-to-drag ratio	24.74	+32.3 %	+3.78 %
Maximum wingspan	46.84 m	/	-1.89 %

The NLF technology gives an extra 5.39 % of fuel savings respect to the braced wing technology, achieving a maximum fuel mass reduction of 36 % compared to the optimized A320. This is a very important result, because one of the goals of the Design Challenge is to achieve a 25 % fuel savings respect to the A320 (CFM) 2009. If we take a look at the original A320 (CFM) 2009 numbers obtained with OPerA in Table 4.4, this aircraft carries a total amount of 13033 kg, which means that the HCW52 SBW+FWS+NLF carries 26.72 % less fuel, meeting this way the requirement. However, it is important to note that these results are not really comparable, because A320 (CFM) 2009 has a different mission (180pax and 1510NM range) as well as different fuel price (2009 versus 2025), and that the comparable results are those shown in Table 14.18.

A point that must be highlighted is the maximum lift coefficients gotten for these optimizations: In some cases, $C_{L,max,TO}$ is getting higher than $C_{L,max,L}$, which does not happen in current aircraft. This is because of the landing and takeoff design lines in the Matching chart: In them, the optimum design point tends to make that the optimum ratio between $C_{L,max,TO}$ and $C_{L,max,L}$ get closer to 1, and sometimes is bigger. For this reason, there was a new constraint set for the last optimization, and is that $C_{L,max,TO}$ can never be higher than $C_{L,max,L}$. In addition, the takeoff and landing field lengths were limited to 2000 m instead of the previous 2700 m, so the DLR requirements are met. The cruise Mach number is still let free, since it has been proved that flying slower has a very significant and positive impact on the results.

The complete results of the second round of optimizations can be found in the CD-Rom copy in an Excel file called “SBW optimization results.xls” and “Second Round results.xls”.

4.6 Final Design Optimization Results

Up to this point of the process, two different rounds of optimizations were performed. The first one had the goal to evaluate all the possible configurations and choose the ones that have the best potential. After it, a second round was performed to further understand the benefits of the chosen configuration, and to look for their best potential. Finally, after seeing and understanding the results, a last optimization is performed to obtain the best possible aircraft that matches the requirements.

As a summary: in the first round of optimizations all the possible configurations were tested. The one with the lowest COC potential was HXW52 SBW, followed closely by HCW52 SBW. However, HXW52 SBW had the problem that this configuration is under risk of deep stall. In addition, HCW52 gave better result than HXW52 when adding folding wing. These reasons made HCW52 a more attractive configuration. For the same reason, and for keeping similarity between the 36 m and 52 m meter models, HCW36 was picked over HXW36.

In the second round those configurations were tested with free requirements, so the maximum saving potential could be estimated. The optimizations were done with several objective functions like minimum COC or minimum fuel mass. Additionally, the new technologies, namely Folding Wing System and Natural Laminar Flow were implemented to the aircraft, comparing its results to evaluate their benefits.

Finally, two configurations have been selected to become the final models. On the first place, a 52 m span limited aircraft, with high wing, conventional (low) tail and engines mounted on the wing, with struts under the wing and FWS, as NLF. This configuration is the main configuration proposed for the Design Challenge, and will be in this section commented. On the second place, an alternative 36 m span limited version is proposed. This version will include winglets, SBW and NLF. This alternative is offered in the case a potential client do not want to go further with the folded wing aircraft. However, this alternative will be briefly introduced, since it is not the one that will be presented to the design challenge.

For the last optimization, as already said at the end of the previous section, the requirements were set free but limited: the takeoff and landing field lengths are limited between 1500 and 2000 m to fit into the challenge's requirements, and the maximum takeoff and lift coefficients are limited so the takeoff maximum lift coefficient never gets higher than the landing coefficient, to get a result that corresponds more with typical aircraft values. The cruise speed was let free, since the beneficial effects of this have been proved. The objective function is COC, because the main goal of the challenge is to achieve reductions on it. The main results obtained for both aircraft are the following (Table 4.19):

Table 4.19 Main results of the final configurations

	HCW52 SBW + FWS + NLF (versus A320)		HCW36 SBW + NLF (versus A320)	
COC	0.6579 €/ton/NM (-12.71 %)		0.7117 €/ton/NM (-5.57 %)	
MF	9984 kg	(-33.64 %)	12608 kg	(-16.19 %)
MTO	69060 kg	(-12.65 %)	73105 kg	(-7.53 %)
OEW	38890 kg	(-11.26 %)	40311 kg	(-8.02 %)
Max. lift-to-drag ratio	25.50	(+36.36 %)	19.27	(+3.05 %)

The results show a very interesting 12.71 % of COC savings, plus a 33.64 % savings in fuel. This means that the presented aircraft has the potential to meet the fuel saving requirement of the challenge. The 35 % COC reduction is, on the other side, not achieved. However, this is not considered a problem, since this requirement is very complicated to meet, especially with an aircraft that, despite being a new concept, is based on classical cantilever aircraft.

The fuel saving comes mainly from the advantage that comes by having a strut installed under the wing. The wing reduction allowed helps achieving an aspect ratio of 24.88 that together with the NLF technology offers a 36.36 % increase in E_{max} . Table 4.20 shows some of the results of the new configuration:

Table 4.20 Optimization results for HCW52 SBW + FWT + NLF

Parameter	Value	COC €/ton/mile	MTO kg	OEW kg	MF Kg
$TOFL$	1992 m	0.6579	69060	38890	9984
LFL	1705 m				
$C_{L,max,L}$	3.1338				
$C_{L,max;TO}$	3.1311				
m_{ML}/m_{MTO}	0.9245				
AR	24.89				
n_{PAX}	190				
n_{SA}	6				
φ_{25}	9.68°				
λ	0.19				
h_p/D_N	0.193				
BPR	11.9				

M_{CR}		0.64
SP		0.7366 m
w_{AISLE}		0.508 m
w_{SEAT}		0.508 m
$w_{ARMREST}$		0.0508 m
$s_{CLEARANCE}$		0.015 m
Thrust weight T/W	to	0.2751
Wing loading m_{MTO}/S_W		729
Cruise altitude h_{CR}		11321 m
t/c		0.157
c_{MAC}		2.252 m
S_W		94.77 m ²
T_{TO}		93194 N
Wing mass m_W		5428 kg
b		48.57 m
Horizontal tail mass m_H	tail	386 kg
Vertical tail mass m_V	tail	674 kg

The results show a plane with high aspect ratio and great span (48.57 m). This means that the mean aerodynamic chord of the wing is small (2.252 m) and this will have an effect in the horizontal tail size, as it can be seen in the table. The wing thickness is also a little bigger than expected, but the reason is that the aircraft flights at $M_{CR} = 0.64$, which is not so close to the transonic regime. This means that the wing thickness does not need to be so thin to avoid compressibility effects or use NLF. The design point (thrust-to-weight ratio and wing loading) is in similar terms as the design point of A320. Interesting is as well the low sweep angle, but that was expected when performing the single parameter optimization, because this way the airplane is more aerodynamic efficient.

To finally analyze the cost results, a bar chart was plotted to show in a visual way the differences between the cost of the designed aircraft and the reference A320. It is included as well in the graphic the alternative 36 m limited airplane.

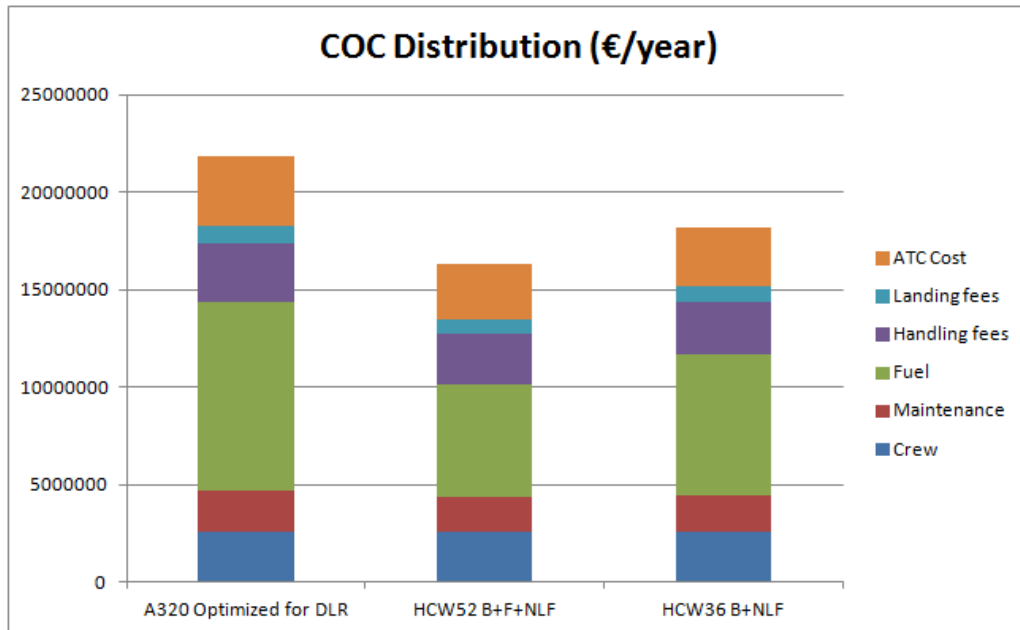


Figure 4.26 COC chart comparison of the optimized aircraft

It can be easily seen in the chart that the biggest part of COC is actually fuel. Especially when cost for year 2025 is estimated, since the fuel price is expected to rise for that year. The important reduction in fuel consumption achieved in both the designed airplanes is responsible of the respective descent in COC. The ATC cost, the landing and the maintenance costs are reduced as well, since they depend on the aircraft weight. However, handling fees depend mainly of the payload, which is the same for the three aircraft, and so no savings are visible there. The crew cost is dependent on the payload as well, so it is the same situation as with the handling fees. Figure 4.27 show the COC distribution for HCW52 SBW + FWS + NLF with more detail.

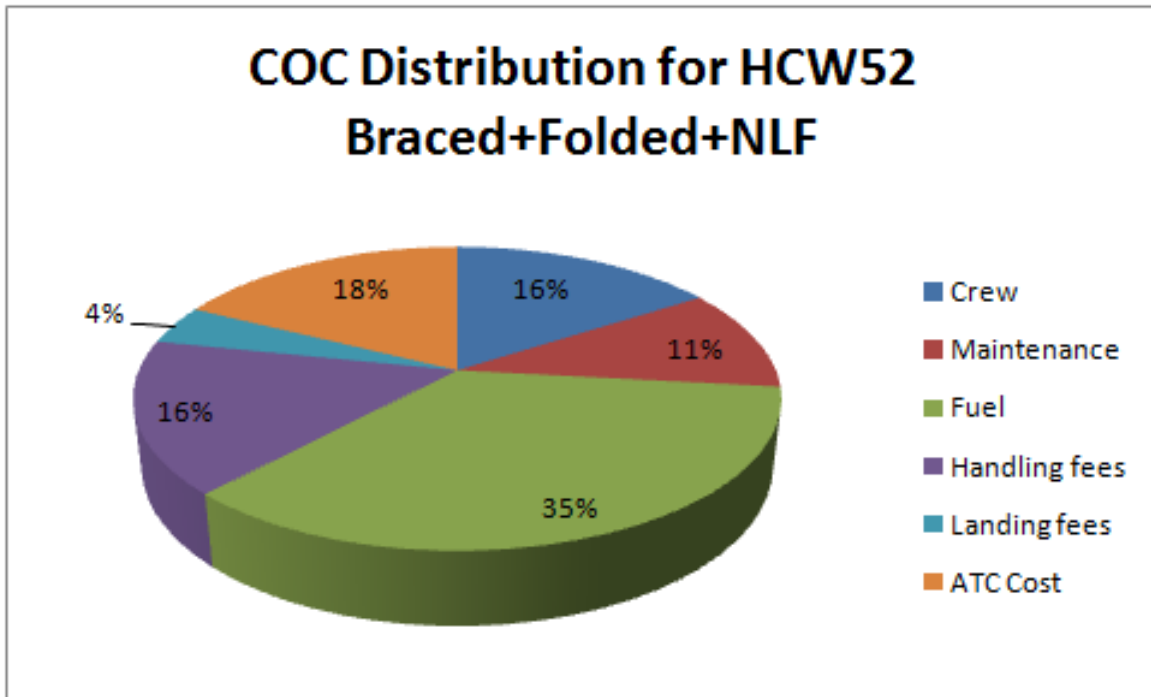


Figure 4.27 COC distribution of the designed airplane

4.7 Visual Representation of the HCW52 SBW + FWS + NLF

To conclude this study, an electronic model of the chosen aircraft was created. In order to do so, a program called OpenVSP was used. OpenVSP stands for Open source Vehicle Sketch Pad, and was created by J.R. Gloudemans and others for NASA in the early 1990's. It was later released as an open source program under the NASA Open Source Agreement (NOSA) on January 2012. OpenVSP is a parametric tool that allows the user to create aircraft geometry using common engineering parameters. OpenVSP was using for this project together with OpenVSP Connect, a tool developed in AERO Group at the Hamburg University of Applied Sciences that simplifies the design with OpenVSP by automatically generating an OpenVSP file according to the parameters introduced by the user.

The final design is represented in Figures 4.28, 4.29, 4.30 and 4.31. There is it possible to see what was already commented about the small size of the horizontal tail: since the horizontal tail volume coefficient depends on the mean aerodynamic chord of the aircraft, by making this smaller, the tail gets smaller as well. Physical explanation for this is that the gravity centre and neutral point are now closer, and therefore the moment to balance by the tail is smaller. In addition, horizontal tail aspect ratio is directly related with the wing aspect ratio in a half proportion, so extending the wing aspect ratio comes along with an extension in the horizontal tail aspect ratio, reducing this way the induced drag of the tail. The vertical tail gets bigger because, conversely as the horizontal tail, its tail volume coefficient depends on the wingspan, and the wingspan for this aircraft is 48.57 m, way longer than the standard 36m for category C. In further phases of the design process (remember that this is a preliminary design phase) might

be convenient to perform analysis to confirm that the standard statistical value is completely valid for an airplane such as the SBW.

The strut shown in the picture is a concept approximation to the real strut design. In this model, the strut was placed at the leading edge of the wing, which is beneficial for the aero elasticity characteristics of the airplane, and forms an angle of about 35° with the wing, because this a compromise angle to minimize the wing weight and use the biggest bending relieve. A small offset between the strut and the wing was added in order to avoid complicated aerodynamic interferences (Ko 2002). However, this strut design is not yet definitive, and must be object of Finite Element and CFD analysis in order to find the proper shape and position for it.

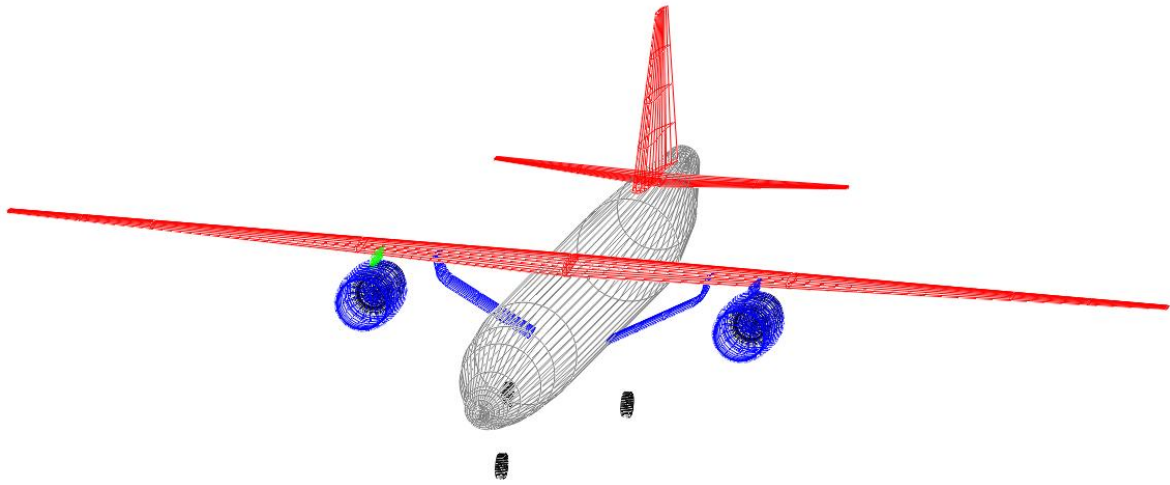


Figure 4.28 3D representation of the final design

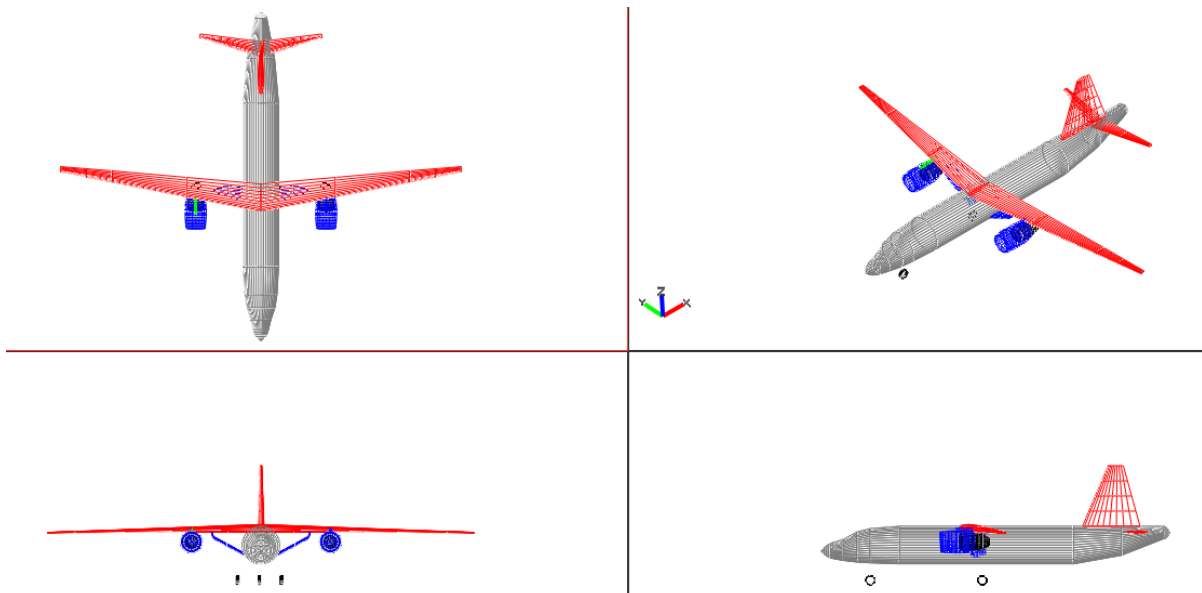


Figure 4.29 4 view representation of the final design

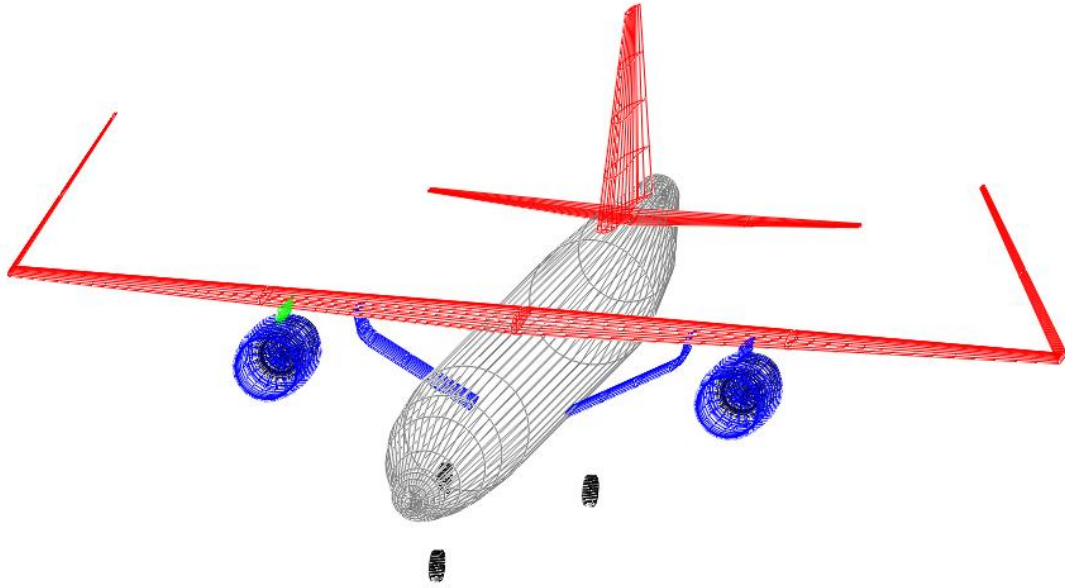


Figure 4.30 Final design with folded wings



Figure 4.31 Artistic representation of the final design

5 Conclusions and Future Work

After completing the preliminary design of a Strut Braced Wing aircraft, many conclusions can be extracted:

On the first place, the saving potential of the SBW has been proven. Following the guidelines of the DLR Design Challenge, final savings up to 12.71 % compared to the reference A320 optimized for comparison purposes were achieved. This is far from the 35 % goal of the contest. However, it was not expected to achieve such a high difference with an aircraft that is very similar to the classic cantilever concept of A320. In addition, fuel savings up to 33.74 % are possible with the strut braced wing configuration, which is way up of the 25 % goal for the challenge. This way, the SBW Aircraft positions itself as a firm alternative to the classic cantilever design in future aircraft.

The future work is clear now: SBW is a configuration with possibilities. Further work must be done in this direction. The design here presented is a preliminary design that must be reviewed and refined in following design phases. This work can be done using the AERO tool PreSTo, useful for the conceptual aircraft design phase. Different analysis, such as FEM analysis and CFD analysis can be carried out, so the final geometry of the aircraft can be defined. The real potential of the SBW configuration will be then checked and proved.

References

- Airbus 2012** J. LEAHY. *Navigating the Future*. Global Market Forecast 2012-2031. Airbus, 2012
- AERO 2013** Box Wing Concept Image from the Database of AERO Research Group of Hamburg University of Applied Sciences, where this Thesis was written
- Agentsmart 2013** Picture taken from the Internet. URL: <http://www.agentsmart.co.uk/blog/wp-content/uploads/2009/10/Sopwith-tabloid2.jpg>
- Carrier 2012** G. CARRIER, O ATINAULT, S. DEQUAND, J.-L. HANTRAIS-GERVOIS, C.LIAUZUN, B. PALUCH, A.-M. RODDE, C.TOUSSAINT. *Investigation of a Strut-Braced Wing Configuration for future commercial transport*. Onera, the French Aerospace Lab. Meudon, France, 2012
- Cessna 2013** Picture taken from the Internet. URL: www.cessna.com
- COSCAP 1999** COOPERATIVE DEVELOPMENT OF OPERATIONAL SAFETY AND CONTINUING AIRWORTHINESS. *Aerodrome Standards. Aerodrome Design and Operations*. Manual based on ICAO Annex 14, July 1999
- FlyBaby 2013** Picture taken from the Internet. URL: <http://www.bowersflybaby.com/tech/alternatives.html>
- Gern 2000** F. H. GERN, A. KO, E. SULAEMAN, R. K. KAPANIA, W.H. MASON, B. GROSSMAN, R.T. HAFTKA. *Passive Load Alleviation in the Design of A Strut-Braced Wing Transonic Transport*. AAIA-2000-4826. Long Beach, CA, 2000
- Grassmeyer 1998** J.M. GRASSMEYER, A. NAGHSHINEH-POUR, P.-A. TETRAULT, B. GROSSMAN, R.T. HAFTKA, R.K. KAPANIA, W.H. MASON, J.A. SCHETZ. *Multidisciplinary Design Optimization of a Strut Braced Wing Aircraft with Tip-Mounted Engines*. Department of Aerospace and Ocean Engineering. Virginia Polytechnic Institute and State University, Blacksburg, VA, USA, 1998
- Gundlach 1999** J.F GUNDLACH IV, A. NAGHSHINEH-POUR, F. GERN, P.-A. TETRAULT, A.KO, J.A. SCHETZ, W.H. MASON, R.K. KAPANIA, B.GROSSMAN, R.T.HAFTKA. *Multidisciplinary Design Optimization and Industry Review of a 2010 Strut-Braced Wing Transonic Transport*. Department of Aerospace and Ocean Engineering. Virginia Polytechnic Institute and State University, Blacksburg, VA, USA, 1999
- Gundlach 2000** J.F GUNDLACH IV, A. NAGHSHINEH-POUR, F. GERN, P.-A. TETRAULT, A.KO, J.A. SCHETZ, W.H. MASON, R.K. KAPANIA, B.GROSSMANN, R.T.HAFTKA. *Multidisciplinary Design Optimization of a Strut-Braced Wing Transonic Transport*. 38th Aerospace Sciences Meeting & Exhibit. 10-13 January 2000. Reno, Nevada

- Herrmann 2010** S. HERRMAN. *Untersuchung des Einusses des Motorenzahl auf die Wirtschaftlichkeit eines Verkehrsflugzeuges unter Berücksichtigung eines optimalen Bypassverhältnisses*. Graduation Thesis, Technical University Berlin, 2010
- Hurel 1952** M. HUREL. *The Advantages of High Aspect Ratios*. *Interavia*, Volume VII, No. 12, 1952, pp 695-699
- Jane 92** JANE'S INFORMATION GROUP. *Jane's All the World's Aircraft '92-'93*. Edited by Mark Lambert, 1993
- Jane 08** JANE'S INFORMATION GROUP. *Jane's All the World's Aircraft '08-'09*. Edited by Paul Jackson, 2009
- Ko 2002** A.KO, W.H.MASON, B.GROSSMANN, J.A.SCHETZ. *A-7 Strut Braced Wing Concept Transonic Wing Design*. Department of Aerospace and Ocean Engineering. Virginia Polytechnic Institute and State University, Blacksburg, VA, USA. Prepared for NASA Langley Research Center. VPI-AOE-275. July, 2012
- Kundu 2010** A.K. KUNDU. *Aircraft Design*, Cambridge Aerospace Series, Cambridge University Press, 2010
- LTH 2008** *Luftfahrttechnisches Handbuch Edition 2008*, MA Band Masseanalyse, 2008. URL: <http://www.lth-online.de/>
- NASA 1980** R.V TURRIZIANI, W.A. LOVELL, G.L. MARTIN, J.E. PRICE, E.E.SWANSON, G.F.WASHBURN. *Preliminary Design Characteristics of a Subsonic Business Jet Concept Employing an Aspect Ratio 25 Strut-Braced Wing*. Kentron International Inc., Hampton Technical Center, Hampton, Virginia, 1980.
- NASA 1981** P.M. SMITH, J.DEYOUNG, W.A. LOVELL, J.E. PRICE, G.F. WASHBURN. *A Study of High-Altitude Manned Research Aircraft Employing Strut-Braced Wings of High Aspect Ratio*. Kenton International, Inc. Hampton Technical Center. Hampton, Virginia, 1981
- NASA 1997** *The Blended Wing Body*, FS-1997-07-24-LaRC, Langley Research Center, Hampton, Virginia, July 1997. URL: <http://scholar.lib.vt.edu/theses/available/etd-07112008-182200/unrestricted/FS-1997-07-24-LaRC.pdf>
- Nita 2012** M. NIȚĂ. *Contributions to Aircraft Preliminary Design and Optimization*. Hamburg University of Applied Sciences, Polytechnic University of Bucharest, 2012
- Price 1997** K. PRICE, N. STORN. *Differential Evolution*. *Dr. Dobbs's Journal*, pp 18-29, April 1997
- Raymer 2006** D.P. RAYMER. *Aircraft Design: A conceptual Approach*, AAIA Education Series, 2006

- Roskam 1989** J.ROSKAM. *Airplane Design, Vol. 1:Preliminary Sizing of Airplanes*. Ottawa, Kansas, 1989
- Scholz 1999** D. SCHOLZ. *Flugzeugentwurf (Airport Design)*. Hamburg University of Applied Sciences, Department of Automotive and Aeronautical Engineering. Lecture Notes, 1999
- Torenbeek 1992** E. TORENBEEK. *Development and Application of a Comprehensive, Design Sensitive Weight Prediction Method for Wing Structures of Transport Category Aircraft*. Delft University of Technology, Faculty of Aerospace Engineering, Report LR-693, 1992
- TUB 2013** TECHNISCHE UNIVERSITÄT BERLIN. *DOC-Assesment Method*. Aircraft Design & Aero Structures. Power Point Presentation. 2013
- Pfenninger 1958** W. PFENNINGER. *Desing considerations of Large Subsonic Long Range Transport Airplanes with Low Drag Boundary Layer Suction*. Northrop Aircraft, Inc., Report NAI-58-529 (BLC-III), 1958
- Yarygina 2012** M.V. YARYGINA, YU.I. POPOV. *Development of the Weight Formula for a Folding Wing*. Paper, (written in Russian) 2012.
- Yarigyna 2013** M.V. YARYGINA. Method of calculation and analysis design weight compartment with folding hinge of wing. Paper (written in Russian), 2013

Acknowledgements

This Thesis was possible thanks to many people. On the first place, I would like to express my gratitude to Prof. Dr.-Ing. Dieter Scholz, MSME, who gave me the opportunity to join the AERO research group of Hamburg University of Applying Sciences, to start this exciting journey into world of Aircraft Design, and for tutoring me during the time this Thesis lasted and helping with all the problems I could find.

On the second place, my eternal gratitude to my partner researchers at AERO group: Andreas, Tim, Tahir, Pryianka, Roberto and Ricardo, who became during this time not only just partners, but good friends. Many thanks to them for helping me to complete this Thesis, for their advice, and for their friendship.

I want also to thank my home University, ETSI Aeronáuticos of the Polytechnical University of Madrid, for giving me the opportunity to write my Final Thesis abroad, as an international student.

Naturally, my deepest gratitude goes to my family. To my parents, Lidia and Julián, who were always supporting me in the good and in the bad moments, always there for me. Thank you. And to my brother, Julio, for his support and help, for being the best partner one could expect in this adventure. Thank you as well to Corpa, Dani, Fran, Iker, Alba and Julio, for being always there and helping me when needed.

Finally, I would like to thank the person that encouraged me to come to Hamburg and write this Thesis, because without that support this Thesis would not have been possible on the first place.

Appendix A

Results of First Iteration Round

Table A.1 Fuel results (kg)

Absolut data	Normal	Braced	Folded	B+F
LCW36	15045	/	/	/
LCW52	13792	/	14629	/
LXW36	15356	/	/	/
LXW52	14435	/	15103	/
LXF36	15989	/	/	/
LXF52	14553	/	15545	/
LTW36	15338	/	/	/
LTW52	14516	/	15048	/
LTF36	15899	/	/	/
LTF52	14902	/	15841	/
HCW36	15669	15116	/	/
HCW52	13903	12959	15228	13143
HXW36	15683	14789	/	/
HXW52	14656	12918	15120	13937
HXF36	16246	14787	/	/
HXF52	15231	13688	15740	15017
HTW36	15698	15023	/	/
HTW52	14780	13072	15431	13983
HTF36	15859	15035	/	/
HTF52	15000	14141	15692	14499

Table A.2 Fuel results compared to reference A320

Comparison	Normal	Braced	Folded	B+F
LCW36	0.00 %	/	/	/
LCW52	-8.33 %	/	-2.76 %	/
LXW36	2.07 %	/	/	/
LXW52	-4.05 %	/	0.39 %	/
LXF36	6.28 %	/	/	/
LXF52	-3.27 %	/	3.32 %	/
LTW36	1.95 %	/	/	/
LTW52	-3.52 %	/	0.02 %	/
LTF36	5.68 %	/	/	/
LTF52	-0.95 %	/	5.29 %	/
HCW36	4.15 %	0.47 %	/	/
HCW52	-7.59 %	-13.87 %	1.22 %	-12.64 %
HXW36	4.24 %	-1.70 %	/	/
HXW52	-2.58 %	-14.14 %	0.50 %	-7.36 %
HXF36	7.98 %	-1.71 %	/	/
HXF352	1.24 %	-9.02 %	4.62 %	-0.19 %
HTW36	4.34 %	-0.14 %	/	/
HTW52	-1.76 %	-13.11 %	2.56 %	-7.06 %
HTF36	5.41 %	-0.06 %	/	/
HTF52	-0.30 %	-6.01 %	4.30 %	-3.63 %

Table A.3 MTO results (kg)

Absolut data	Normal	Braced	Folded	B+F
LCW36	79057	/	/	/
LCW52	80863	/	81263	/
LXW36	79370	/	/	/
LXW52	80996	/	80596	/
LXF36	82129	/	/	/
LXF52	83539	/	82349	/
LTW36	81103	/	/	/
LTW52	82289	/	81696	/
LTF36	82900	/	/	/
LTF52	84531	/	84032	/
HCW36	79986	77132	/	/
HCW52	82267	76281	80758	75836
HXW36	81839	75547	/	/
HXW52	80533	76274	82298	75950
HXF36	82501	77086	/	/
HXF52	84863	77695	85429	78714
HTW36	81431	76629	/	/
HTW52	84111	79249	82373	77530
HTF36	83935	77613	/	/
HTF52	85992	83260	85788	79251

Table A.4 MTO results compared with reference A320

Comparison	Normal	Braced	Folded	B+F
LCW36	0.00 %	/	/	/
LCW52	2.28 %	/	2.79 %	/
LXW36	0.40 %	/	/	/
LXW52	2.45 %	/	1.95 %	/
LXF36	3.89 %	/	/	/
LXF52	5.67 %	/	4.16 %	/
LTW36	2.59 %	/	/	/
LTW52	4.09 %	/	3.34 %	/
LTF36	4.86 %	/	/	/
LTF52	6.92 %	/	6.29 %	/
HCW36	1.18 %	-2.44 %	/	/
HCW52	4.06 %	-3.51 %	2.15 %	-4.07 %
HXW36	3.52 %	-4.44 %	/	/
HXW52	1.87 %	-3.52 %	4.10 %	-3.93 %
HXF36	4.36 %	-2.49 %	/	/
HXF352	7.34 %	-1.72 %	8.06 %	-0.43 %
HTW36	3.00 %	-3.07 %	/	/
HTW52	6.39 %	0.24 %	4.19 %	-1.93 %
HTF36	6.17 %	-1.83 %	/	/
HTF52	8.77 %	5.32 %	8.51 %	0.25 %

Appendix B

CD-ROM Contents

The CD-Rom enclosed with this Thesis includes the following content:

- This Thesis in a PDF file.
- Complete results of the first round of iterations, in an Excel file called “First Round Results.xls”. The file is saved both in .xls and .xlsx formats.
- Complete results of the second round of iterations, in an Excel file called “Second Round Results.xls” The file is saved both in .xls and .xlsx formats.
- Summary of all the results, including complete results of last round of iterations, in an Excel file named “SBW Optimizations General Results.xls”. The file is saved in both .xls and .xlsx formats.
- Latest OPerA version created for this Thesis. It comes in an Excel file called “OPerA_SanchezBarreda_Thesis.xls” This file requires the use of Excel Macros to work properly.